UNIVERSITY OF CALIFORNIA, SAN DIEGO

The Role of Twist1 in Promoting Tumor Invasion and Metastasis by Regulation of Invadopodia Formation

A dissertation in partial satisfaction of the
requirements for the degree Doctor of Philosophy

in

Molecular Pathology

by

Mark Adam Eckert

Committee in charge:

Professor Jing Yang, Chair
Professor Sara Courtneidge
Professor Shelley Halpain
Professor James Quigley
Professor David Schlaepfer

2012

The dissertation of Mark Adam Eckert is approved, and it is acceptable in quality and form for publication on microfilm and electronically:

Chair

University of California, San Diego

2012

DEDICATION

To all of my family and friends who have always

been there for me no matter what has happened.

You've all made my life a much more

pleasant and interesting experience for the last six years.

EPIGRAPH

"Whereof one cannot speak, thereof one must be silent."

Ludwig Wittgenstein, *Tractatus Logico-Philosophicus*

TABLE OF CONTENTS

LIST OF FIGURES

Chapter I

Chapter II

Chapter III

LIST OF COMMON ABBREVIATIONS

ADAM12: A disintegrin and metalloprotease 12

IF: Immunofluorescence

IHC: Immunohistochemistry

IP: Immunoprecipitation

ECM: Extracellular matrix

EMT: Epithelial-mesenchymal transition

MMP: Matrix metalloprotease

MT1-MMP: Membrane-type 1 metalloprotease

PDGFR: Platelet-derived growth factor receptor

RT-PCR: Real-time polymerase chain reaction

SDS-PAGE: Sodium dodecyl sulfate polyacrylamide gel electrophoresis

SEM: Standard error of the mean

shRNA: Short hairpin ribonucleic acid

WB: Western blot

ACKNOWLEDGEMENTS

I would like to thank Dr. Jing Yang for all of her support and mentorship over the past six years. Graduate school has been a truly life-altering experience and thanks to Dr. Yang it has been altered for the best. All of the people that have passed through the lab since I've been here have taught me something and I have appreciated the chance to learn from such a wonderful group of people. In particular, however, I would like to thank Helmi Lwin for all of her assistance in the early years of the lab and Jeff Tsai for being an incredibly knowledgeable and helpful person whom I have turned to many times in lab.

I would also like to thank Dr. Sara Courtneidge for her contributions to getting my project started. Without her assistance, my time in graduate school would have been much less successful. In addition, members of her lab, especially Begoña Diaz and Danielle Murphy, were always willing to help me with advice and reagents when I most needed them.

Chapter II was reproduced with permission from co-authors, modified from the publication: Mark A. Eckert, Thinzar M. Lwin, Andrew T. Chang, Jihoon Kim, Etienne Danis, Lucila Ohno-Machado, and Jing Yang. "Twist1-induced invadopodia formation promotes tumor metastasis." Cancer Cell. Vol. 19, Issue 3, 372-386, March 8, 2011.

VITA

EDUCATION

2006-2012 University of California, San Diego, La Jolla, CA
Ph.D., Molecular Pathology

2002-2006 North Carolina State University, Raleigh, NC
B.S., Biochemistry
B.S., Chemistry
Minor, Genetics

PUBLICATIONS

Eckert, MA, Yang J. (2011). Targeting invadopodia to block breast cancer metastasis. Oncotarget. *2*, 562-8.

Eckert MA, Lwin TM, Chang AT, Kim J, Danis E, Ohno-Machado L, Yang J. (2011). Twist1-induced invadopodia formation promotes tumor metastasis. Cancer Cell. *19* 372-86.

RESEARCH EXPERIENCE

2006-2012 **Graduate Student, Molecular Pathology Graduate Program**
University of California, San Diego, La Jolla, CA
Research in Dr. Jing Yang's laboratory on the mechanisms of Twist1-induced local invasion and metastasis.

2004-2006 **Undergraduate Research Assistant, Department of Chemistry**
North Carolina State University, Raleigh, NC
Research in Dr. Lin He's laboratory on analyzing the efficiency of chemically-induced DNA ligation with surface plasmon resonance spectroscopy.

ABSTRACT OF THE DISSERTATION

The Role of Twist1 in Promoting Tumor Invasion and Metastasis by Regulation of Invadopodia Formation

by

Mark Adam Eckert

Doctor of Philosophy in Molecular Pathology

University of California, San Diego, 2012

Professor Jing Yang, Chair

Metastasis is a multistep process during which cancer cells gain the ability to invade through the extracellular matrix (ECM) to disseminate to distant organs. Cancer cells can degrade ECM by forming invasive structures called invadopodia which concentrate protease activities to areas of the cell in contact with the ECM. Twist1 is a key transcription factor known to promote the epithelial mesenchymal transition (EMT)

and tumor metastasis. We find that Twist1 promotes local invasion in metastasis by inducing invadopodia formation via transcriptional regulation of platelet-derived growth factor α (PDGFRα) and a disintegrin and metalloprotease 12 (ADAM12).

We find that Twist1 is both necessary and sufficient for invadopodia formation and ECM degradation in multiple cell lines. Twist1 induces PDGFRα expression, which in turn activates Src, to promote invadopodia formation. We demonstrate that Twist1 and PDGFRα are central mediators of invadopodia formation in response to various EMT-inducing signals. Induction of PDGFRα and invadopodia is essential for Twist1 to promote tumor metastasis. Consistent with PDGFRα being a direct transcriptional target of Twist1, co-expression of Twist1 and PDGFRα predicts poor survival in breast tumor patients. Therefore, invadopodia-mediated matrix degradation is a key function of Twist1 in promoting tumor metastasis.

Moreover, we find that the transmembrane metalloprotease ADAM12 is strongly induced by Twist1 and localizes to both invadopodia and focal adhesions. Knockdown of ADAM12 reduces both migration and invasion while increasing adhesion and focal adhesion number. We show that ADAM12 is required for formation of invadopodia and gelatin degradation. Using a series of ADAM12 mutants, we find that the disintegrin domain of ADAM12 is involved in both regulation of focal adhesions and invadopodia while the metalloprotease domain is specifically required for efficient invadopodia formation. Functionally, ADAM12 is required for efficient metastasis of tumor cells to the lung in a human xenograft breast cancer metastasis model in mice.

Our work defines a novel role for Twist1 in regulating ECM degradation during tumor invasion and metastasis. These results could lead to new biomarkers and targeted therapeutics for invasive and metastatic breast cancer.

Chapter I

Introduction: Roles of the Epithelial-Mesenchymal Transition and Invadopodia in Local Invasion and Metastasis

MECHANISMS OF METASTASIS

Cancer arises from the transformation of a single normal cell into a malignant cell that subsequently develops into a tumor. Over the course of cancer development, a pattern of abnormalities develops that sustain and drive the progression of the disease. In 2000, Hanahan and Weinberg synthesized and summarized the existing literature to develop a list of the "hallmarks of cancer." They propose that cancer development requires sustained proliferative signaling, evasion of growth suppressors, gain of replicative immortality, resistance to apoptosis, activation of angiogenesis, and an induction of invasion and metastasis. Importantly, the authors note that there may be variation in the order in which key events in cancer progression occur between individual tumors (Hanahan and Weinberg, 2000). In 2011, Hanahan and Weinberg revisited the hallmarks of cancer and added two emerging hallmarks, avoidance of immune destruction and deregulation of cellular energetics, and two enabling characteristics, genome instability and tumor-promoting inflammation (Hanahan and Weinberg, 2011). These papers have been enormously influential in driving research and hypotheses in the field of cancer biology over the last decade. Importantly, one hallmark, metastasis, is responsible for over 90% of cancer deaths (Chaffer and Weinberg, 2011).

Metastasis itself is a multistep process (Hanahan and Weinberg, 2000; Schedin and Elias, 2004). Most cancers are carcinomas that arise from epithelial tissues. In the first steps of metastasis, carcinoma cells that proliferate abnormally lose polarity and become dysplastic. In breast cancer, this is characteristic of ductal carcinoma in situ, one of the first clinically detectable lesions in breast cancer (Virnig et al., 2010).

Carcinoma cells go on to breach the basement membrane that underlies all epithelial tissues. Following local invasion through the stroma or surrounding tissues, cancer cells intravasate into the circulatory system. Those cells that survive transit in the circulatory system extravasate at distant sites to form metastases. Eventually, some micrometastases will proliferate at distant sites leading to formation of overt macrometastases. Alternatively, cancer metastasis may be thought of as a two step process: in the first step, cancer cells invade and disseminate to distant organs. In the second step, outgrowth of micrometastases occurs in distant organs. This model reflects the hypothesis that the rate-limiting steps of metastasis are late events involving growth at the metastatic site (Chaffer and Weinberg, 2011).

Recently, a process termed the epithelial-mesenchymal transition, or EMT, has been recognized as important in promoting multiple steps of the metastatic process. EMT itself is a developmentally-conserved program in which epithelial cells gain properties typically associated with mesenchymal cells including increased motility and invasiveness (Boyer and Thiery 1993; Hay 1995). In the first description of the EMT process, this process was characterized primarily by the morphological changes associated with the individual cell migration of lens epithelial cells in 3D culture: migrating cells lost their characteristic cobblestone morphology with strong apical-basal polarity and became spindle-shaped (Greenburg, 1982).

At the molecular level, EMT is defined by a repression of epithelial genes and a complementary induction of mesenchymal genes. Loss of epithelial cadherin (E-cadherin) is one of the most characteristic features of EMT. Normal epithelial cells form tight connections with one another via E-cadherin mediated junctions that are linked to

the cytoskeleton via catenins (Yap et al., 1997). During EMT, these E-cadherin-mediated junctions are lost in a process that promotes the cell-cell dissociation associated with metastasis (Onder et al., 2008). Catenins associated with epithelial junctions, including α, β, and γ-catenin, are also reduced at the protein level during EMT (Yang et al., 2004). In concert with the loss of epithelial junctions, a host of mesenchymal markers are upregulated. A weaker, neural-cadherin (N-cadherin) is upregulated in place of E-cadherin and cells replace cytokeratin intermediate filaments with vimentin filaments (Yang and Weinberg, 2008; Lee et al., 2006). In addition to the forward EMT process, the reverse process, mesenchymal-epithelial transition (MET), also occurs (Chaffer et al., 2007). It is hypothesized that EMT in the primary tumor is followed by a reversion through an MET process following metastasis to explain the observation that the cytological properties of metastases are usually identical to those found in the primary tumor (Thiery, 2002).

The EMT process is primarily a transcriptional program that is activated by a suite of zinc-finger and basic helix-loop-helix (bHLH) transcription factors. The zinc-finger transcription factors Snail, Slug, Zeb1, and Zeb2 directly inhibit E-cadherin expression via binding to E-box elements in the E-cadherin promoter (Hajra et al., 2002; Peinado et al., 2003; Sánchez-Tilló et al., 2010; Vandewalle et al., 2005). All of these transcription factors are sufficient to induce the characteristic features of EMT including increased migration and invasion in epithelial cells (Medici et al., 2008; Vandewalle et al., 2005; Sánchez-Tilló et al., 2010). As β-catenin associates with the intracellular portion of cadherin-mediated junctions, destabilization of E-cadherin junctions also has the effect of increasing the cytoplasmic pool of β-catenin (Orsulic et

al., 1999). Under certain cellular contexts, this can lead to nuclear accumulation of β-catenin (Papkoff and Aikawa, 1998). In the nucleus, β-catenin has additional roles as a transcriptional co-activator that associates with lymphoid enhancer-binding factor 1 (LEF1) and transcription factor 4 (TCF4) to drive further changes characteristic of EMT via induction of Slug and Twist1 (Conacci-Sorrell et al., 2003; Onder et al., 2008). In addition, the bHLH transcription factors Twist1 and Twist2 are sufficient to induce a robust EMT in epithelial cells (Yang et al., 2004; Fang et al., 2011). The roles of Twist1 in EMT are discussed further in the subsequent section.

EMT processes occur on multiple occasions during development. During gastrulation, the primitive ectoderm invaginates to form the mesoderm in a process that involves a loss of cell-cell adhesion and local breaching of the basement membrane (Kimelman, 2006; Viebahn, 1995). This process requires a Snail1-mediated EMT in mice; knockout of Snail1 leads to a dramatic failure of mesoderm formation in which the mesoderm continues to express E-cadherin (Carver et al., 2001). An additional EMT occurs during neural crest formation in early embryonic development. The neural crest arises from the ectodermal neural tube via a process that involves individual cell migration and loss of cadherin-mediated junctions (Tucker et al., 1988). Within the cranial and cardiac neural crest, this process also entails breaching a basement membrane similar to the process that occurs during gastrulation (Sternberg and Kimber, 1986). Knockout of Twist1 in mice leads to a failure of proper neural crest formation and embryonic lethality (Chen & Behringer 1995; Soo et al. 2002). Additional Twist1-dependent EMT events occur during cardiac valve formation and secondary palate formation (Fitchett and Hay, 1989; Morabito et al., 2001).

Multiple markers of EMT have been associated with increased invasiveness and metastasis in human cancers. Loss of E-cadherin, a defining feature of EMT, occurs in many aggressive cancers. Reduced staining for E-cadherin by immunohistochemistry is associated with disease prognosis in breast and gastric carcinomas (Gould Rothberg and Bracken, 2006; Guilford et al., 1998). Nuclear β-catenin staining associated with EMT is strongly correlated with poor survival and prognosis in colorectal cancer (Horst et al., 2009) Slug expression is also increased in subpopulations of colorectal and squamous cell cancers that have poor prognosis (Shioiri et al., 2006; Uchikado et al., 2005). Increased Snail1 expression also correlates with both poor survival and metastasis in adenoid cystic carcinoma of the salivary gland (Jiang et al., 2010). Twist1 is associated with poor prognosis and reduced survival in multiple cancers, which is discussed more fully in the subsequent section.

TWIST1 AND EMT

In 2004, Yang et al. described a crucial role for the transcription factor Twist1 in promoting breast cancer metastasis. Knockdown of Twist1 in the highly metastatic 4T1 mouse mammary carcinoma cell line led to a reduction in metastasis to the lungs in an orthotopic mouse model of metastasis. In addition, overexpression of Twist1 in human mammary epithelial cells promoted an EMT process in which cells lost E-cadherin mediated junctions, upregulated mesenchymal genes such as N-cadherin and fibronectin, and became more invasive and metastatic. Importantly, Twist1 expression was found to be upregulated in more invasive cell lines and in invasive lobular carcinoma (Yang et al. 2004). In subsequent years, Twist1 has been associated with

aggressiveness and metastasis in melanomas, neuroblastomas, prostate cancers, and gastric cancers, among others (Peinado et al., 2007).

Mammalian Twist1 is a Class B basic helix-loop-helix (bHLH) transcription factor which lacks a transactivation domain (Franco et al., 2010). In order to regulate transcription, Twist1 must dimerize with other class A or B bHLH transcription factors such as E12/47 or Hand2 (Firulli et al., 2005; Laursen et al., 2007). There is additional evidence that Twist1 homodimers play a role in fibroblast growth factor receptor (FGFR) regulation during cranial suture development (Connerney et al., 2008). As either a homodimer or heterodimer, Twist1 binds E-box elements with the consensus sequence 5'-CANNTG-3' in promoter regions of target genes to regulate gene expression (Franco et al., 2010). Depending on the binding partner for Twist1, gene expression may be upregulated or downregulated following recruitment of the complex to a promoter (Castanon et al., 2001). Twist1 also possesses a domain called a TWIST-box which can interact with and repress the transcriptional activation properties of runt-related transcription factor 1 (RunX1) and (Sex determining region Y)-box 9 (SOX9) (Gu et al., 2012; Kronenberg, 2004).

Twist1 is regulated at both the transcriptional and post-translational level. Hypoxia directly induces Twist1 transcription via both hypoxia inducible factor 1 (HIF-1) α and β (Gort et al. 2007; Yang et al. 2008). Tumor necrosis factor alpha (TNF-α) induces an EMT in some cell lines via direct upregulation of Twist1 by nuclear factor kappa B (NF-KB) (Li et al., 2012; Pham et al., 2007). This suggests a strong link between inflammatory processes that occur in many cancers and Twist1-induced EMT and invasion. Finally, the Wnt pathway, which is often aberrantly activated in cancers

and associated with stem cells, induces Twist1 transcription via stabilization of cytoplasmic β-catenin in mammary carcinoma cells (Howe et al., 2003).

Phosphorylation of Twist1 at several different residues regulates both the stability and the localization of Twist1. Protein kinase B (PKB or Akt) serine phosphorylates Twist1 and induces nuclear translocation of Twist1. This phosphorylation event is also associated with an attenuation of p53 in response to pro-apoptotic signals. Significantly, a monoclonal antibody against serine-phosphorylated Twist was generated and found to localize specifically to the nucleus in multiple human cancer samples (Vichalkovski et al., 2010). In response to transforming growth factor β (TGF-β) signaling, Twist1 is serine phosphorylated by a mitogen activated protein kinase (MAPK). This phosphorylation event leads to increased stability of the Twist1 protein and associated regulation of Twist1 target genes and invasion (Hong et al., 2011). In addition to being phosphorylated, Twist1 is also a substrate for ubiquitination mediated by the E3-ligase partner of paired (PPa) (Lander et al., 2011). This provides yet another potential mechanism for regulation of Twist1 stability and protein levels.

In *Drosophila*, Twist1 is required for induction of mesoderm formation and myogenic differentiation (Furlong et al., 2001). In mammalian systems, Twist1 is essential for formation of the neural crest as described in the preceding section. The differing roles of *Drosophila* and mammalian Twist1 proteins is hypothesized to be due to the fact that *Drosophila* Twist1 possesses a transactivation domain and does not require a dimerization partner to regulate gene transcription (Franco et al., 2010). Twist1 knockout mice are not viable due to failure of neural tube closure (Soo et al., 2002). Interestingly, Twist1 haploinsufficiency induces craniofacial abnormalities due

to premature fusion of cranial sutures in heterozygous knockout mice (Franco et al., 2010). This possesses remarkable similarity to Saerthe-Chotzen syndrome in humans, a developmental disorder characterized by abnormal craniofacial development associated with mutations in both Twist1 and FGFRs (Kress et al., 2005). This suggests additional roles for Twist1 in cranial bone development and differentiation.

Interestingly, Yang et al. report that transducing cancer cells that express Twist1 with E-cadherin is not sufficient to suppress invasion (Yang et al. 2004). This suggests that Twist1 promotes other cellular processes independent of E-cadherin loss to promote local invasion and metastasis. Defining these active processes associated with local invasion and metastasis is essential to understanding how EMT promotes disease progression.

INVADOPODIA STRUCTURE AND FUNCTION

Subcellular structures called invadopodia play key roles in driving local invasion during cancer progression. Invadopodia are dynamic actin-based protrusions occurring on the basal surface of some cancer cells or Src-transformed fibroblasts that localize proteoytic activity to areas of the cell in contact with the ECM to drive local invasion. By convention, in non-transformed cells similar structures are termed podosomes. When referring to both structures in general terms, the term invadosome may be used (Murphy and Courtneidge, 2011). Although first identified in Src-tranformed fibroblasts, invadopodia and podosomes have subsequently been identified in a large number of cancer and normal cell types. Breast, prostate, head and neck cancer, bladder, and pancreatic cancer cell lines all form invadopodia under normal cell culture conditions (Bowden et al., 1999; Desai et al., 2008; Neel et al., 2012). Untransformed

cells that invade or remodel the ECM, including macrophages, osteoclasts, dendritic cells, and activated endothelial cells, also form podosomes (Evans et al., 2003; Gawden-Bone et al., 2010; Pfaff and Jurdic, 2001; Moreau et al., 2003).

The fundamental structure of an invadosome consists of a core of F-actin associated with actin-regulatory proteins, scaffolding and adhesion proteins, and proteases. The overall structure of an invadopodia is typically a projection 0.5-2 μm in diameter that may extend over 5 μm into the surrounding ECM (Murphy and Courtneidge, 2011). Invadopodia length is highly-dependent on matrix composition and depth, with intact peritoneal membrane substrates leading to formation of long-lived invadopodia up to 12 μm long (Schoumacher et al., 2010). Invadopodia can be identified with fluorescence microscopy by the colocalization of invadopodia marker proteins, such as tyrosine kinase substrate 5 (Tks5) or cortactin, with F-actin puncta on the basal surface of the cell (Seals et al. 2005; Bowden et al. 2006). Cortactin or F-actin positive puncta can also be positively identified as invadopodia by colocalization with phosphotyrosine staining due to the fact that many of the components of invadopodia are tyrosine phosphorylated by Src kinase (Bowden et al., 2006).

Live-cell imaging experiments using fluorescently-tagged invadopodia proteins such as cortactin and membrane-type metalloprotease 1 (MT1-MMP) reveal that individual invadopodia are dynamic structures with lifetimes ranging from minutes to hours depending on the ECM substrate (Yamaguchi et al., 2005; Schoumacher et al., 2010). Electron microscopy studies of invadopodia suggest that invadopodia form in close association with collagen fibrils and concentrate metalloproteases, including secreted matrix metalloproteases 2 and 9 (MMP2 and 9) and membrane-type 1

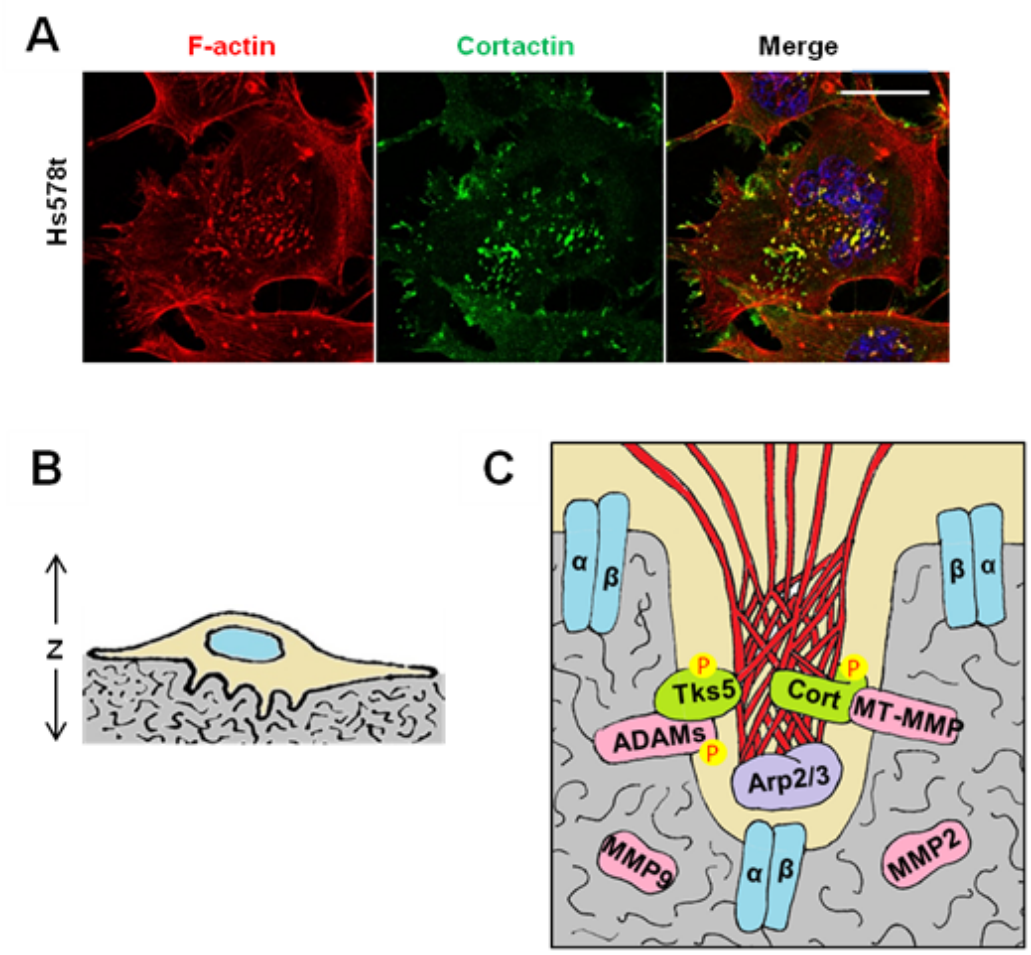

Figure 1.1: Invadopodia. (A) Hs578t breast cancer cell stained with cortactin and F-actin. Invadopodia are clearly apparent as punctuate areas of yellow colocalization in the merged image. Scale bar = 5 μm. (B) Z-projection demonstrating that invadopodia are projections from the basal surface of the cell in contact with the ECM (grey). Not to scale. (C) Cartoon of invadopodia emphasizing key aspects of structure. The center of the invadopodia is a branched F-actin core (red) that is formed through the action of the Arp2/3 complex (lavender) and other actin-regulatory proteins. Integrin α/β heterodimers (blue) may play adhesive and signaling roles both at the tip of the invadopodia and in a ring surrounding the structure. Multiple scaffolding and structural proteins, including Tks5 and cortactin (cort, green) are involved in regulating actin polymerization, interaction with other proteins, and delivery of proteases to the invadopodia. Several metalloproteases are highlighted (pink), including the transmembrane MT-MMPs and ADAMs. Other matrix metalloproteases, including MMP2 and MMP9, are secreted locally at invadopodia. Src activity is necessary for invadopodia, and multiple component of invadopodia are tyrosine phosphorylated (yellow circles, Tks5, cortactin, and ADAMs). Not to scale.

metalloprotease (MT1-MMP) to the tip of individual invadopodia (Vishnubhotla et al., 2007). Tolde et al. report that invadopodia in a dermis-derived 3D culture system form significantly larger invadopodia in which proteolytic activity is concentrated near the base of the invadopodia (Tolde et al., 2010). There are few reports of invadopodia in *in vivo* systems, although Quintavalle et al. identify podosomes in intact mouse aorta smooth muscle tissue via immunoelectron microscopy (Quintavalle et al., 2010).

Although they possess many similarities, invadosomes are distinct from other actin-based cellular protrusions such as filopodia, lamellopodia, and focal adhesions. Filopodia are thin, actin based protrusions often associated with lamellopodia thought to function as cellular probes of the surrounding environment (Mattila and Lappalainen, 2008). In contrast to filopodia, invadosomes form exclusively on the basal surface of the cell and are capable of proteolytic processing of ECM components. In addition, invadosomes contain both branched and parallel actin fibers while filopodia are composed entirely of parallel actin filaments (Murphy and Courtneidge, 2011). Although also composed primarily of branched F-actin, lamellipodia are distinct sheet-like projections from the lateral edges of cells involved in cell motility (Small et al., 2002). Invadosomes differ from lamellipodia in their localization to the basal surface of the cell and their narrow, punctate architecture (Murphy and Courtneidge, 2011). Focal adhesions perhaps possess the greatest similarity to invadosomes. Both focal adhesions and invadosomes are associated with branched and parallel F-actin and associate with integrins. Many structural proteins are shared between focal adhesions and invadopodia, including paxillin and actinin (Hirooka et al., 2011; Badowski et al., 2007). Complicating differentiation of invadopodia from focal adhesions, Wang et al. recently

described a novel function for focal adhesions in mediating MT1-MMP-dependent focal matrix degradation. In the same manuscript, however, Wang et al. describe a key difference between invadosomes and focal adhesions: focal adhesion-mediated degradation occurs on the cell periphery and has a distinctive elongated shape characteristic of focal adhesions (Wang and McNiven, 2012). In contrast, invadosome-mediated degradation consists of circular, punctate degradation associated with F-actin (Murphy and Courtneidge, 2011). This is consistent with previous reports that invadopodia preferentially form in areas of the cell in close proximity to the Golgi apparatus (Baldassarre, 2002).

Although invadopodia formation correlates well with *in vitro* models of invasion in Matrigel and collagen matrices (Yu and Machesky, 2012; Schoumacher et al., 2010), relatively few studies have directly addressed the role of invadopodia in metastasis. Although cortactin is expressed at high levels in invasive human colorectal and head and neck cancers, cortactin has other functions outside of invadopodia as an actin-bundling protein associated with cortical actin (Cai et al., 2010; Hofman et al., 2008). The most direct evidence that cortactin-mediated invadopodia formation is essential for metastasis comes from animal experiments in which mice were injected with MDA-MB231 cells overexpressing wild type or mutant cortactin that lacked several tyrosine phosphorylation sites. The MDA-MB231 cells expressing the mutant form of cortactin metastasized at a significantly lower rate than those expressing the wild type cortactin (Li et al., 2001). Interestingly, the tyrosine phosphorylation sites Li et al. mutated have been identified as essential sites of phosphorylation for invadopodia formation (Ayala et al., 2008). Tks5 is perhaps the protein most specifically related to invadopodia.

Knockdown of the invadopodia-specific scaffolding protein Tks5 in Src-transformed fibroblasts led to a reduction in tumor growth and angiogenesis in a subcutaneous tumor model (Blouw et al. 2008). The authors suggested a role for invadopodia in shedding or release of growth factors from the matrix in driving proliferation and angiogenesis *in vivo*. More work is clearly necessary to fully characterize the effects and roles of invadopodia using *in vivo* models of metastasis.

COMPONENTS OF INVADOPODIA

Actin-Regulatory Proteins

As the primary core of invadopodia consists of polymerized F-actin, many actin regulatory proteins are associated with invadopodia formation and regulation. The actin regulatory protein 2/3 complex (Arp2/3 complex) consists of a seven unit complex that promotes actin nucleation and polymerization (D'Agostino, 2005). Arp2/3 is enriched at invadopodia where it is required for formation of branched actin filaments and invadopodia formation (Weed et al., 2000; DesMarais et al., 2009). A recently developed small-molecule inhibitor of the Arp2/3 complex completely abrogates podosome formation in monocytes (Nolen et al., 2009). Another class of actin-nucleating proteins, the formins, is also enriched at invadopodia in breast cancer cells (Lizárraga et al., 2009). In contrast to Arp2/3, formins mediate linear actin polymerization (Goode and Eck, 2007). It is hypothesized that formins are necessary for elongation of invadopodia and extension into the ECM (Lizárraga et al., 2009). In addition to actin-nucleating proteins, the actin-severing protein cofilin cleaves F-actin filaments at invadopodia to create new barbed ends that promote additional actin polymerization at invadopodia (Oser and Condeelis, 2009). The actin-bundling protein

fascin is also necessary for initiation and stabilization of invadopodia formation and promotes ECM degradation and invasion (Li et al., 2010). Similarly the actin-bundling protein cortactin is an essential component of invadopodia with roles in actin bundling and trafficking of proteases to invadopodia (Ayala et al., 2008; Artym et al., 2006). Phosphorylation of cortactin by Arg or Src has important effects on initiating invadopodia formation in some models of invadopodia formation (Mader et al., 2011).

Adhesive Proteins

Invadopodia and podosomes are tightly linked to the ECM via cluster-of-differentiation 44 (CD44) and integrin-mediated interactions. CD44 is a transmembrane receptor with high affinity for many components of the ECM, including hyaluronic acid and fibronectin (Goodison et al., 1999). In both osteoclast podosomes and cancer cell invadopodia, there is evidence that CD44 is involved in membrane trafficking of MMP9 to the cell surface (Yu and Stamenkovic, 1999; Samanna et al., 2007). Despite the strong localization of CD44 with invadopodia and podosomes, there have been few studies characterizing its function at invadosomes.

Integrin heterodimers, composed of one alpha and one beta subunit, bind to ECM components through an extracellular domain that can bind a diverse range of substrates, including collagens, fibronectin, vitronectin, and gelatin, with the specificity of the interaction depending on the specific alpha-beta heterodimers involved (Destaing et al, 2011). The intracellular domains of integrin heterodimers mediate interactions with the cytoskeleton through proteins including vinculin, α-actinin, and talin (Hood and Cheresh, 2002; Kanchanawong et al., 2010). In addition, integrins can mediate signal transduction through interactions with intracellular kinases including focal

adhesion kinase (FAK) and Src (Mitra and Schlaepfer, 2006). Both β1 and β3 integrins have been localized to invadopodia and podosomes via immunofluorescence staining (Mersich et al., 2010; Mueller and Chen, 1991). Interestingly, in Src-transformed fibroblasts that express both β1 and β3 integrins, inhibition of β1 integrin eliminated invadopodia formation while β3 was dispensable (Destaing et al., 2010). In addition, different integrins have been localized to different areas of invadopodia. In oral squamous carcinoma cells, α3β1 integrin localized to rings surrounding the F-actin rich core of the invadopodia. The invadopodia project itself was strongly positive for αvβ5 integrin (Takkunen et al., 2010). The specific integrin heterodimers involved in invadopodia may vary by cell-type and depend on the range of integrins expressed by the cell line being examined. More work is clearly necessary to identify the specific roles of integrins at invadopodia and the significance of integrin localization to the invadopodia protrusion versus the surrounding area.

Scaffolding Proteins

Scaffolding proteins play an integral role in invadopodia, linking the actin cytoskeleton to the adhesive and proteolytic components of invadopodia. Tks5 is a large scaffolding protein consisting of an amino-terminal Phox-homology (PX) domain following by five SH3 domains that was first described as an essential component of invadopodia in Src-transformed fibroblasts, breast cancer cells, and melanoma cells (Seals et al., 2005). The PX domain of Tks5 regulates localization of the protein to phosphatidylinositol 3-and-4-phosphate 2 (PI(3,4)P2) enriched areas of the cell membrane associated with lipid-rafts while the five SH3 domains mediate interactions with intracellular proteins containing PxxP or RxxK amino acid sequences (Mayer,

2001; Oikawa et al., 2009). Tks5 interaction with Nck, Grb2, and neural Wiskott-Aldrich Syndrome protein (N-WASP) promote invadopodia formation via promotion of Arp2/3-mediated actin nucleation and polymerization (Stylli et al., 2009). Alternatively, recruitment of Tks5 to focal adhesions may promote a transition from focal-adhesion mediated attachment to invadopodia-mediated degradation (Oikawa et al., 2009). Tks5 also interacts with the transmembrane metalloproteases ADAM12 and 19 that are also enriched in invadopodia (Abram et al., 2003). A related scaffolding protein, Tks4, resembles Tks5 in possessing a PX domain and four SH3 domains and is hypothesized to play complementary roles in localization of MT1-MMP to invadopodia (Buschman et al., 2009).

In addition to Tks4 and 5, cortactin and N-WASP play important structural roles in invadopodia. N-WASP is activated by phosphorylation by Src or Abl kinases, leading to an association with the Arp2/3 complex that then promotes Arp2/3-mediated actin nucleation and polymerization (Yamaguchi et al., 2005). Interaction of N-WASP with cortactin also promotes Arp2/3 activation and actin polymerization at invadopodia (DesMarais et al., 2009). Cortactin is an additional adaptor protein that functions as an actin bundling protein and regulator of actin polymerization, primarily via its interaction with N-WASP (DesMarais et al., 2009). Cortactin appears to have key roles in transport of proteases to invadopodia. Upon knockdown of cortactin, invadopodia-like structures still form in head and neck cancer cells but fail to degrade ECM components (Clark et al., 2007). Even when MT1-MMP is overexpressed in MDA-MB231 cells, cortactin co-expression is required for efficient transport of MT1-MMP to invadopodia and subsequent ECM degradation (Clark and Weaver, 2008). Live-cell imaging suggests

that cortactin is one of the earliest proteins recruited to invadopodia, preceding even actin polymerization (Artym et al., 2006). The mechanism by which cortactin is recruited to the membrane prior to invadopodia formation remains uncharacterized and poorly understood.

Proteases

Consistent with a role for invadopodia in mediating ECM degradation and local invasion, a wide variety of proteases are enriched at invadopodia. The serine proteases fibroblast activation protein α (FAPα, or seprase) and dipeptidyl peptidase 4 (DPPiv) are both highly enriched at invadopodia in multiple cell types (O'Brien and O'Connor, 2008). FAPα and DPPiv are both dipeptidyl peptidases that possess gelatinase and collagenase activity (Kelly, 2005). In addition, FAPα localizes to invadopodia via an interaction with α3β1 integrin (Mueller et al., 1999). Interestingly, FAPα activity is also associated with formation of more ordered, linear collagen matrices that are associated with increased cell velocity and migration (Lee et al., 2011). Although inhibition of DPPiv activity with a specific monoclonal blocking antibody abrogated invasion in cells on collagen matrices, the exact role for these proteases in invadopodia formation and regulation are still poorly understood (Ghersi et al., 2002). Similarly to knockdown of Tks5, FAPα appears to have roles in cancer growth and proliferation (Huang et al., 2011). This may suggest a more general role for invadopodia in promoting tumor growth through an unknown mechanism that may involve release of growth factors from the cell surface or the surrounding ECM. The recent development of small-molecule inhibitors specific for both FAPα and DPPiv will allow more thorough

investigation of the unique roles of these proteases in invadopodia biogenesis and metastasis (Brennen et al., 2012).

Matrix metalloproteases (MMPs) are zinc-dependent metalloproteases that have important roles in cleavage of membrane components and other substrates. Both secreted and membrane bound MMPs are involved in invadopodia formation and function. Due to the central role of MMPs in mediating ECM degradation and the observation that the metalloproteases inhibitor BB94 inhibits invadopodia formation, the role of MMPs in invadopodia has been a popular topic for investigation (Ayala et al., 2008).

MT1-MMP is a transmembrane endopeptidase with critical roles in mediating local invasion and metastasis. Substrates for MT1-MMP include collagens, vitronectin, fibronectin, and laminins (Sabeh et al., 2004). In multiple cancer cell lines and endothelial cells and osteoclasts, MT1-MMP localizes to invadopodia (Poincloux et al., 2009). Knockdown of MT1-MMP is sufficient to abrogate invadopodia-mediated degradation and formation (Steffen et al., 2008). Interestingly, in addition to roles in degrading ECM components, MT1-MMP can activate other, secreted MMPs. Via an αvβ3 integrin-dependent mechanism, MT1-MMP cleaves the propeptidase domain from MMP2 leading to localized activation of soluble MMP2 (Deryugina et al., 2001). Interestingly, immunoelectron microscopy reveals that MT1-MMP localizes to the extreme tip of invadopodia where both MMP2 and MMP9 are also localized (Vishnubhotla et al., 2007). Components of the exocyst complex, including exocyst complex component 7 (Exo70 or Sec8) localize to invadopodia and are required for efficient delivery of MMPs (Liu et al., 2009). As MT1-MMP is constitutively activated

by cleavage of its prodomain by furin peptidase, its activity is primarily regulated by localization. Protein kinase C (PKC)-mediated phosphorylation of the cytoplasmic tail of MT1-MMP is sufficient to induce membrane localization of MT1-MMP (Urena et al., 1999).

Several members of the a disintegrin and metalloprotease (ADAM) family of proteases, including ADAM12 and ADAM19, localize to invadopodia (Seals et al., 2005; Abram et al., 2003). ADAM family proteases are zinc-dependent transmembrane metalloproteases that possess additional cysteine-rich and disintegrin domains that mediate interactions with the ECM through syndecans and integrins, respectively (Kveiborg et al., 2008). ADAM12 and 19 are known to act as sheddases, capable of cleaving and releasing ligands including epidermal growth factor (EGF) and delta-like 1 (Dl1) from the cell surface (Dyczynska et al., 2007; Horiuchi et al., 2006). Both ADAM12 and ADAM19 directly interact with Tks5, implying a potential role in invadopodia formation or regulation (Abram et al., 2003). Current functional studies in invadopodia are limited to the observation that inducing clustering of ADAM12 with a monoclonal antibody leads to localized shedding of EGF and formation of invadopodia (Albrechtsen et al., 2011). The biological relevance of this antibody-directed ligation to a potential role for ADAM12 in invadopodia formation remains unresolved.

Due to the central role of proteases in invadopodia, techniques have been developed to allow visualization and quantification of invadopodia-mediated degradation of ECM components. Fluorescently-labeled gelatin can be covalently conjugated to a poly-L-lysine coated coverslip substrate via gluteraldehyde crosslinking. Areas that are degraded by cells plated on the fluorescent substrate will

appear as dark areas in a uniformly fluorescent background. Relative degradation can be assayed by calculating the relative area degraded per cell to investigate the effects of small-molecule inhibitors or mRNA knockdown on invadopodia-mediated degradation (Even-Ram and Artym, 2009). Substrates other than gelatin, including fibronectin, collagen, and gelatin-Matrigel mixtures, have also been used as fluorescent substrates in similar assays (Nascimento et al., 2009; Aga et al., 2008; Furmaniak-Kazmierczak et al., 2007). These data suggest that invadopodia are capable of degrading a diverse array of ECM components.

REGULATION OF INVADOPODIA

Consistent with their diverse protein components, multiple signaling pathways converge to regulate invadopodia formation and activity. These include Src, PKC, and integrins. Although numerous biochemical pathways have been implicated in invadopodia formation, there is a paucity of information on the role of transcriptional regulation in invadopodia biogenesis.

The nonreceptor tyrosine kinase Src has always been recognized as an important regulator of invadopodia formation. Invadopodia were, in fact, first described in Src-transformed fibroblasts: upon transformation with constitutively active chicken Src, fibroblasts formed numerous rosettes of invadopodia capable of degrading ECM components (David-Pfeuty and Singer, 1980; Tarone et al., 1985; Chen et al., 1985). Transduction of other cell lines with constitutively active Src similarly induces robust invadopodia formation (Kelley et al., 2010), while inhibition with Src kinase inhibitors, such as SU6656 and PP2, prevent invadopodia formation (Mader et al., 2011; Balzer et al., 2010). Src phosphorylates multiple components of invadopodia, including cortactin

and Tks5 (Ayala et al., 2008; Stylli et al., 2009). In a series of mutagenesis experiments, tyrosine resides in cortactin were found to be necessary for invadopodia formation in a Src-dependent manner (Ayala et al., 2008). Phosphorylation of Tks5 by Src leads to recruitment of the adaptor protein Nck and subsequent actin polymerization, indicating a role for Src signaling in invadopodia formation (Stylli et al., 2009). Osteoclasts derived from Src knockout mice form significantly fewer podosomes. Paradoxically, the podosomes that do form in Src-null osteoclasts have much longer half-lives, suggesting that Src can have dual roles in promoting both invadopodia formation and turnover (Destaing et al., 2007).

Regulation of Src activity in the context of invadopodia formation has primarily focused on activation of Src via the EGF receptor pathway. A recent publication describes the observation that the Abl-related kinase Arg is activated by Src downstream of EGFR and that Arg itself phosphorylates cortactin to induce invadopodia formation (Mader et al., 2011). A potential role for localized shedding of EGF at invadopodia is suggested by the observation that ADAM12 clustering correlates with increased EGF shedding at invadopodia (Albrechtsen et al., 2011). Understanding the cellular contexts during metastasis during which Src is activated is clearly a priority in understanding the regulation of invadopodia during metastasis.

There are multiple lines of evidence indicating that protein kinase C (PKC) plays important roles in regulating invadopodia formation and structure. PKCμ localizes to invadopodia with cortactin and paxillin in MDA-MB231 cells (Bowden et al., 1999). Although the function of PKC activity was not described in this paper, a subsequent paper by Li et al. found that phosphorylation of fascin by PKC is required for

localization of fascin to invadopodia (Li et al., 2010). This suggests a role for PKC in regulating actin dynamics and stability in invadopodia. Activation of PKCα with phorbol esters also induces Src activation and invadopodia formation in a mechanism that is dependent on phosphoinositide-3-kinase (PI3K) activity (Walker et al., 2007). Interestingly, PKC activity promotes membrane localization of both MT1-MMP and ADAM12. For both MT1-MMP and ADAM12, this relocalization is dependent on a region in the cytoplasmic tail that sequesters the proteins away from the membrane in the absence of PKC signaling (Sundberg et al., 2004; Urena et al., 1999). This suggests that PKC may play dual roles in regulating invadopodia formation or stability and recruitment of essential proteases to invadopodia.

Although a wide variety of integrins localize to invadopodia and podosomes in different cell lines, the role of integrin signaling in invadosome regulation remains controversial. There are multiple models for invadopodia formation. In one model, focal adhesions are converted to invadopodia via recruitment of Tks5 to nascent focal adhesions (Oikawa et al., 2009). Conversely, other models propose that Tks5 or cortactin phosphorylation by Src or Arg, respectively, promotes de novo actin synthesis at areas of invadopodia with other proteins subsequently being recruited to the invadopodia (Stylli et al., 2009; Mader et al., 2011). It should be noted that these models do not preclude the possibility that focal adhesions induce the Src activation required for invadopodia formation.

Consistent with these multiple models, focal adhesions have been described as both essential for invadopodia formation and as potent inhibitors of invadopodia formation. In Src-transformed cells, FAK promotes Src kinase recruitment to

invadopodia and subsequent invasion (Schlaepfer and Hunter, 1997). Similarly, Pan et al. report that formation of rosettes of invadosomes in Src-transformed fibroblasts, endothelial cells, and cancer cells requires FAK signaling, with FAK localizing to invadosomes (Pan et al., 2011). In addition, increased matrix stiffness, which potentiates focal adhesion mediated signaling, was found to promote invadopodia formation in breast cancer cells (Alexander et al., 2008).

Conversely, Chan et al. report that focal adhesion formation and FAK inhibit invadopodia formation by sequestering Src kinase activity (Chan et al., 2009). It has also been reported that FAK is not necessary for invadopodia formation in colon cancer cells with overexpression of FAK actually suppressing invadopodia formation (Vitale et al., 2008). Bowden et al. report that invadopodia can be discriminated from focal adhesions with immunofluorescence by the observation that invadopodia are negative for FAK (Bowden et al., 2006). These contradictory results regarding the contributions of FAK and focal adhesions to invadopodia formation suggest that multiple pathways may regulate invadopodia formation in a manner that may depend on cell type, ECM substrate, or status of signaling pathways in the cells. The recent observation that MT1-MMP localizes to focal adhesions to promote local invasion and ECM degradation raises many new questions in the field regarding the relative contribution of focal adhesions and invadopodia to local invasion and metastasis (Wang and McNiven, 2012).

CONCLUDING REMARKS

EMT provides a new paradigm in which to understand how cancer cells gain the ability to complete multiple steps of the metastatic process. Although the transcriptional

networks governing EMT and the downstream effectors of EMT essential for metastasis are beginning to be understood, major unanswered questions still remain. Identifying the most important and conserved pathways regulating invasion downstream of these transcription factors is essential in identifying new treatment modalities and biomarkers. In particular, identifying the active processes responsible for driving invasion independent of loss of E-cadherin is necessary to reveal in detail the mechanisms driving metastasis during EMT.

Invadopodia provide an elegant explanation for how cells can direct proteolysis to areas of the cell in contact with the ECM. A picture is beginning to emerge of how the interplay of adhesive, actin-regulatory, and proteolytic proteins unite in the formation of invadopodia. Although much is understood about the components of invadopodia and the basic signaling pathways driving their formation, major unanswered questions remain. In particular, the relevance of invadopodia to *in vivo* metastasis has yet to be resolved for multiple cancer types. Targeted disruption of invadopodia formation in *in vivo* models of cancer invasion and dissemination are required to answer this urgent question.

In light of the advances made in understanding transcriptional regulation of metastasis via the EMT program, it will be interesting to determine how transcriptional networks influence invadopodia formation. Regulation of invadopodia by transcription factors could occur via direct regulation of gene products involved in invadopodia structure, or by indirectly affecting pathways essential for invadopodia formation. Finally, following the observation that focal adhesions are capable of proteolysis of the ECM, more research is necessary to better understand the relative contributions of

invadopodia and focal adhesions to cancer cell invasion, migration, and metastasis. This will likely require not only methods to specifically disrupt only invadopodia or focal adhesion-mediated degradation, but also use of robust *in vitro* and *in vivo* models that mirror the metastatic process in human disease.

ACKNOWLEDGEMENTS

I would like to thank Dr. Jing Yang and Dr. Jeff Tsai for their helpful comments on the structure and content of this portion of the dissertation.

REFERENCES

Abram, C. L., Seals, D. F., Pass, I., Salinsky, D., Maurer, L., Roth, T. M., and Courtneidge, S. A. (2003). The adaptor protein fish associates with members of the ADAMs family and localizes to podosomes of Src-transformed cells. J Biol Chem *278*, 16844–16851.

Aga, M., Bradley, J. M., Keller, K. E., Kelley, M. J., and Acott, T. S. (2008). Specialized podosome- or invadopodia-like structures (PILS) for focal trabecular meshwork extracellular matrix turnover. Invest Ophthalmol Vis Sci *49*, 5353–5365.

Albrechtsen, R., Stautz, D., Sanjay, A., Kveiborg, M., and Wewer, U. M. (2011). Extracellular engagement of ADAM12 induces clusters of invadopodia with localized ectodomain shedding activity. Exp Cell Res *317*, 195–209.

Alexander, N. R., Branch, K. M., Parekh, A., Clark, E. S., Iwueke, I. C., Guelcher, S. A., and Weaver, A. M. (2008). Extracellular matrix rigidity promotes invadopodia activity. Curr Biol *18*, 1295–1299.

Artym, V. V., Zhang, Y., Seillier-Moiseiwitsch, F., Yamada, K. M., and Mueller, S. C. (2006). Dynamic interactions of cortactin and membrane type 1 matrix metalloproteinase at invadopodia: defining the stages of invadopodia formation and function. Cancer Res *66*, 3034–3043.

Ayala, I., Baldassarre, M., Giacchetti, G., Caldieri, G., Tete, S., Luini, A., and Buccione, R. (2008). Multiple regulatory inputs converge on cortactin to control invadopodia biogenesis and extracellular matrix degradation. J Cell Sci *121*, 369–378.

Blouw, B., Seals, D., Pass, I., Diaz, B., and Courtneidge, S. (2008). A role for the podosome/invadopodia scaffold protein Tks5 in tumor growth *in vivo*. Eur J Cell Biol *87*, 555–567.

Boyer, B., and Theiry, J. P. (1993). Epithelium-mesenchyme interconversion as example of epithelial plasticity. APMIS *101*, 257–268.

Badowski, C., Pawlak, G., Grichine, A., Chabadel, A., Oddou, C., Jurdic, P., Pfaff, M., Albiges-Rizo, C., and Block, M. R. (2007). Paxillin phosphorylation controls invadopodia/podosomes spatiotemporal organization. Mol Biol Cell *19*, 633–645.

Baldassarre, M., Pompeo, A., Beznoussenko, G., Castaldi, C., Cortellino, S., McNiven, M. A., Luini, A., and Buccione, R. (2002). Dynamin participates in focal extracellular matrix degradation by invasive cells. Mol Biol Cell *14*, 1074–1084.

Balzer, E. M., Whipple, R. A., Thompson, K., Boggs, A. E., Slovic, J., Cho, E. H., Matrone, M. A., Yoneda, T., Mueller, S. C., and Martin, S. S. (2010). c-Src differentially regulates the functions of microtentacles and invadopodia. Oncogene *29*, 6402–6408.

Bowden, E. T., Barth, M., Thomas, D., Glazer, R. I., and Mueller, S. C. (1999). An invasion-related complex of cortactin, paxillin and PKCμ associates with invadopodia at sites of extracellular matrix degradation. Oncogene *18*, 4440–4449.

Bowden, E. T., Onikoyi, E., Slack, R., Myoui, A., Yoneda, T., Yamada, K. M., and Mueller, S. C. (2006). Co-localization of cortactin and phosphotyrosine identifies active invadopodia in human breast cancer cells. Exp Cell Res *312*, 1240–1253.

Brennen, W. N., Isaacs, J. T., and Denmeade, S. R. (2012). Rationale behind targeting fibroblast activation protein-expressing carcinoma-associated fibroblasts as a novel chemotherapeutic strategy. Mol Cancer Ther *11,* 257–266.

Buschman, M. D., Bromann, P. A., Cejudo-Martin, P., Wen, F., Pass, I., and Courtneidge, S. A. (2009). The novel adaptor protein Tks4 (SH3PXD2B) is required for functional podosome formation. Mol Biol Cell *20*, 1302–1311.

Cai, J.-hua, Zhao, R., Zhu, J.-wei, Jin, X.-long, Wan, F.-jun, Liu, K., Ji, X.-pin, Zhu, Y.-bo, and Zhu, Z.-gang (2010). Expression of cortactin correlates with a poor prognosis in patients with Stages II–III colorectal adenocarcinoma. J Gastrointest Surg *14*, 1248–1257.

Carver, E. A., Jiang, R., Lan, Y., Oram, K. F., and Gridley, T. (2001). The mouse snail gene encodes a key regulator of the epithelial-mesenchymal transition. Mol Cell Biol *21*, 8184–8188.

Castanon, I., Von Stetina, S., Kass, J., and Baylies, M. K. (2001). Dimerization partners determine the activity of the Twist bHLH protein during *Drosophila* mesoderm development. Development *128*, 3145–3159.

Chaffer, C. L., Thompson, E. W., and Williams, E. D. (2007). Mesenchymal to epithelial transition in development and disease. Cells Tissues Organs *185*, 7–19.

Chaffer, C. L., and Weinberg, R. A. (2011). A perspective on cancer cell metastasis. Science *331*, 1559–1564.

Chan, K. T., Cortesio, C. L., and Huttenlocher, A. (2009). FAK alters invadopodia and focal adhesion composition and dynamics to regulate breast cancer invasion. J Cell Biol *185*, 357–370.

Chen, W.-T., Chen, J.-M., Parsons, S. J., and Parsons, J. T. (1985). Local degradation of fibronectin at sites of expression of the transforming gene product pp60src. Nature *316*, 156–158.

Chen, Z. F., and Behringer, R. R. (1995). twist is required in head mesenchyme for cranial neural tube morphogenesis. Genes Dev *9*, 686–699.

Clark, E. S., and Weaver, A. M. (2008). A new role for cortactin in invadopodia: regulation of protease secretion. Eur J Cell Biol *87*, 581–590.

Clark, E. S., Whigham, A. S., Yarbrough, W. G., and Weaver, A. M. (2007). Cortactin is an essential regulator of matrix metalloproteinase secretion and extracellular matrix degradation in invadopodia. Cancer Res *67*, 4227–4235.

Conacci-Sorrell, M., Simcha, I., Ben-Yedidia, T., Blechman, J., Savagner, P., and Ben-Ze'ev, A. (2003). Autoregulation of E-cadherin expression by cadherin-cadherin interactions: the roles of beta-catenin signaling, Slug, and MAPK. J Cell Biol *163*, 847–857.

Connerney, J., Andreeva, V., Leshem, Y., Mercado, M. A., Dowell, K., Yang, X., Lindner, V., Friesel, R. E., and Spicer, D. B. (2008). Twist1 homodimers enhance FGF responsiveness of the cranial sutures and promote suture closure. Dev Biol *318*, 323–334.

David-Pfeuty, T., and Singer, S. J. (1980). Altered distributions of the cytoskeletal proteins vinculin and alpha-actinin in cultured fibroblasts transformed by Rous sarcoma virus. Proc Natl Acad Sci *77*, 6687–6691.

Deryugina, E. I., Ratnikov, B., Monosov, E., Postnova, T. I., DiScipio, R., Smith, J. W., and Strongin, A. Y. (2001). MT1-MMP initiates activation of pro-MMP-2 and integrin

alphavbeta3 promotes maturation of MMP-2 in breast carcinoma cells. Exp Cell Res *263*, 209–223.

DesMarais, V., Yamaguchi, H., Oser, M., Soon, L., Mouneimne, G., Sarmiento, C., Eddy, R., and Condeelis, J. (2009). N-WASP and cortactin are involved in invadopodium-dependent chemotaxis to EGF in breast tumor cells. Cell Motil Cytoskel *66*, 303–316.

Desai, B., Ma, T., and Chellaiah, M. A. (2008). Invadopodia and matrix degradation, a new property of prostate cancer cells during migration and invasion. J Biol Chem *283*, 13856–13866.

Destaing, O., Block, M. R., Planus, E., and Albiges-Rizo, C. (2011). Invadosome regulation by adhesion signaling. Curr Opin Cell Biol *23*, 597–606.

Destaing, O., Planus, E., Bouvard, D., Oddou, C., Badowski, C., Bossy, V., Raducanu, A., Fourcade, B., Albiges-Rizo, C., and Block, M. R. (2010). Beta-1A integrin is a master regulator of invadosome organization and function. Mol Biol Cell *21*, 4108–4119.

Destaing, O., Sanjay, A., Itzstein, C., Horne, W. C., Toomre, D., De Camilli, P., and Baron, R. (2007). The tyrosine kinase activity of c-Src regulates actin dynamics and organization of podosomes in osteoclasts. Mol Biol Cell *19*, 394–404.

Dyczynska, E., Sun, D., Yi, H., Sehara-Fujisawa, A., Blobel, C. P., and Zolkiewska, A. (2007). Proteolytic processing of delta-like 1 by ADAM proteases. J Biol Chem *282*, 436–444.

D'Agostino, J. L. (2005). Dissection of Arp2/3 complex actin nucleation mechanism and distinct roles for Its nucleation-promoting Factors in Saccharomyces cerevisiae. Genetics *171*, 35–47.

Evans, J. G., Correia, I., Krasavina, O., Watson, N., and Matsudaira, P. (2003). Macrophage podosomes assemble at the leading lamella by growth and fragmentation. J Cell Biol *161*, 697–705.

Even-Ram, S., and Artym, V. (2009). Extracellular Matrix Protocols (Totowa, NJ: Humana Press).

Fang, X., Cai, Y., Liu, J., Wang, Z., Wu, Q., Zhang, Z., Yang, C. J., Yuan, L., and Ouyang, G. (2011). Twist2 contributes to breast cancer progression by promoting an epithelial-mesenchymal transition and cancer stem-like cell self-renewal. Oncogene *30*, 4707–4720.

Firulli, B. A., Krawchuk, D., Centonze, V. E., Vargesson, N., Virshup, D. M., Conway, S. J., Cserjesi, P., Laufer, E., and Firulli, A. B. (2005). Altered Twist1 and Hand2 dimerization is associated with Saethre-Chotzen syndrome and limb abnormalities. Nat Genet *37*, 373–381.

Fitchett, J. E., and Hay, E. D. (1989). Medial edge epithelium transforms to mesenchyme after embryonic palatal shelves fuse. Dev Biol *131*, 455–474.

Franco, H. L., Casasnovas, J., Rodriguez-Medina, J. R., and Cadilla, C. L. (2010). Redundant or separate entities?--roles of Twist1 and Twist2 as molecular switches during gene transcription. Nucleic Acids Res *39*, 1177–1186.

Furlong, E. E., Andersen, E. C., Null, B., White, K. P., and Scott, M. P. (2001). Patterns of gene expression during *Drosophila* mesoderm development. Science *293*, 1629–1633.

Furmaniak-Kazmierczak, E., Crawley, S. W., Carter, R. L., Maurice, D. H., and Côté, G. P. (2007). Formation of extracellular matrix-digesting invadopodia by primary aortic smooth muscle cells. Circul Res *100*, 1328–1336.

Gawden-Bone, C., Zhou, Z., King, E., Prescott, A., Watts, C., and Lucocq, J. (2010). Dendritic cell podosomes are protrusive and invade the extracellular matrix using metalloproteinase MMP-14. J Cell Sci *123*, 1427–1437.

Ghersi, G., Dong, H., Goldstein, L. A., Yeh, Y., Hakkinen, L., Larjava, H. S., and Chen, W.-T. (2002). Regulation of fibroblast migration on collagenous matrix by a cell surface peptidase complex. J Biol Chem *277*, 29231–29241.

Goode, B. L., and Eck, M. J. (2007). Mechanism and function of formins in the control of actin assembly. Annu Rev Biochem *76*, 593-627.

Goodison, S., Urquidi, V., and Tarin, D. (1999). CD44 cell adhesion molecules. Mol Pathol *52*, 189–196.

Gort, E. H., van Haaften, G., Verlaan, I., Groot, A. J., Plasterk, R. H. A., Shvarts, A., Suijkerbuijk, K. P. M., van Laar, T., van der Wall, E., Raman, V., et al. (2007). The TWIST1 oncogene is a direct target of hypoxia-inducible factor-2α. Oncogene *27*, 1501–1510.

Gould Rothberg, B. E., and Bracken, M. B. (2006). E-cadherin immunohistochemical cxpression as a prognostic factor in infiltrating ductal carcinoma of the breast: a systematic review and meta-analysis. Breast Cancer Res Treat *100*, 139–148.

Greenburg, G. and Hay, E. D. (1982). Epithelia suspended in collagen gels can lose polarity and express characteristics of migrating mesenchymal cells. J Cell Biol *95*, 333–339.

Gu, S., Boyer, T. G., and Naski, M. C. (2012). Basic helix-loop-helix transcription factor twist1 inhibits the transacivator function of the master chondrogenic regulator Sox9. J Biol Chem, *287*, 328567–328576.

Guilford, P., Hopkins, J., Harraway, J., McLeod, M., McLeod, N., Harawira, P., Taite, H., Scoular, R., Miller, A., and Reeve, A. E. (1998). E-cadherin germline mutations in familial gastric cancer. Nature *392*, 402–405.

Hajra, K. M., Chen, D. Y.S., and Fearon, E. R. (2002). The SLUG Zinc-Finger Protein Represses E-Cadherin in Breast Cancer. Cancer Res *62*, 1613–1618.

Hanahan, D., and Weinberg, R. A. (2011). Hallmarks of cancer: the next generation. Cell *144*, 646–674.

Hanahan, D., and Weinberg, R. A. (2000). The hallmarks of cancer. Cell *100*, 57–70.

Hay, E. D. (1995). An overview of epithelio-mesenchymal transformation. Cells Tissues Organs *154*, 8–20.

Hirooka, S., Akashi, T., Ando, N., Suzuki, Y., Ishida, N., Kurata, M., Takizawa, T., Kayamori, K., Sakamoto, K., and Fujiwara, N. (2011). Localization of the invadopodia-related proteins actinin-1 and cortactin to matrix-contact-side cytoplasm of cancer cells in curgically resected lung adenocarcinomas. Pathobiology *78*, 10–23.

Hofman, P., Butori, C., Havet, K., Hofman, V., Selva, E., Guevara, N., Santini, J., and Van Obberghen-Schilling, E. (2008). Prognostic significance of cortactin levels in head and neck squamous cell carcinoma: comparison with epidermal growth factor receptor status. Br J Cancer *98*, 956–964.

Hong, J., Zhou, J., Fu, J., He, T., Qin, J., Wang, L., Liao, L., and Xu, J. (2011). Phosphorylation of serine 68 of Twist1 by MAPKs stabilizes Twist1 protein and promotes breast cancer cell invasiveness. Cancer Res *71*, 3980–3990.

Hood, J. D., and Cheresh, D. A. (2002). Role of integrins in cell invasion and migration. Nat Rev Cancer *2*, 91–100.

Horiuchi, K., Le Gall, S., Schulte, M., Yamaguchi, T., Reiss, K., Murphy, G., Toyama, Y., Hartmann, D., Saftig, P., and Blobel, C. P. (2006). Substrate selectivity of epidermal growth factor-receptor ligand sheddases and their regulation by phorbol esters and calcium influx. Mol Biol Cell *18*, 176–188.

Horst, D., Reu, S., Kriegl, L., Engel, J., Kirchner, T., and Jung, A. (2009). The intratumoral distribution of nuclear β-catenin is a prognostic marker in colon cancer. Cancer *115*, 2063–2070.

Howe, L. R., Watanabe, O., Leonard, J., and Brown, A. M. C. (2003). Twist is up-regulated in response to Wnt1 and inhibits mouse mammary cell differentiation. Cancer Res *63*, 1906–1913.

Huang, Y., Simms, A. E., Mazur, A., Wang, S., León, N. R., Jones, B., Aziz, N., and Kelly, T. (2011). Fibroblast activation protein-α promotes tumor growth and invasion of breast cancer cells through non-enzymatic functions. Clin Exp Metastasis *28*, 567–579.

Jiang, J., Tang, Y., Zhu, G., Zheng, M., Yang, J., and Liang, X. (2010). Correlation between transcription factor Snail1 expression and prognosis in adenoid cystic carcinoma of salivary gland. Oral Surg Oral Med Oral Pathol Oral Radiol Endod *110*, 764–769.

Kelly, T. (2005). Fibroblast activation protein-α and dipeptidyl peptidase IV (CD26): Cell-surface proteases that activate cell signaling and are potential targets for cancer therapy. Drug Resist Updates *8*, 51–58.

Kanchanawong, P., Shtengel, G., Pasapera, A. M., Ramko, E. B., Davidson, M. W., Hess, H. F., and Waterman, C. M. (2010). Nanoscale architecture of integrin-based cell adhesions. Nature *468*, 580–584.

Kelley, L. C., Ammer, A. G., Hayes, K. E., Martin, K. H., Machida, K., Jia, L., Mayer, B. J., and Weed, S. A. (2010). Oncogenic Src requires a wild-type counterpart to regulate invadopodia maturation. J Cell Sci *123*, 3923–3932.

Kimelman, D. (2006). Mesoderm induction: from caps to chips. Nat Rev Genet *7*, 360–372.

Kress, W., Schropp, C., Lieb, G., Petersen, B., Büsse-Ratzka, M., Kunz, J., Reinhart, E., Schäfer, W.-D., Sold, J., Hoppe, F., et al. (2005). Saethre–Chotzen syndrome caused by TWIST 1 gene mutations: functional differentiation from Muenke coronal synostosis syndrome. Eur J Hum Genet *14*, 39–48.

Kronenberg, H. M. (2004). Twist genes regulate Runx2 and bone formation. Dev Cell *6*, 317–318.

Kveiborg, M., Albrechtsen, R., Couchman, J. R., and Wewer, U. M. (2008). Cellular roles of ADAM12 in health and disease. Int J Biochem Cell Biol *40,* 1685–1702.

Lander, R., Nordin, K., and LaBonne, C. (2011). The F-box protein Ppa is a common regulator of core EMT factors Twist, Snail, Slug, and Sip1. J Cell Biol *194*, 17–25.

Laursen, K. B., Mielke, E., Iannaccone, P., and Füchtbauer, E.-M. (2007). Mechanism of transcriptional activation by the proto-oncogene Twist1. J Biol Chem *282*, 34623–34633.

Lee, H.O., Mullins, S. R., Franco-Barraza, J., Valianou, M., Cukierman, E., and Cheng, J. D. (2011). FAP-overexpressing fibroblasts produce an extracellular matrix that enhances invasive velocity and directionality of pancreatic cancer cells. BMC Cancer *11*, 245.

Lee, J. M., Dedhar, S., Kalluri, R., and Thompson, E. W. (2006). The epithelial-mesenchymal transition: new insights in signaling, development, and disease. J Cell Biol *172*, 973–981.

Li, A., Dawson, J. C., Forero-Vargas, M., Spence, H. J., Yu, X., König, I., Anderson, K., and Machesky, L. M. (2010). The actin-bundling protein fascin stabilizes actin in invadopodia and potentiates protrusive invasion. Curr Biol *20*, 339–345.

Li, C.W., Xia, W., Huo, L., Lim, S.O., Wu, Y., Hsu, J. L., Chao, C.-H., Yamaguchi, H., Yang, N.-K., Ding, Q., et al. (2012). Epithelial-mesenchyme transition induced by TNF-a requires NF-kB mediated transcriptional upregulation of Twist1. Cancer Res *72*, 1290–1300.

Li, Y., Tondravi, M., Liu, J., Smith, E., Haudenschild, C. C., Kaczmarek, M., and Zhan, X. (2001). Cortactin potentiates bone metastasis of breast cancer cells. Cancer Res *61*, 6906–6911.

Liu, J., Yue, P., Artym, V. V., Mueller, S. C., and Guo, W. (2009). The role of the exocyst in matrix metalloproteinase secretion and actin dynamics during tumor cell invadopodia formation. Mol Biol Cell *20*, 3763–3771.

Lizárraga, F., Poincloux, R., Romao, M., Montagnac, G., Le Dez, G., Bonne, I., Rigaill, G., Raposo, G., and Chavrier, P. (2009). Diaphanous-related formins are required for invadopodia formation and invasion of breast tumor cells. Cancer Res *69*, 2792–2800.

Mader, C. C., Oser, M., Magalhaes, M. A. O., Bravo-Cordero, J., Condeelis, J. S., Koleske, A. J., and Gil-Henn, H. (2011). An EGFR-Src-Arg-cortactin pathway mediates functional maturation of invadopodia and breast cancer cell invasion. Cancer Res *71*, 1730–1741.

Mattila, P. K., and Lappalainen, P. (2008). Filopodia: molecular architecture and cellular functions. Nat Rev Mol Cell Biol *9*, 446–454.

Mayer, B. (2001). SH3 domains: complexity in moderation. J Cell Sci *114*, 1253–1263.

Medici, D., Hay, E. D., and Olsen, B. R. (2008). Snail and Slug promote epithelial-mesenchymal transition through beta-catenin-T-cell factor-4-dependent expression of transforming growth factor-beta3. Mol Biol Cell *19*, 4875–4887.

Mersich, A. T., Miller, M. R., Chkourko, H., and Blystone, S. D. (2010). The formin FRL1 (FMNL1) is an essential component of macrophage podosomes. Cytoskel *67*, 573–585.

Mitra, S. K., and Schlaepfer, D. D. (2006). Integrin-regulated FAK-Src signaling in normal and cancer cells. Curr Opin Cell Biol *18*, 516–523.

Morabito, C. J., Dettman, R. W., Kattan, J., Collier, J. M., and Bristow, J. (2001). Positive and negative regulation of epicardial-mesenchymal transformation during avian heart development. Dev Biol *234*, 204–215.

Moreau, V., Tatin, F., Varon, C., and Genot, E. (2003). Actin can reorganize into podosomes in aortic endothelial cells, a process controlled by Cdc42 and RhoA. Mol Cell Biol *23*, 6809–6822.

Mueller, S. C., Ghersi, G., Akiyama, S. K., Sang, Q. X., Howard, L., Pineiro-Sanchez, M., Nakahara, H., Yeh, Y., and Chen, W. T. (1999). A novel protease-docking function of integrin at invadopodia. J Biol Chem *274*, 24947–24952.

Mueller, S., and Chen, W. (1991). Cellular invasion into matrix beads: localization of beta 1 integrins and fibronectin to the invadopodia. J Cell Sci. *99*, 213–225.

Murphy, D. A., and Courtneidge, S. A. (2011). The “ins” and “outs” of podosomes and invadopodia: characteristics, formation and function. Nat Rev Mol Cell Biol *12*, 413–426.

Nascimento, C. F., Gama-De-Souza, L. N., Freitas, V. M., and Jaeger, R. G. (2009). Role of MMP9 on invadopodia formation in cells from adenoid cystic carcinoma. Study by laser scanning confocal microscopy. Microsc Res Tech *73*, 99-108.

Neel, N. F., Rossman, K. L., Martin, T. D., Hayes, T. K., Yeh, J. J., and Der, C. J. (2012). The RalB small GTPase mediates invadopodia formation through a GTPase activating protein-independent function of the RalBP1/RLIP76 effector. Mol Cell Biol *32*, 1374-1386.

Nolen, B. J., Tomasevic, N., Russell, A., Pierce, D. W., Jia, Z., McCormick, C. D., Hartman, J., Sakowicz, R., and Pollard, T. D. (2009). Characterization of two classes of small molecule inhibitors of Arp2/3 complex. Nature *460*, 1031–1034.

Oikawa, T., and Takenawa, T. (2009). PtdIns(3,4)P2 instigates focal adhesions to generate podosomes. Cell Adh Migr *3*, 195–197.

Onder, T. T., Gupta, P. B., Mani, S. A., Yang, J., Lander, E. S., and Weinberg, R. A. (2008). Loss of E-cadherin promotes metastasis via multiple downstream transcriptional pathways. Cancer Res *68*, 3645–3654.

Orsulic, S., Huber, O., Aberle, H., Arnold, S., and Kemler, R. (1999). E-cadherin binding prevents beta-catenin nuclear localization and beta-catenin/LEF-1-mediated transactivation. J Cell Sci *112*, 1237–1245.

Oser, M., and Condeelis, J. (2009). The cofilin activity cycle in lamellipodia and invadopodia. J Cell Biochem *108*, 1252–1262.

O'Brien, P., and O'Connor, B. F. (2008). Seprase: an overview of an important matrix serine protease. Biochim Biophys Acta *1784*, 1130–1145.

Pan, Y.-R., Chen, C.-L., and Chen, H.C. (2011). FAK is required for the assembly of podosome rosettes. J Cell Biol *195*, 113–129.

Papkoff, J., and Aikawa, M. (1998). WNT-1 and HGF regulate GSK3β activity and β-catenin signaling in mammary epithelial cells. Biochem Biophys Res Commun *247*, 851–858.

Peinado, H., Ballestar, E., Esteller, M., and Cano, A. (2003). Snail mediates E-Cadherin repression by the recruitment of the Sin3A/Histone Deacetylase 1 (HDAC1)/HDAC2 complex. Mol Cell Biol *24*, 306–319.

Pfaff, M., and Jurdic, P. (2001). Podosomes in osteoclast-like cells: structural analysis and cooperative roles of paxillin, proline-rich tyrosine kinase 2 (Pyk2) and integrin {alpha}V{beta}3. J Cell Sci *114*, 2775–2786.

Pham, C. G., Bubici, C., Zazzeroni, F., Knabb, J. R., Papa, S., Kuntzen, C., and Franzoso, G. (2007). Upregulation of Twist-1 by NF- B blocks cytotoxicity induced by chemotherapeutic drugs. Mol Cell Biol *27*, 3920–3935.

Poincloux, R., Lizárraga, F., and Chavrier, P. (2009). Matrix invasion by tumour cells: a focus on MT1-MMP trafficking to invadopodia. J Cell Sci *122*, 3015–3024.

Quintavalle, M., Elia, L., Condorelli, G., and Courtneidge, S. A. (2010). MicroRNA control of podosome formation in vascular smooth muscle cells *in vivo* and *in vitro*. J Cell Biol *189*, 13–22.

Seals, D., Azucenajr, E., Pass, I., Tesfay, L., Gordon, R. Woodrow, M., Resau, J., and Courtneidge, S. (2005). The adaptor protein Tks5/Fish is required for podosome formation and function, and for the protease-driven invasion of cancer cells. Cancer Cell *7*, 155–165.

Sabeh, F., Ota, I., Holmbeck, K., Birkedal-Hansen, H., Soloway, P., Balbin, M., Lopez-Otin, C., Shapiro, S., Inada, M., Krane, S., et al. (2004). Tumor cell traffic through the extracellular matrix is controlled by the membrane-anchored collagenase MT1-MMP. J Cell Biol *167*, 769–781.

Samanna, V., Ma, T., Mak, T. W., Rogers, M., and Chellaiah, M. A. (2007). Actin polymerization modulates CD44 surface expression, MMP-9 activation, and osteoclast function. J Cell Physiol *213*, 710–720.

Schedin, P., and Elias, A. (2004). Multistep tumorigenesis and the microenvironment. Breast Cancer Res *6,* 93–101.

Schlaepfer, D. D., and Hunter, T. (1997). Focal adhesion kinase overexpression enhances ras-dependent integrin signaling to ERK2/mitogen-activated protein kinase through interactions with and activation of c-Src. J Biol Chem *272*, 13189–13195.

Schoumacher, M., Goldman, R. D., Louvard, D., and Vignjevic, D. M. (2010). Actin, microtubules, and vimentin intermediate filaments cooperate for elongation of invadopodia. J Cell Biol *189*, 541–556.

Shioiri, M., Shida, T., Koda, K., Oda, K., Seike, K., Nishimura, M., Takano, S., and Miyazaki, M. (2006). Slug expression is an independent prognostic parameter for poor survival in colorectal carcinoma patients. Br J Cancer *94*, 1816–1822.

Small, J. V., Stradal, T., Vignal, E., and Rottner, K. (2002). The lamellipodium: where motility begins. Trends Cell Biol *12*, 112–120.

Soo, K., O'Rourke, M. P., Khoo, P. L., Steiner, K. A., Wong, N., Behringer, R. R., and Tam, P. P. L. (2002). Twist function is required for the morphogenesis of the cephalic neural tube and the differentiation of the cranial neural crest cells in the mouse embryo. Dev Biol *247*, 251–270.

Steffen, A., Le Dez, G., Poincloux, R., Recchi, C., Nassoy, P., Rottner, K., Galli, T., and Chavrier, P. (2008). MT1-MMP-dependent invasion is regulated by TI-VAMP/VAMP7. Curr Biol *18*, 926–931.

Sternberg, J., and Kimber, S. J. (1986). The relationship between emerging neural crest cells and basement membranes in the trunk of the mouse embryo: a TEM and immunocytochemical study. J Embryol Exp Morphol *98*, 251–268.

Stylli, S. S., Stacey, T. T. I., Verhagen, A. M., Xu, S. S., Pass, I., Courtneidge, S. A., and Lock, P. (2009). Nck adaptor proteins link Tks5 to invadopodia actin regulation and ECM degradation. J Cell Sci *122*, 2727–2740.

Sundberg, C., Thodeti, C. K., Kveiborg, M., Larsson, C., Parker, P., Albrechtsen, R., and Wewer, U. M. (2004). Regulation of ADAM12 cell-surface expression by protein kinase C epsilon. J Biol Chem *279*, 51601–51611.

Sánchez-Tilló, E., Lázaro, A., Torrent, R., Cuatrecasas, M., Vaquero, E. C., Castells, A., Engel, P., and Postigo, A. (2010). ZEB1 represses E-cadherin and induces an EMT by recruiting the SWI/SNF chromatin-remodeling protein BRG1. Oncogene *29*, 3490–3500.

Takkunen, M., Hukkanen, M., Liljeström, M., Grenman, R., and Virtanen, I. (2010). Podosome-like structures of non-invasive carcinoma cells are replaced in epithelial-mesenchymal transition by actin comet-embedded invadopodia. J Cell Mol Med *14*, 1569–1593.

Tarone, G., Cirillo, D., Giancotti, F. G., Comoglio, P. M., and Marchisio, P. C. (1985). Rous sarcoma virus-transformed fibroblasts adhere primarily at discrete protrusions of the ventral membrane called podosomes. Exp Cell Res *159*, 141–157.

Thiery, J. P. (2002). Epithelial-mesenchymal transitions in tumour progression. Nat Rev Cancer *2*, 442–454.

Tolde, O., Rösel, D., Veselý, P., Folk, P., and Brábek, J. (2010). The structure of invadopodia in a complex 3D environment. Eur J Cell Biol *89*, 674–680.

Tucker, G. C., Duband, J. L., Dufour, S., and Thiery, J. P. (1988). Cell-adhesion and substrate-adhesion molecules: their instructive roles in neural crest cell migration. Development *103*, 81–94.

Uchikado, Y., Natsugoe, S., Okumura, H., Setoyama, T., Matsumoto, M., Ishigami, S., and Aikou, T. (2005). Slug expression in the E-cadherin preserved tumors is related to prognosis in patients with esophageal squamous cell carcinoma. Clin Cancer Res *11*, 1174–1180.

Urena, J., Merlos-Suarez, A., Baselga, J., and Arribas, J. (1999). The cytoplasmic carboxy-terminal amino acid determines the subcellular localization of proTGF-(alpha) and membrane type matrix metalloprotease (MT1-MMP). J Cell Sci *112*, 773–784.

Vitale, S., Avizienyte, E., Brunton, V., and Frame, M. (2008). Focal adhesion kinase is not required for Src-induced formation of invadopodia in KM12C colon cancer cells and can interfere with their assembly. Eur J Cell Biol *87*, 569–579.

Vandewalle, C., Comijn, J., De Craene, B., Vermassen, P., Bruyneel, E., Andersen, H., Tulchinsky, E., Van Roy, F., and Berx, G. (2005). SIP1/ZEB2 induces EMT by repressing genes of different epithelial cell-cell junctions. Nucleic Acids Res *33*, 6566–6578.

Vichalkovski, A., Gresko, E., Hess, D., Restuccia, D. F., and Hemmings, B. A. (2010). PKB/AKT phosphorylation of the transcription factor Twist-1 at Ser42 inhibits p53 activity in response to DNA damage. Oncogene *29*, 3554–3565.

Viebahn, C. (1995). Epithelio-mesenchymal transformation during formation of the mesoderm in the mammalian embryo. Cells Tissues Organs *154*, 79–97.

Virnig, B. A., Tuttle, T. M., Shamliyan, T., and Kane, R. L. (2010). Ductal carcinoma in situ of the breast: a systematic review of incidence, treatment, and outcomes. J Natl Cancer Inst *102*, 170–178.

Vishnubhotla, R., Sun, S., Huq, J., Bulic, M., Ramesh, A., Guzman, G., Cho, M., and Glover, S. C. (2007). ROCK-II mediates colon cancer invasion via regulation of MMP-2 and MMP-13 at the site of invadopodia as revealed by multiphoton imaging. Lab Investigation *87*, 1149–1158.

Walker, V. G., Ammer, A., Cao, Z., Clump, A. C., Jiang, B. H., Kelley, L. C., Weed, S. A., Zot, H., and Flynn, D. C. (2007). PI3K activation is required for PMA-directed activation of cSrc by AFAP-110. Am J Physiol Cell Physiol *293*, C119–C132.

Wang, Y., and McNiven, M. A. (2012). Invasive matrix degradation at focal adhesions occurs via protease recruitment by a FAK-p130Cas complex. J Cell Biol *196*, 375–385.

Weed, S.A., Karginov, A.V., Schafer, D.A., Weaver, A.M., Kinley, A.W., Cooper, J.A., Parsons, J.T. (2000). Cortactin localization to sites of actin assembly in lamellipodia requires interactions with F-Actin and the Arp2/3 complex. J Cell Biol *151*, 29.

Yamaguchi, H., Lorenz, M., Kempiak, S., Sarmiento, C., Coniglio, S., Symons, M., Segall, J., Eddy, R., Miki, H., Takenawa, T., et al. (2005). Molecular mechanisms of invadopodium formation: the role of the N-WASP-Arp2/3 complex pathway and cofilin. J Cell Biol *168*, 441–452.

Yang, J., Mani, S. A., Donaher, J. L., Ramaswamy, S., Itzykson, R. A., Come, C., Savagner, P., Gitelman, I., Richardson, A., and Weinberg, R. A. (2004). Twist, a master regulator of morphogenesis, plays an essential role in tumor metastasis. Cell *117*, 927–939.

Yang, J., and Weinberg, R. A. (2008). Epithelial-mesenchymal transition: at the crossroads of development and tumor metastasis. Dev Cell *14*, 818–829.

Yang, M. H., Wu, M.-Z., Chiou, S.-H., Chen, P. M., Chang, S. Y., Liu, C. J., Teng, S. C., and Wu, K. J. (2008). Direct regulation of TWIST by HIF-1alpha promotes metastasis. Nat Cell Biol *10*, 295–305.

Yap, A. S., Brieher, W. M., and Gumbiner, B. M. (1997). Molecular and functional analysis of cadherin-based adherens junctions. Ann Rev Cell Dev Biol *13*, 119–146.

Yu, Q., and Stamenkovic, I. (1999). Localization of matrix metalloproteinase 9 to the cell surface provides a mechanism for CD44-mediated tumor invasion. Genes Dev *13*, 35–48.

Yu, X., and Machesky, L. M. (2012). Cells assemble invadopodia-like structures and invade into matrigel in a matrix metalloprotease dependent manner in the circular invasion assay. PloS One *7*, e30605.

Chapter II

PDGFRα is Essential for Twist1-Induced Invadopodia Formation and Metastasis

ABSTRACT

The Twist1 transcription factor is known to promote tumor metastasis and induce the epithelial-mesenchymal transition (EMT). Here, we report that Twist1 is both necessary and sufficient for the formation of invadopodia in multiple cells lines. Invadopodia are specialized membrane protrusions on the basal surface of cells that regulate localized degradation of the extracellular matrix. Twist1 induces PDGFRα expression, which in turn activates Src, to promote invadopodia formation. Src signaling is essential for invadopodia formation. We show that Twist1 and PDGFRα are central mediators of invadopodia formation in response to various EMT-inducing signals, including the transcription factor Snail and TGFB. Induction of PDGFRα and invadopodia is essential for Twist1 to promote tumor metastasis in a mouse model of breast cancer metastasis. Consistent with the observation that PDGFRα is a direct transcriptional target of Twist1, coexpression of Twist1 and PDGFRα predicts poor survival in human breast cancer patients. Therefore, invadopodia-mediated matrix degradation is a key and specific function of Twist1 in promoting tumor metastasis during the EMT process.

INTRODUCTION

During metastasis, carcinoma cells acquire the ability to invade surrounding tissues and intravasate through the endothelium to enter systemic circulation. Both the invasion and intravasation processes require degradation of basement membrane and extracellular matrix (ECM). Although proteolytic activity is associated with increased metastasis and poor clinical outcome, the molecular triggers for matrix degradation in tumor cells are largely unknown.

Invadopodia are specialized actin-based membrane protrusions found in cancer cells that degrade ECM via localization of proteases (Tarone et al., 1985; Chen, 1989). Their ability to mediate focal ECM degradation suggests a critical role for invadopodia in tumor invasion and metastasis. However, a definitive role for invadopodia in local invasion and metastasis *in vivo* has not yet been clearly demonstrated. As actin-based structures, invadopodia contain a primarily branched filamentous actin (F-actin) core and actin regulatory proteins, such as cortactin, Wiscott-Aldrich Syndrome protein (WASp), and the actin-related protein 2/3 complex (Arp2/3 complex) (Linder, 2007). The SH3-domain-rich proteins tyrosine kinase substrate 4 (Tks4) (Buschman et al., 2009) and Tks5 (Seals et al., 2005) function as essential adaptor proteins in clustering structural and enzymatic components of invadopodia. The matrix degradation activity of invadopodia has been associated with a large number of proteases, including membrane type 1 metalloproteases (MT1-MMP) (Linder 2007). Invadopodia formation requires tyrosine phosphorylation of several invadopodia components including cortactin (Ayala et al., 2008), Tks4 (Buschmann et al., 2009), and Tks5 (Seals et al., 2005) by Src family kinases.

Our previous study found that the Twist1 transcription factor, a key regulator of early embryonic morphogenesis, was essential for the ability of tumor cells to metastasize from the mammary gland to the lung in a mouse breast tumor model and was highly expressed in invasive human lobular breast cancer (Yang et al., 2004). Since then, studies have also associated Twist1 expression with many aggressive human cancers, such as melanomas, neuroblastomas, prostate cancers, and gastric cancers (Peinado et al., 2007). Twist1 can activate a latent developmental program termed the epithelial-mesenchymal transition (EMT), thus enabling carcinoma cells to dissociate from each other and migrate.

The EMT program is a highly conserved developmental program that promotes epithelial cell dissociation and migration to different sites during embryogenesis. During EMT, cells lose their epithelial characteristics, including cell adhesion and polarity, and acquire a mesenchymal morphology and the ability to migrate (Hay, 1995). Biochemically, cells downregulate epithelial markers such as adherens junction proteins epithelial cadherin (E-cadherin) and catenins and express mesenchymal markers including vimentin and fibronectin (Boyer and Thiery, 1993). In addition to Twist1, the zinc-finger transcription factors, including Snail, Slug, zinc finger E-box binding 1 (ZEB1), and ZEB2 (Peinado et al., 2007), can also activate the EMT program by directly binding the E-boxes of the E-cadherin promoter to suppress its transcription. However, it is unclear how Twist1, as a basic helix-loop-helix (bHLH) transcription factor, controls the EMT program. In this study, we test the hypothesis that Twist1 plays a major role in regulating ECM degradation to promote tumor metastasis.

RESULTS

Twist1 is necessary and sufficient for invadopodia formation. Our previous studies found that Twist1 expression was associated with increased metastatic potentials in a series of mouse mammary tumor cell lines, including 67NR, 168FARN, and 4T1 (Yang et al., 2004). Furthermore, Twist1 is required for the ability of 4T1 cells to metastasize from the mammary gland to the lung. To dissect the cellular functions of Twist1 in promoting tumor metastasis, we first tested whether expression of Twist1 was associated with increased ability to degrade ECM. 67NR, 168FARN, and 4T1 cells were plated onto fluorescein isothiocyanate (FITC)-conjugated gelatin matrix to assess their abilities to degrade matrix. We found that Twist1-expressing metastatic 168FARN and 4T1 cells potently degraded ECM in eight hours, while non-metastatic 67NR cells that do not express Twist1 failed to do so (Figure 2.1A–C). To test whether Twist1 is required for the ability of 168FARN and 4T1 cells to degrade ECM, 168FARN and 4T1 cells expressing two independent shRNAs against Twist1 were processed for the matrix degradation assay (Figure 2.1 A-B). Indeed, we found that suppressing Twist1 expression resulted in a potent reduction in matrix degradation in both cell types (Figure 2.1 B–C). Together, these results demonstrate that Twist1 is required for ECM degradation ability in tumor cells.

Localized matrix degradation can be mediated through actin-based subcellular protrusions called invadopodia. Colocalization of F-actin with the actin-bundling protein cortactin (Bowden et al., 2006) or the unique adaptor protein Tks5 (Abram et al., 2003) can be used to identify invadopodia. To determine whether invadopodia are present in 168FARN and 4T1 cells and whether Twist1 is required for invadopodia

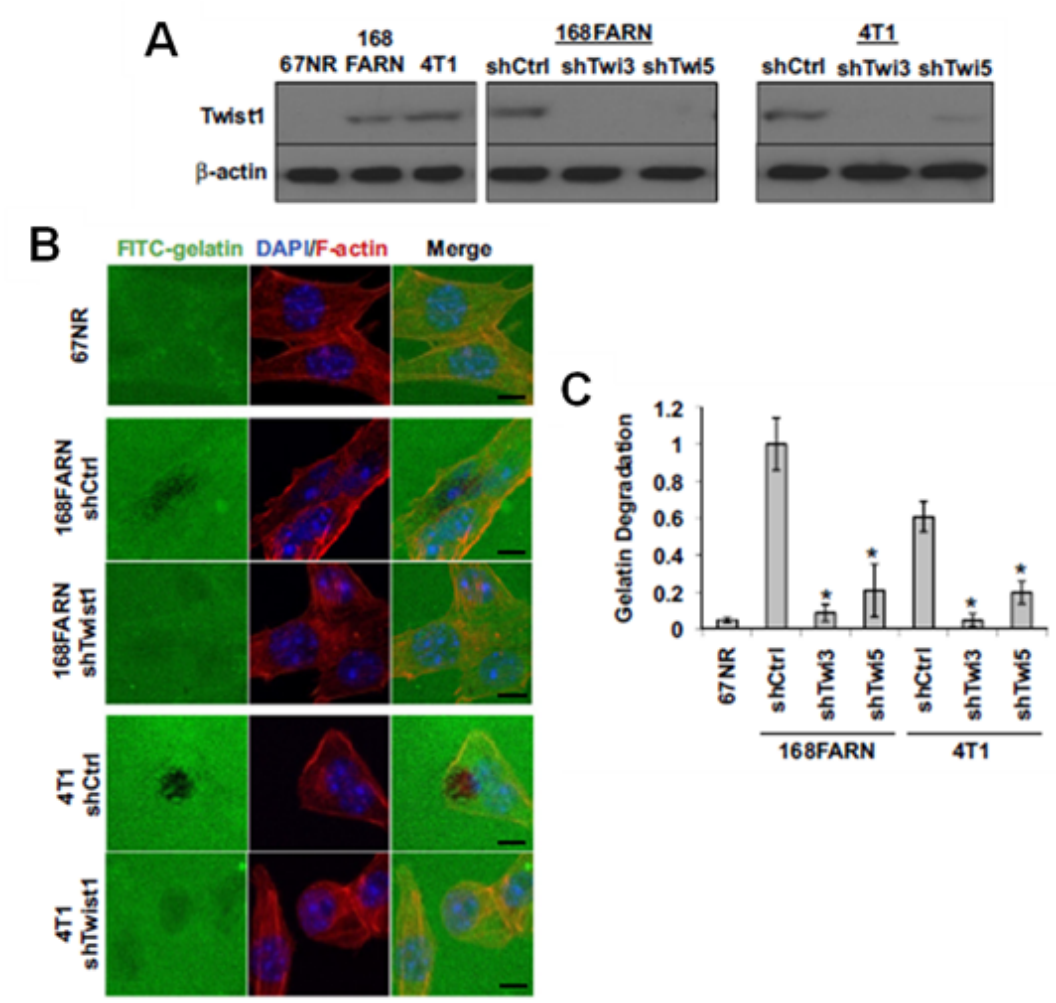

Figure 2.1: Twist1 is necessary for gelatin degradation. (A) Indicated cell lysates were analyzed by SDS-PAGE and probed for Twist1 and β-actin (B) 67NR, 168FARN (expressing control or Twist1 knockdown shRNA), and 4T1 (expressing control or Twist1 knockdown shRNA) cells were plated on FITC-conjugated gelatin (green) for 8 hours. F-actin was stained with phallodin (red) and nuclei with DAPI (blue). Areas of gelatin degradation appear as punctuate black areas beneath the cells. (C) Quantification of FITC-gelatin degradation. Error bars are standard error of mean (SEM). N=3 replicates, n=150 cells/sample. *$p<0.02$. Scale bars are 1 μm for insets, 5 μm for full images.

formation, we examined the presence of invadopodia in 168FARN and 4T1 cells by immunofluorescence. Invadopodia are transient structures, so only a fraction of cells possess invadopodia at any given time. Indeed, over 50% 168FARN and 4T1 cells contain invadopodia, while suppression of Twist1 expression reduced the occurrence of invadopodia to 5–20% in both cell lines (Figure 2.2 A–C). These data indicate that Twist1 is necessary for the formation of invadopodia for ECM degradation.

Since 168FARN and 4T1 mouse tumor cells contain additional genetic and epigenetic changes essential for their tumorigenic and metastatic abilities (Mani et al., 2007), we next tested whether Twist1 is sufficient to promote invadopodia formation and matrix degradation in HMLE cells, immortalized normal human mammary epithelial cells. As reported, expression of Twist1 induced EMT in HMLE cells (Yang et al., 2004). We examined the presence of invadopodia and found that over 60% of HMLE cells expressing Twist1 contained invadopodia, compared to 10% of HMLE control cells with invadopodia (Figure 2.3 A-C). Importantly, these invadopodia were all localized to the basal surface of the cell directly adjacent to the underlying matrix when examined with Z-sectioning (Figure 2.3 D). To determine whether these Twist1-induced invadopodia are functional, we compared the ability of these two cell lines to degrade matrix using the FITC-gelatin degradation assay. Expression of Twist1 increased matrix degradation by approximately 10 fold (Figure 2.3 E-F). Strikingly, focal matrix degradation precisely colocalized with F-actin positive puncta (Figure 2.3 E), indicating that Twist1 is sufficient to promote the formation of functional invadopodia in HMLE cells. Furthermore, Twist1-induced matrix degradation is

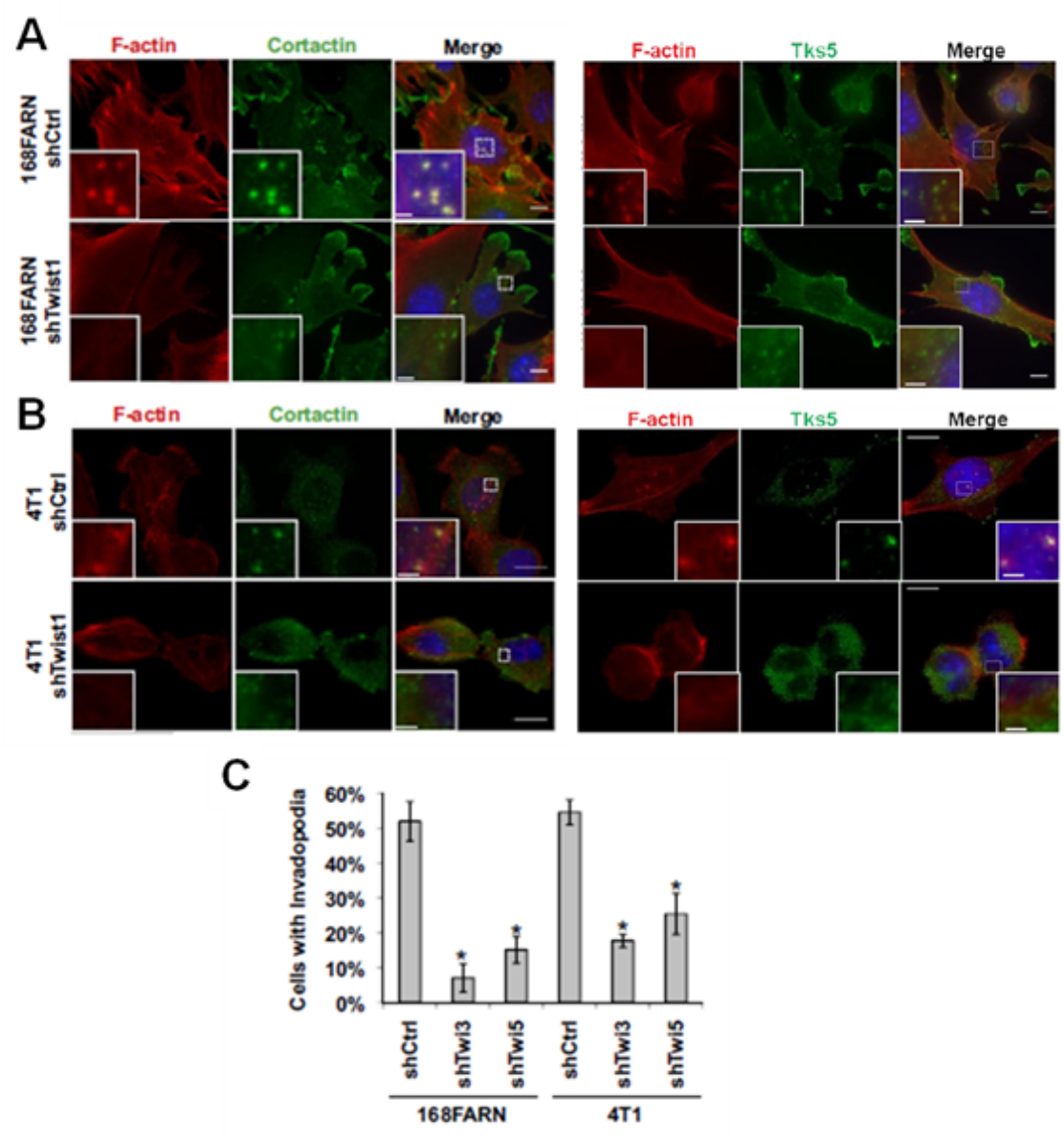

Figure 2.2: Twist1 is necessary for invadopodia formation. (A) 168FARN and (B) 4T1 cells expressing control or Twist1 shRNAs were stained with phalloidin (red), DAPI (blue), and cortactin (green) or Tks5 (green). (C) Quantification of percentage of cells with invadopodia. Error bars are SEM. N=3 replicates, n=150 cells/sample. *p<0.02. Scale bars are 1 μm for insets, 5 μm for full images.

protease-driven since suppression of metalloproteases by GM6001 inhibited the ability of HMLE-Twist1 cells to degrade FITC-gelatin (Figure 2.3 F). Together, these data demonstrate that Twist1 is both necessary and sufficient to promote invadopodia formation and focal matrix degradation.

Twist1-induced degradation is invadopodia and Src-dependent. Since both invadopodia-associated proteases and secreted proteases can mediate matrix degradation, we next set out to determine whether invadopodia, not secreted proteases, are solely responsible for Twist1-induced matrix degradation. In HMLE-Twist1 cells, we expressed shRNAs against Tks5, an adaptor protein that is required for invadopodia formation, but not MMP secretion (Seals et al., 2004). Both shRNAs effectively suppressed Tks5 expression (Figure 2.4 A), and gelatin zymography showed that knockdown of Tks5 did not affect the secretion of proteases, mainly MMP2, into conditioned media (Figure 2.4 G). In contrast, suppression of Tks5 significantly reduced their abilities to form invadopodia (Figure 2.4 B-C) and degrade FITC-gelatin matrix (Figure 2.4 D). Complementary to these data, Boyden chamber migration and invasion assays showed that suppression of Tks5 inhibited the ability of HMLE-Twist1 cells to invade through Matrigel, but did not affect cell migration (Figure 2.4 E-F). Together, these results demonstrate that the protease activity associated with invadopodia is the sole mediator of Twist1-induced matrix degradation.

We next set out to understand how Twist1 promotes invadopodia formation. While no transcription factor has been implicated in invadopodia regulation, tyrosine phosphorylation of invadopodia components, including cortactin and Tks5, is necessary

Figure 2.3: Twist1 is sufficient to promote invadopodia formation. (A) HMLE cells expressing a control vector or Twist1 were plated on 0.2% gelatin matrix for 72 hours and invadopodia were visualized by colocalization of cortactin (green) and F-actin (red). (B) Quantification of cells with invadopodia. (C) HMLE cells expressing a control vector or Twist1 were plated on 0.2% gelatin matrix for 72 hours and invadopodia were visualized by colocalization of Tks5 (green) and F-actin (red). (D) Colocalization of F-actin (red) and cortactin (green) is restricted to the basal side of cells in direct contact with the underlying matrix. (E) HMLE control or HMLE-Twist1 cells were plated on FITC-gelatin for 8 hours and stained for F-actin (red) and nuclei (blue). (F) Quantification of degradation by HMLE-ctrl and HMLE-Twist1 cells and HMLE-Twist1 cells treated with 25 μM GM6001 Negative Control (GMNC) or 25 μM GM6001 for eight hours. Error bars are SEM. N=150 cells/sample. *$p<0.02$. Scale bars are 1 μm for insets, 5 μm for full images.

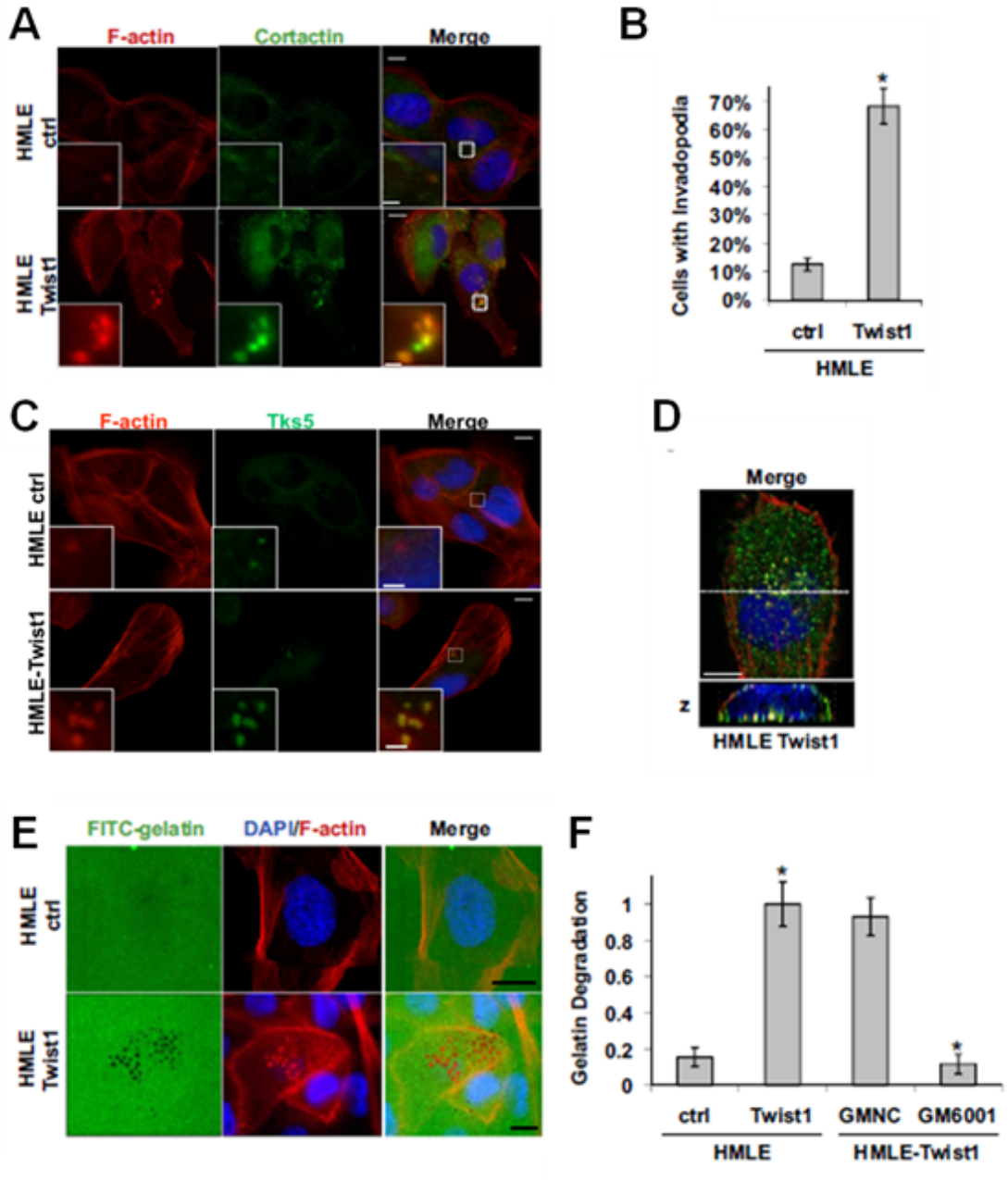
A
F-actin
Cortactin
Merge
HMLE ctrl
HMLE Twist1
B
Cells with Invadopodia
70%
60%
50%
40%
30%
20%
10%
0%
ctrl
Twist1
HMLE
C
F-actin
Tks5
Merge
HMLE ctrl
HMLE-Twist1
D
Merge
z
HMLE Twist1
E
FITC-gelatin
DAPI/F-actin
Merge
HMLE ctrl
HMLE Twist1
F
Gelatin Degradation
1
0.8
0.6
0.4
0.2
0
ctrl
Twist1
GMNC
GM6001
HMLE
HMLE-Twist1

Figure 2.4: Twist1-mediated matrix degradation is invadopodia-driven and Src-dependent. (A) Cell lysates from HMLE-Twist1 cells expressing control or Tks5 shRNA were analyzed by SDS-PAGE and probed for Tks5 and β-actin. Both shRNAs against Tks5 were effective at knocking down Tks5 at the protein level. (B) HMLE-Twist1 cells expressing a control or Tks5 shRNA were plated on 0.2% gelatin and stained for Tks5 (green) or phosphotyrosine (green) and F-actin (red). (C) Quantification of cells with invadopodia. N=150 cells/sample (D) Quantification of FITC-gelatin degradation. N=150 cells/sample (E) 40,000 HMLE-Twist1 cells expressing control or Tks5 shRNAs were plated on Transwell inserts. Cells that migrate through the insert were stained with crystal violet and number of cells quantified by releasing dye with 10% acetic acid and measuring absorbency at 520 nm. No significant differences in migration were observed. (F) 40,000 HMLE-Twist1 cells expressing control or Tks5 shRNAs were plated on Transwell inserts coated with a thin layer of Matrigel to assay invasion. Invasion was quantified identically to migration. Knockdown of Tks5 caused a significant reduction in invasion by HMLE-Twist1 cells. (G) Conditioned media from HMLE-Twist1 cells expressing control or Tks5 shRNA were analyzed with gelatin zymography. No differences in protease activity can be observed between control and shTks5 knockdown cells. Bands correlating to expression of pro-MMP2 and cleaved, active MMP2 are indicated on gel. (H) HMLE-Twist1 cells were plated on 0.2% gelatin and treated with treated with DMSO or 5μM SU6656 for 12 hours and stained for phosphotyrosine (green) and F-actin (red). Error bars are SEM. N=150 cells/sample. *$p<0.02$. Scale bars are 1 μm for insets, 5 μm for full images.

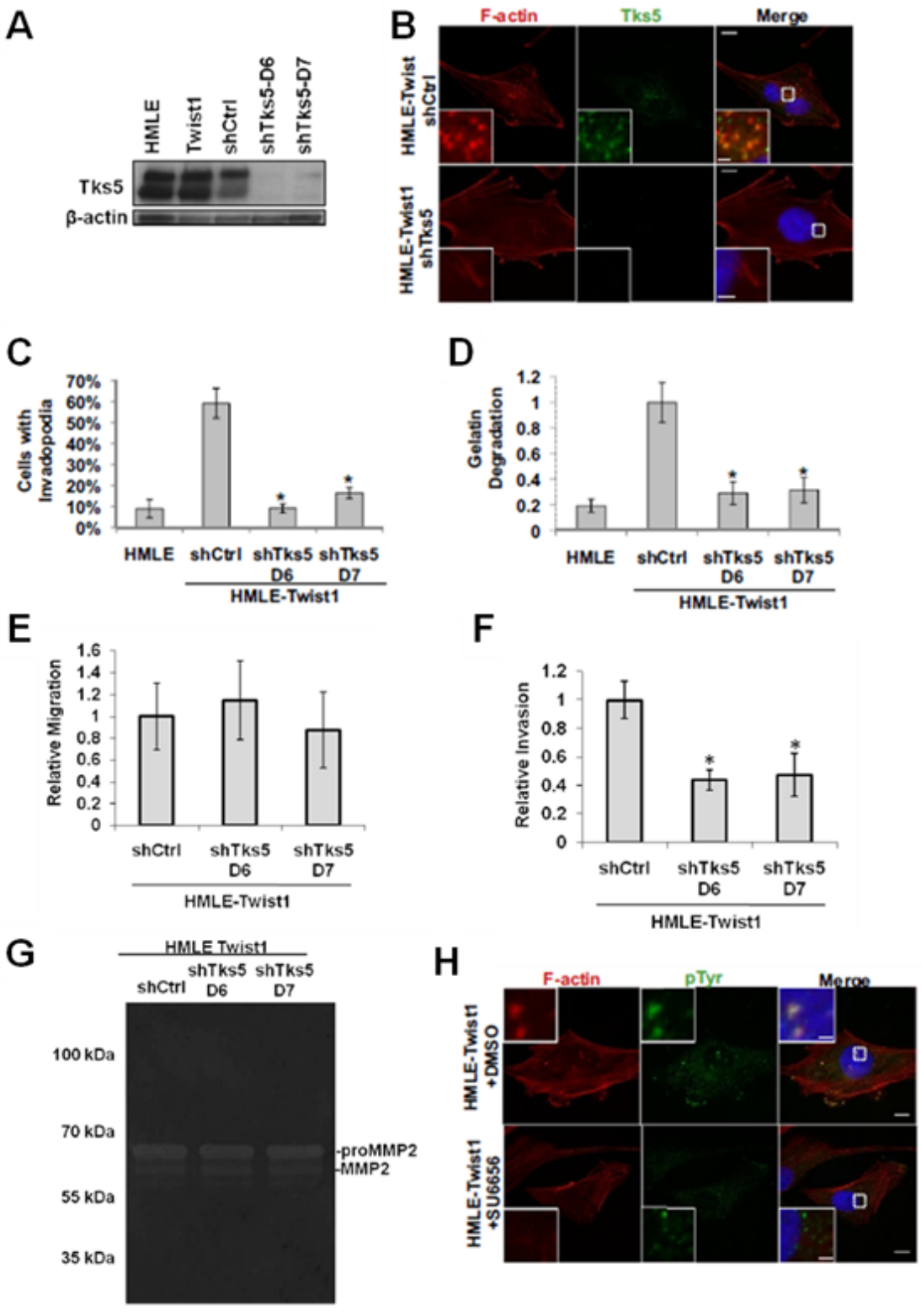
A
HMLE
Twist1
shCtrl
shTks5-D6
shTks5-D7
Tks5
β-actin
B
F-actin
Tks5
Merge
HMLE-Twist shCtrl
HMLE-Twist1 shTks5
C
Cells with Invadopodia
70%
60%
50%
40%
30%
20%
10%
0%
HMLE
shCtrl
shTks5 D6
shTks5 D7
HMLE-Twist1
D
Gelatin Degradation
1.2
1
0.8
0.6
0.4
0.2
0
HMLE
shCtrl
shTks5 D6
shTks5 D7
HMLE-Twist1
E
Relative Migration
1.6
1.4
1.2
1
0.8
0.6
0.4
0.2
0
shCtrl
shTks5 D6
shTks5 D7
HMLE-Twist1
F
Relative Invasion
1.2
1
0.8
0.6
0.4
0.2
0
shCtrl
shTks5 D6
shTks5 D7
HMLE-Twist1
G
HMLE Twist1
shCtrl
shTks5 D6
shTks5 D7
100 kDa
70 kDa
55 kDa
35 kDa
-proMMP2
-MMP2
H
F-actin
pTyr
Merge
HMLE-Twist1 +DMSO
HMLE-Twist1 +SU6656

for invadopodia formation (Ayala et al., 2008). We therefore assessed whether tyrosine phosphorylation at invadopodia was increased in HMLE-Twist1 cells. Immunofluorescence staining with a phosphotyrosine antibody revealed enrichment of phosphotyrosine at invadopodia (Figure 2.4 H). Cortactin immunoprecipitated from HMLE-Twist1 cells also showed increased tyrosine phosphorylation compared to HMLE control cells (Figure 2.5 C).

Src family kinases are the major kinases that promote tyrosine phosphorylation and formation of invadopodia. We therefore examined whether Twist1 induced expression of any of the three major Src family kinases, Src, Yes, and Fyn. Both real-time RT-PCR and immunoblotting analyses showed that none of the three Src kinases were greatly induced by Twist1 (Figure 2.5 A-C). Interestingly, when we probed for the activation status of Src, Yes, and Fyn in HMLE-Twist1 cells using an antibody recognizing the active form of Src family kinases (phosphotyrosine 416), Src was significantly activated upon Twist1 expression (Figure 2.5 C), while Yes and Fyn phosphorylation remained constant (Figure 2.5 B). These data suggest that activation of Src kinase activity, but not transcriptional induction of Src kinase expression, might be responsible for tyrosine phosphorylation at invadopodia in HMLE-Twist1 cells. To determine whether Src kinase activity is required for Twist1-induced invadopodia function, we treated HMLE-Twist1 cells with SU6656, a selective inhibitor of Src family kinases (Blake et al., 2000) (Figure 2.5 D) or expressed a dominant-negative Src (SrcK295M/Y527F) (Figure 2.5 E). Both treatments reduced the ability of HMLE-Twist1 cells to degrade by 5-fold (Figure 2.5 F), indicating that Src kinase activity

Figure 2.5: Twist1-induced activation of Src is necessary for invadopodia formation. (A) mRNA collected from HMLE and HMLE-Twist1 cells was reverse-transcribed and analyzed with real-time PCR for expression levels of three Src family kinases: Src, Fyn, and Yes. Values were normalized against GAPDH values. (B) The Src family kinases Yes and Fyn were immunoprecipitated from cell lysates from HMLE control and HMLE-Twist1 cells and analyzed by SDS-PAGE. Blots were probed with Yes and Fyn antibodies as well as a pTyr416Src antibody that recognizes the active (phosphorylated) form of all Src family kinases. (C) Cortactin and Src were immunoprecipitated from HMLE control and HMLE-Twist1 cell lysates, analyzed by SDS-PAGE, and probed for cortactin and phosphotyrosine and Src and $pTyr^{416}Src$, respectively. Input lysates were probed for β-actin, Src, and cortactin. (D) HMLE-Twist1 cells were treated for eight hours with 5 μM SU6656 or DMSO control. Cell lysates were harvested from these cells and analyzed by SDS-PAGE. Blots were probed for total Src and active $pTyr^{416}Src$. (E) Lysates from HMLE-Twist1 cells transfected with either control or dominant-negative Src (DN-Src) constructs were harvested and cortactin immunoprecipitated, analyzed by SDS-PAGE, and probed for cortactin and phosphotyrosine. (F) Quantification of FITC-gelatin degradation. Indicated cells were treated with 5 μM SU6656 or DMSO for 12 hours or transfected with control or SrcK295M/Y527F vectors. N=3 replicates, n=150 cells/sample. (G) Quantification of cells with invadopodia. N=3 replicates, n=150 cells/sample. Error bars are SEM. *$p<0.02$.

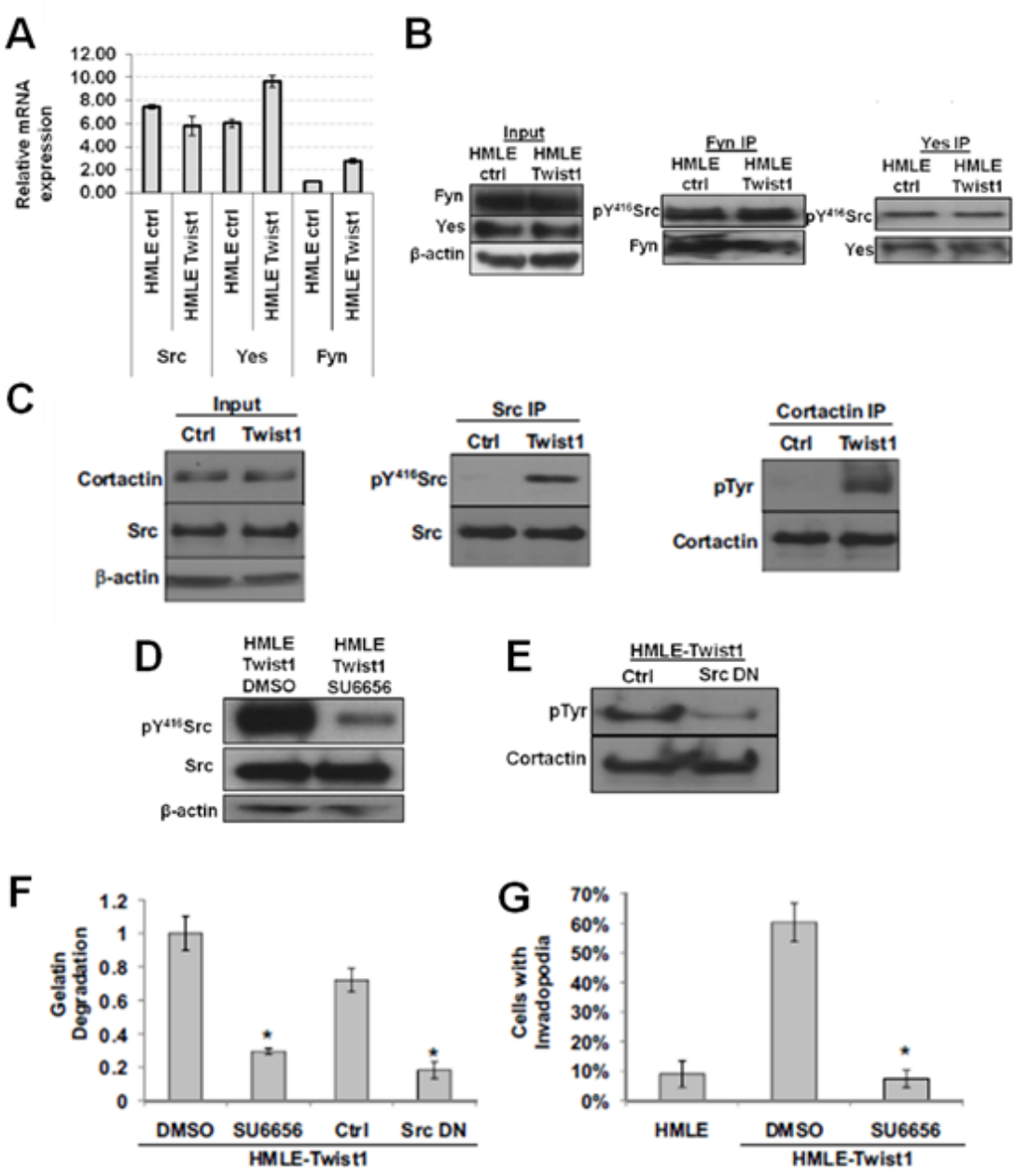
A
Relative mRNA expression
12.00
10.00
8.00
6.00
4.00
2.00
0.00
HMLE ctrl
HMLE Twist1
HMLE ctrl
HMLE Twist1
HMLE ctrl
HMLE Twist1
Src
Yes
Fyn
B
Input
HMLE ctrl
HMLE Twist1
Fyn
Yes
β-actin
Fyn IP
HMLE ctrl
HMLE Twist1
pY416Src
Fyn
Yes IP
HMLE ctrl
HMLE Twist1
pY416Src
Yes
C
Input
Ctrl
Twist1
Cortactin
Src
β-actin
Src IP
Ctrl
Twist1
pY416Src
Src
Cortactin IP
Ctrl
Twist1
pTyr
Cortactin
D
HMLE Twist1 DMSO
HMLE Twist1 SU6656
pY416Src
Src
β-actin
E
HMLE-Twist1
Ctrl
Src DN
pTyr
Cortactin
F
Gelatin Degradation
1.2
1
0.8
0.6
0.4
0.2
0
*
*
DMSO
SU6656
Ctrl
Src DN
HMLE-Twist1
G
Cells with Invadopodia
70%
60%
50%
40%
30%
20%
10%
0%
*
HMLE
DMSO
SU6656
HMLE-Twist1

is essential for Twist1–mediated invadopodia function. Treatment with SU6656 also inhibited colocalization of the phosphotyrosine signal with F-actin (Figure 2.4 H) and caused a significant reduction in the number of cells that formed invadopodia (Figure 2.5 G). Together, these results indicate that Twist1-induced invadopodia formation and function is dependent on activation of the Src kinase.

Twist1-induced PDGFR expression and activation is required for invadopodia formation. As a transcription factor, Twist1 cannot directly activate Src kinase, so we probed how Twist1 promotes activation of Src in HMLE-Twist1 cells. Since activation of Src kinase is downstream of growth factor receptor (GFR) activation, we examined induction of known GFRs upstream of Src by Twist1. Using an inducible Twist1 (Twist1-ER) construct (Mani et al., 2008), we found that expression of platelet-derived growth factor α (PDGFRα) mRNAs increased 3-fold within 3 hours of Twist1 activation and reached over 6000-fold induction at Day 15, while induction of PDGFRβ mRNAs occurred significantly later (Figure 2.6 A). PDGFRs can directly activate Src family kinases by tyrosine phosphorylation (Kypta et al., 1990), and activation of a PDGF autocrine loop is associated with the EMT program (Jechlinger et al., 2003). We found that PDGFRα and β proteins were also induced in HMLE-Twist1 cells and both PDGFR α and β were phosphorylated at tyrosine residues corresponding to their active states (Figure 2.6 B). This activation of PDGFR without exogenous PDGF ligands implies the existence of an autocrine activation loop *in vitro* most likely mediated by PDGF-C, the only PDGF ligand significantly expressed and upregulated upon activation of Twist1 in HMLE cells (Figure 2.6 C). Upregulation of PDGFRs by Twist1 therefore presented a potential mechanism for activation of Src by Twist1.

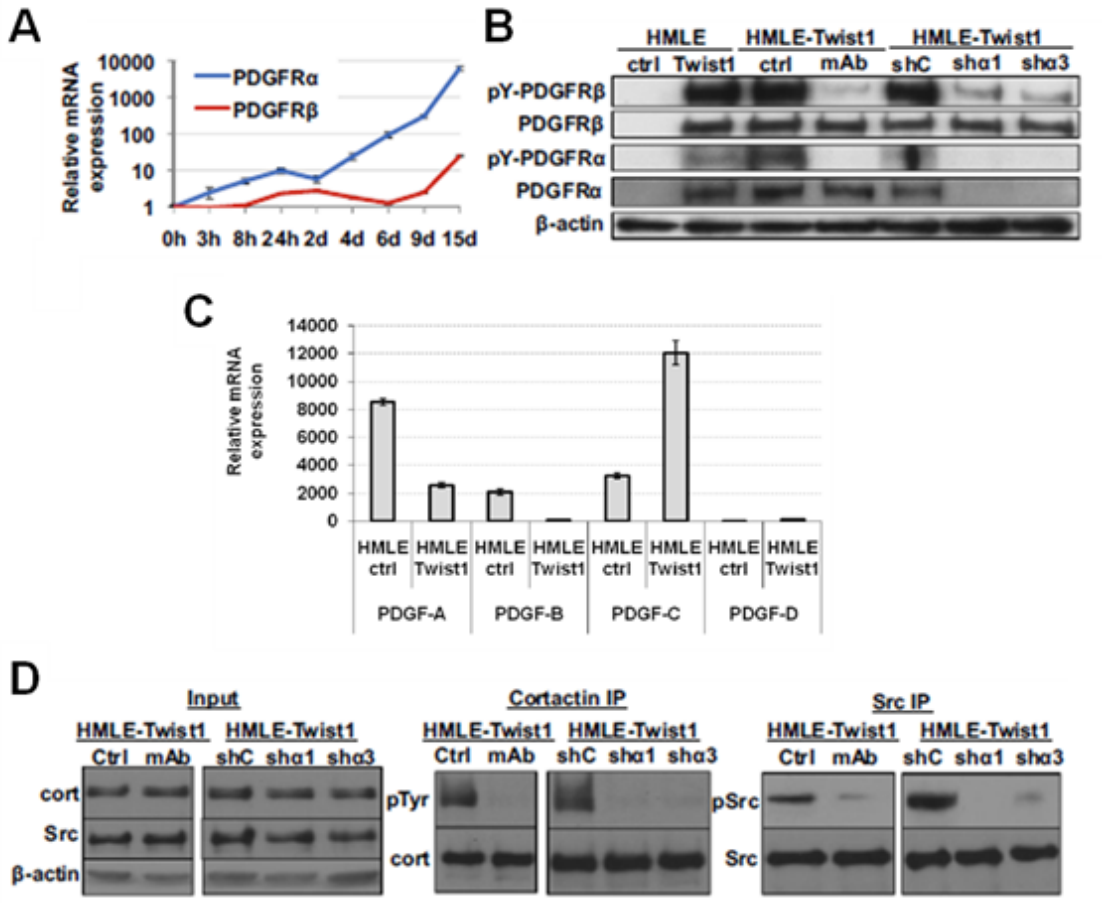

Figure 2.6: Induction of PDGFRα by Twist1 induces phosphorylation of invadopodia components. (A) Real-time PCR analysis of PDGFRα and PDGFRβ expression in HMLE-Twist1-ER cells treated with 20 nM 4-hydroxy-tamoxifen for indicated amount of time. (B) Cell lysates from HMLE control, HMLE-Twist1 cells, HMLE-Twist1 cells treated with vehicle or 8μg/ml PDGFRα blocking antibody (ctrl and mAb), and HMLE-Twist1 cells expressing control (shC) or PDGFR (shα1 and 3) shRNA were analyzed by SDS-PAGE and probed for β-actin, PDGFRα, PDGFRβ, pTyr^{754}PDGFRα, and pTyr^{1009}PDGFRβ. (C) mRNA from HMLE control and HMLE-Twist1 cells was analyzed for expression of all PDGF ligands (PDGF-A, PDGF-B, PDGF-C, and PDGF-D) normalized to GAPDH expression. (D) Cortactin and Src were immunoprecipitated from cell lysates of HMLE-Twist1 cells treated with 8 μg/mL PDGFRα blocking antibody (mAb) or vehicle control (ctrl) or HMLE-Twist1 cells expressing indicated shRNAs (control, shC; shPDGFRα, shα1 and shα3) and probed for total cortactin and phosphotyrosine or total Src and pTyr^{419}Src, respectively. Input lysates were probed for β-actin, cortactin, and total Src. Error bars are SEM.

We next set out to determine whether activation of PDGFRs is required for Twist1-induced invadopodia formation and matrix degradation. Given the immediate and robust induction of PDGFRα upon Twist1 activation, we focused on inhibiting PDGFRα to examine its role in mediating Twist1-induced Src activation and invadopodia formation. We first treated the HMLE-Twist1 cells with a monoclonal blocking antibody against PDGFRα and examined invadopodia formation and matrix degradation. This antibody effectively inhibited PDGFRα activation (Figure 2.6 B), Src activation, and tyrosine phosphorylation of cortactin in HMLE-Twist1 cells (Figure 2.6 D). This PDGFRα blocking antibody significantly inhibited invadopodia formation and tyrosine phosphorylation at invadopodia and suppressed the ability of HMLE-Twist1 cells to degrade FITC-gelatin by over 5-fold (Figure 2.7 A-C). To verify the results observed with the PDGFRα blocking antibody, we also expressed two independent shRNAs against PDGFRα in HMLE-Twist1 cells to stably suppress and inhibit PDGFRα signaling. Both shRNAs potently suppressed PDGFRα expression (Figure 2.6 B), Src activation, and cortactin phosphorylation (Figure 2.6 D), and effectively suppressed the ability of HMLE-Twist1 cells to degrade matrix (Figure 2.7 C). Importantly, expression or secretion of proteases was not affected by PDGFRα knockdown as measured with gelatin zymography (Figure 2.7 D). Together, these data indicate that PDGFRα expression and activation is required for Twist1-induced invadopodia formation and invasion.

We also examined expression of PDGFRα in 168FARN cells expressing control and Twist1 knockdown constructs. PDGFRα was highly expressed in control cells and significantly reduced upon knockdown of Twist1 (Figure 2.7 E). These results provide

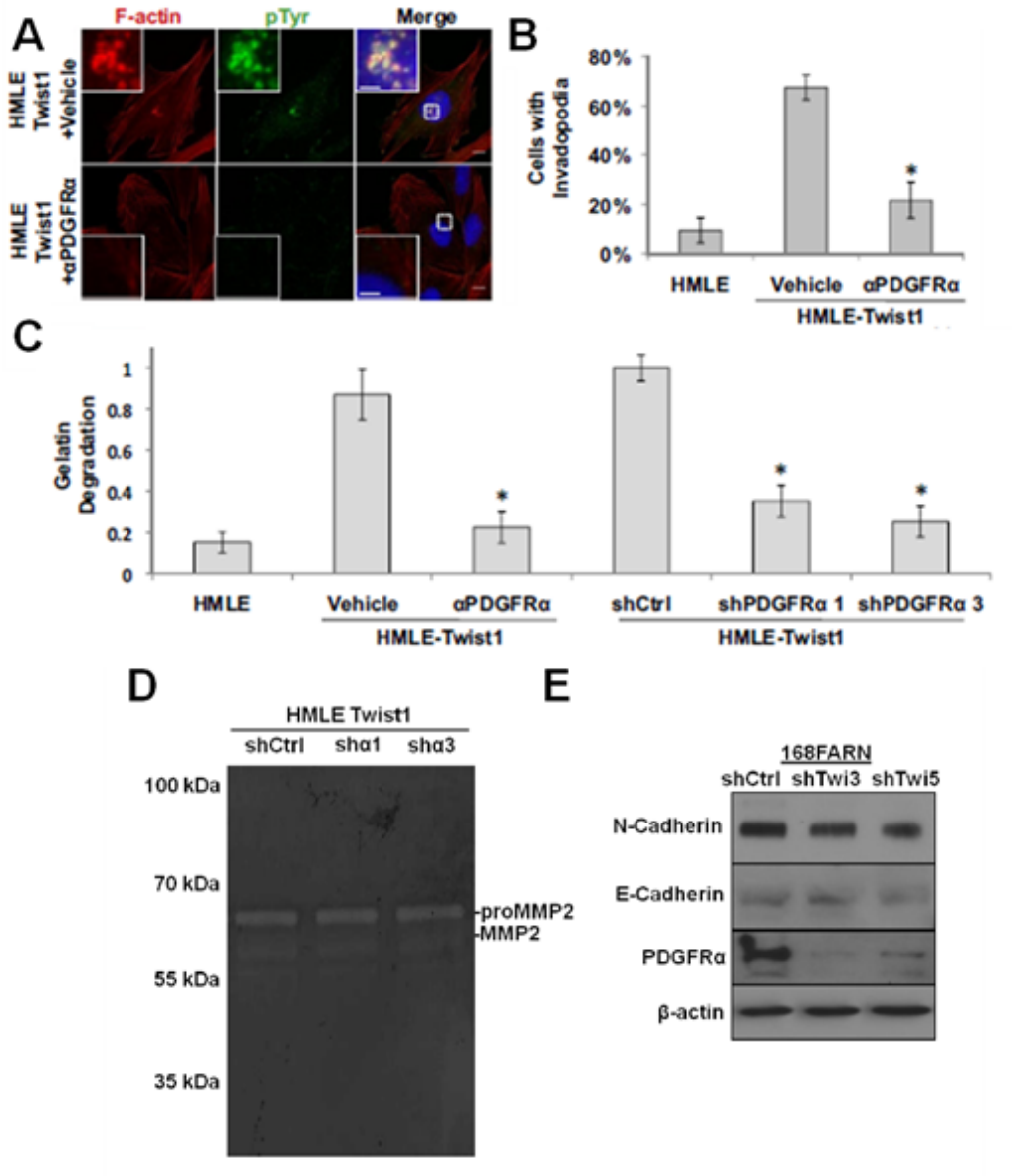

Figure 2.7: PDGFRα is necessary for Twist1-induced invadopodia formation. (A) HMLE-Twist1 cells were treated for 24 hours with 8 μg/mL PDGFRα blocking antibody (αPDGFRα) or control and stained for phosphotyrosine (green), F-actin (red), and nuclei (blue). (B) Quantification of invadopodia formation. (C) Quantification of gelatin degradation. (D) Conditioned media from HMLE-Twist1 cells expressing control or PDGFRα shRNA were analyzed with gelatin zymography. (E) SDS-PAGE analysis of lysates from 168FARN cells expressing indicated shRNA probed for N-cadherin, E-cadherin, PDGFRα, and β-actin. Scale bars are 1 μm for insets, 5 μm for full images. N=3 replicates, n=150 cells/sample. Error bars are SEM. *p<0.02.

further evidence that expression of PDGFRα depends on the presence of Twist1 in breast tumor cells.

Invadopodia formation is a specific function of Twist1 in EMT. Since other inducers of EMT, such as transforming growth factor B (TGFβ) and Snail, have also been associated with tumor invasion and metastasis, we sought to understand whether invadopodia formation also occurs in response to other EMT-inducing signals and whether Twist1 mediates invadopodia formation in response to these signals.

To do so, we first tested the ability of Snail, another EMT-inducing transcription factor, to promote invadopodia formation and matrix degradation. As previously reported, Snail overexpression induces EMT similarly to Twist1 in HMLE cells (Mani et al., 2009). HMLE-Snail cells have similar numbers of invadopodia and ECM-degradation activities as HMLE-Twist1 cells (Figure 2.8 A-D). To determine whether Snail, like Twist1, could induce the expression of PDGFRα to promote invadopodia formation, we examined the expression of PDGFRα mRNA in HMLE cells that express an inducible Snail (Snail-ER) construct. In contrast to the immediate induction of PDGFRα upon Twist1 activation, PDGFRα mRNA only began to increase 6 days after Snail activation, indicating that induction of PDGFRα by Snail is indirect (Figure 2.8 E). Interestingly, endogenous Twist1 mRNA levels increased significantly after 4 days of Snail activation, before PDGFRα mRNA began to increase (Figure 2.8 E). These data suggest that induction of endogenous Twist1 could be responsible for PDGFRα expression and invadopodia formation upon Snail activation.

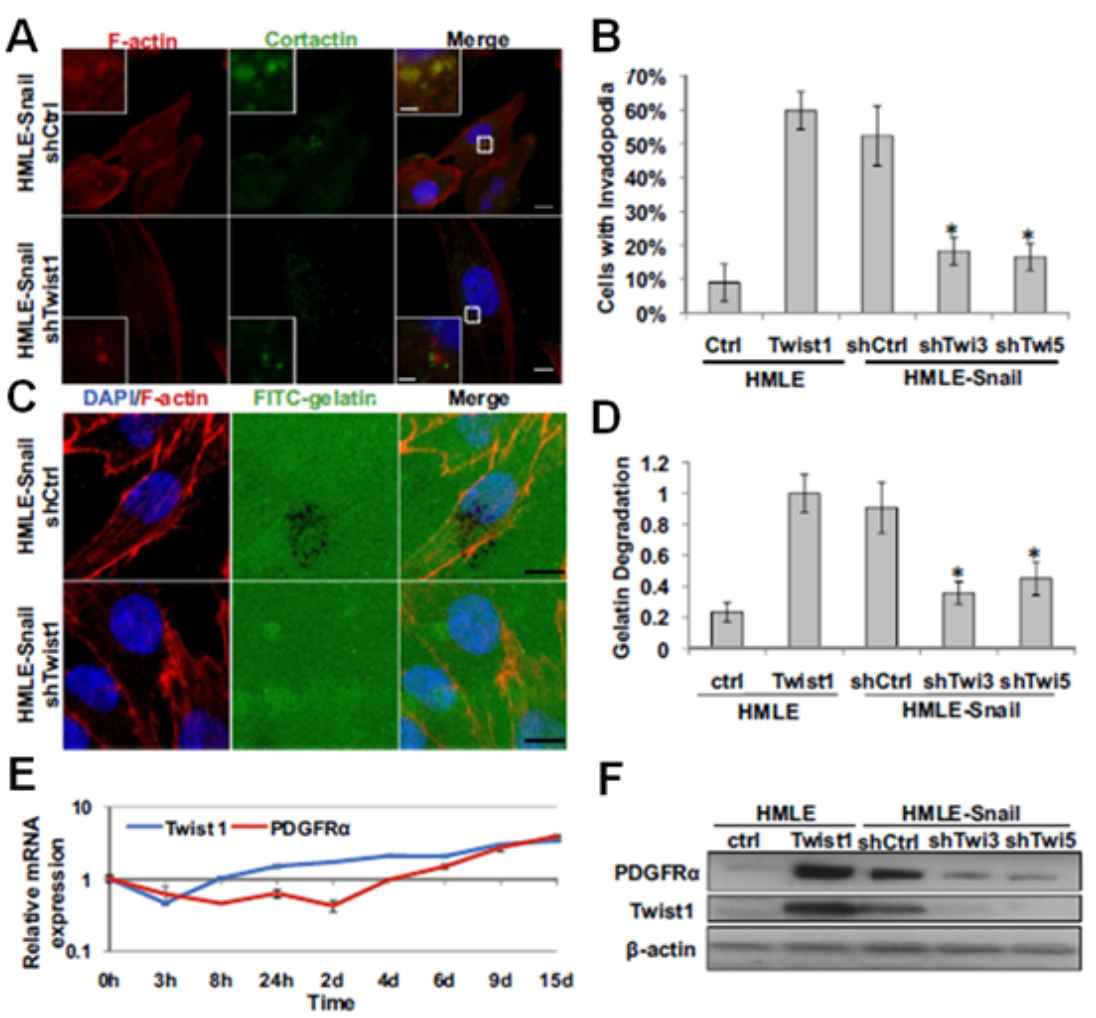

Figure 2.8: Twist1 is necessary for Snail-induced invadopodia formation. (A) HMLE-Snail cells expressing indicated shRNA were seeded on 0.2% gelatin for 72 hours, and stained for cortactin (green), F-actin (red), and nuclei (blue). (B) Quantification of cells with invadopodia. (C) HMLE-Snail cells expressing control or Twist1 shRNA were seeded on FITC-gelatin (green) for 8 hours and stained for F-actin (red) and nuclei (blue). (D) Quantification of FITC-gelatin degradation. (E) Real-time PCR analysis of PDGFRα and Twist1 mRNA expression in HMLE-Snail-ER cells treated with 20 nM 4-hydroxy-tamoxifen. (F) Cell lysates from indicated cells were analyzed by SDS-PAGE and probed for PDGFRα, Twist1, and β-actin. Scale bars are 1 μm for insets, 5 μm for full images. N=3 replicates, n=150 cells/sample. Error bars are SEM. *$p<0.02$.

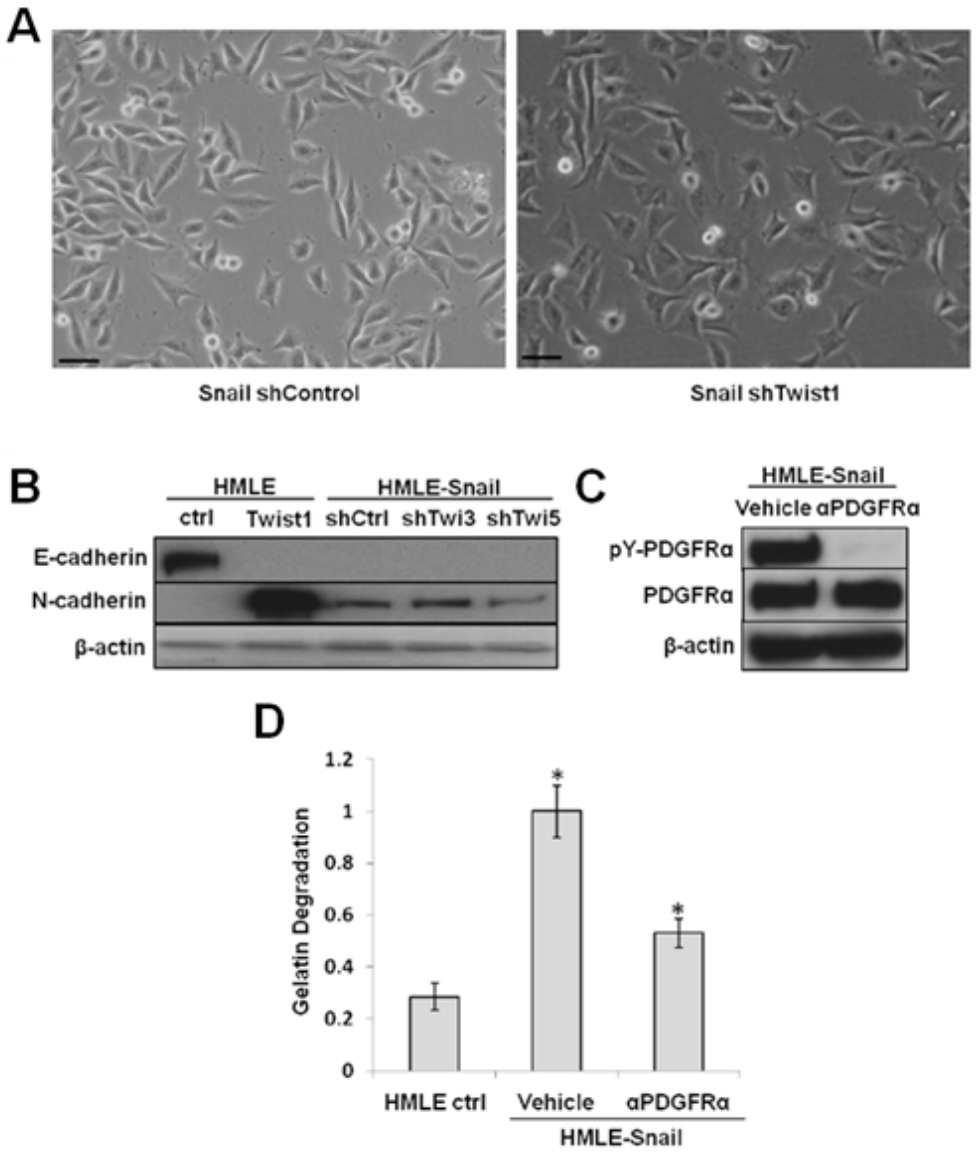

Figure 2.9: Twist1 is not necessary for Snail-induced EMT. (A) Brightfield images of HMLE-Snail cells expressing control or Twist1 shRNA. Both cells have similar mesenchymal morphologies with loss of cell adhesions and cell scattering. Scale bars are 10 μm. (B) Cell lysates from HMLE control, HMLE-Twist1, and HMLE-Snail cells expressing indicated shRNA were analyzed with SDS-PAGE and probed for markers of mesenchymal cells (N-cadherin) or epithelial cells (E-cadherin) and β-actin. (C) Cell lysates from HMLE-Snail cells treated with vehicle or 8 μg/ml PDGFRα blocking antibody were analyzed with SDS-PAGE and probed for phosphorylated PDGFRα, total PDGFRα, and β-actin. (D) Quantification of degradation in HMLE-Snail cells treated with 8 μg/ml PDGFRα blocking antibody or vehicle control. Error bars are SEM, N=3 experiments, n=150 cells/experiment. * $p<0.05$.

To assess whether Twist1 mediates the induction of invadopodia and PDGFRα in HMLE-Snail cells, we expressed shRNAs against endogenous Twist1 in HMLE-Snail cells. Indeed, suppression of endogenous Twist1 significantly inhibited expression of PDGFRα in HMLE-Snail cells (Figure 2.8 F). Significantly, suppression of Twist1 expression inhibited invadopodia formation in HMLE-Snail cells and reduced their ability to degrade matrix (Figure 2.8 A-D). Importantly, HMLE-Snail cells that express shRNAs against Twist1 presented an EMT phenotype with loss of E-cadherin expression and a mesenchymal morphology (Figure 2.9 A-B), indicating that suppression of E-cadherin by Snail and induction of invadopodia by Twist1 are regulated independently. Treating HMLE-Snail cells with the PDGFRα blocking antibody also significantly suppressed the ability of HMLE-Snail cells to degrade FITC-gelatin (Figure 2.9 C-D). Together, these results indicate that Twist1 and PDGFRα are responsible for invadopodia formation in response to Snail activation.

To further generalize our finding, we also investigated the role of Twist1 and PDGFRα in regulating invadopodia formation in response to TGFβ. In EpH4 mouse mammary epithelial cells, TGFβ has been shown to collaborate with Ras to promote EMT and activates an autocrine PDGF loop (Jechlinger et al., 2003). When we examined the invadopodia formation and matrix degradation in EpH4-Ras cells treated with TGFβ, we found that TGFβ treatment induced over 5-fold increase of invadopodia formation and matrix degradation in 2D culture (Figure 2.10 A-C). When these cells grew in 3D culture with TGFβ, invadopodia were visible at the leading edge of cells invading out of the organoids (Figure 2.10 E). Both Twist1 and PDGFRα were induced upon TGFβ treatment (Figure 2.10 D). When endogenous Twist1 induction was

Figure 2.10: Twist1 is required for TGFB-induced invadopodia formation in EpH4Ras cells. (A) EpH4Ras cells expressing control or Twist1 shRNAs were seeded on 0.2% gelatin for 72 hours before and after treatment with 5 ng/ml TGFβ1 for seven days and stained for cortactin (green), F-actin (red), and nuclei (blue). (B) Quantification of cells with invadopodia before and after seven days of 5 ng/ml TGFβ1 treatment for EpH4Ras cells expressing indicated shRNAs. N=150 cells/sample. *$p<0.02$. (C) Quantification of FITC-gelatin degradation for cells expressing indicated shRNA before and after seven days of 5 ng/ml TGFβ1 treatment. (D) Cell lysates from indicated cells before and after treatment with 5 ng/mL TGFβ1 for seven days were analyzed by SDS-PAGE and probed for PDGFRα, Twist1, and β-actin. (E) Indicated cells were embedded in 1:1 mixture of Matrigel and collagen, allowed to form 3D structures, and processed for IF before and after 7 days of induction with 7 ng/ml TGFβ1. Cells were stained for Tks5 (green) and F-actin (red). Error bars are SEM, N=3 experiments, n=150 cells/experiment. * $p<0.05$.

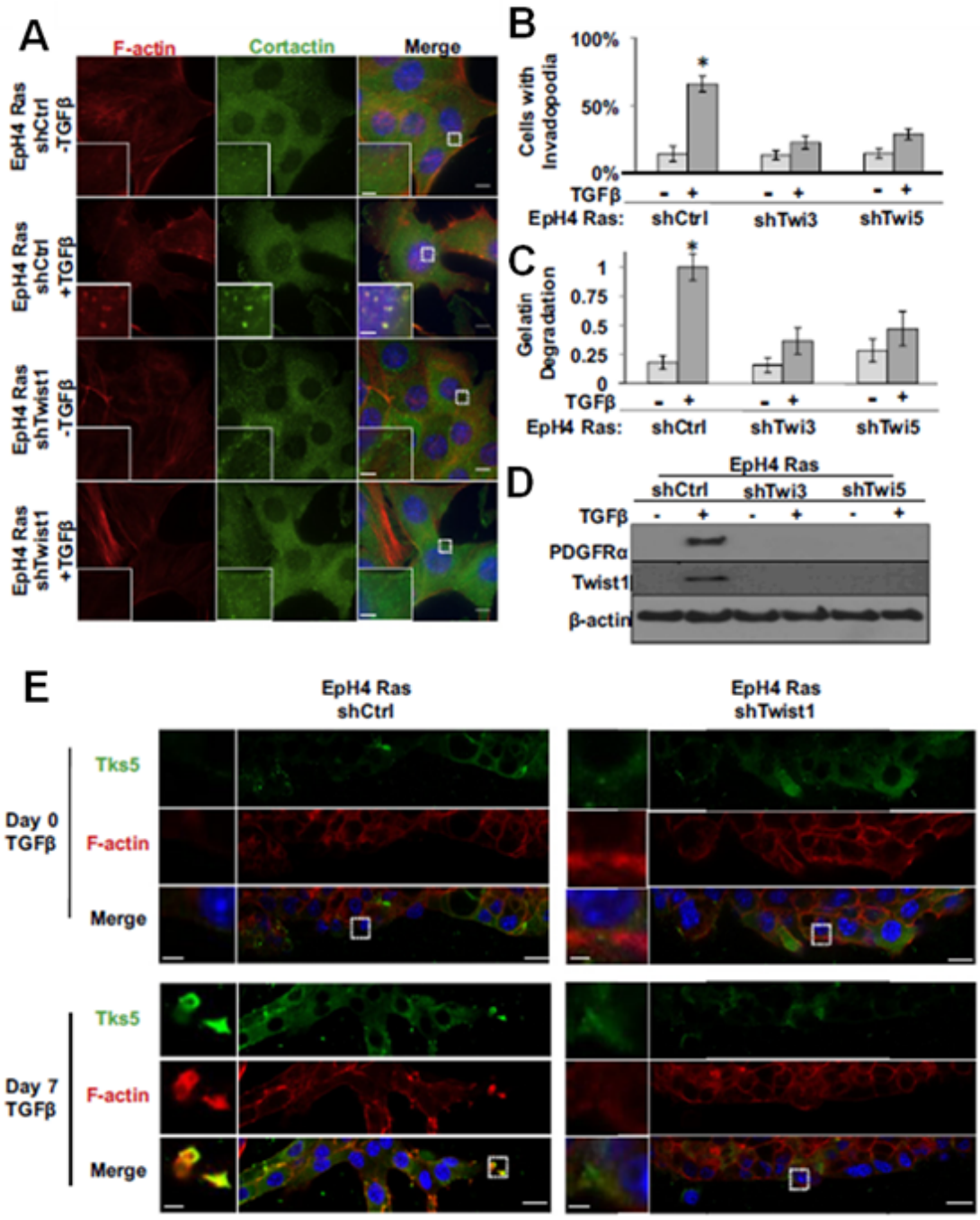
A
F-actin
Cortactin
Merge
EpH4 Ras shCtrl -TGFβ
EpH4 Ras shCtrl +TGFβ
EpH4 Ras shTwist1 -TGFβ
EpH4 Ras shTwist1 +TGFβ
B
Cells with Invadopodia
100%
50%
0%
TGFβ
EpH4 Ras:
shCtrl
shTwi3
shTwi5
C
Gelatin Degradation
1
0.75
0.5
0.25
0
D
EpH4 Ras
PDGFRα
Twist1
β-actin
E
EpH4 Ras shCtrl
EpH4 Ras shTwist1
Day 0 TGFβ
Day 7 TGFβ
Tks5
F-actin
Merge

Figure 2.11: Twist1 is not required for TGFB-induced EMT in EpH4Ras cells. (A) Brightfield images of Eph4-Ras cells expressing control or Twist1 shRNA before and after seven days of 5 ng/ml TGFβ1 treatment. Scale bars are 10 μm. (B) Cell lysates from EpH4-Ras cells expressing control or Twist1 shRNA were collected before and after 7 days of treatment with 5 ng/m TGFβ1 treatment, analyzed by SDS-PAGE, and probed for E-cadherin, N-cadherin, and β-actin. (C) Cell lysates from EpH4-Ras cells treated with 5 ng/ml TGFβ1 for 7 days and DMSO or 25 μg/ml STI571 for 1 day were analyzed by SDS-PAGE and probed for phosphorylated PDGFRα, total PDGFRα, and β-actin. (D) Quantification of degradation in Eph4-Ras cells treated with TGFβ1 and 25 μM STI571 or DMSO. (E) Cell lysates from cells with indicated treatment of TGFβ1 or STI571were analyzed by SDS-PAGE and probed for E-cadherin, and N-cadherin, β-actin. Error bars are SEM, N=3 experiments, 150 cells. * $p<0.05$.

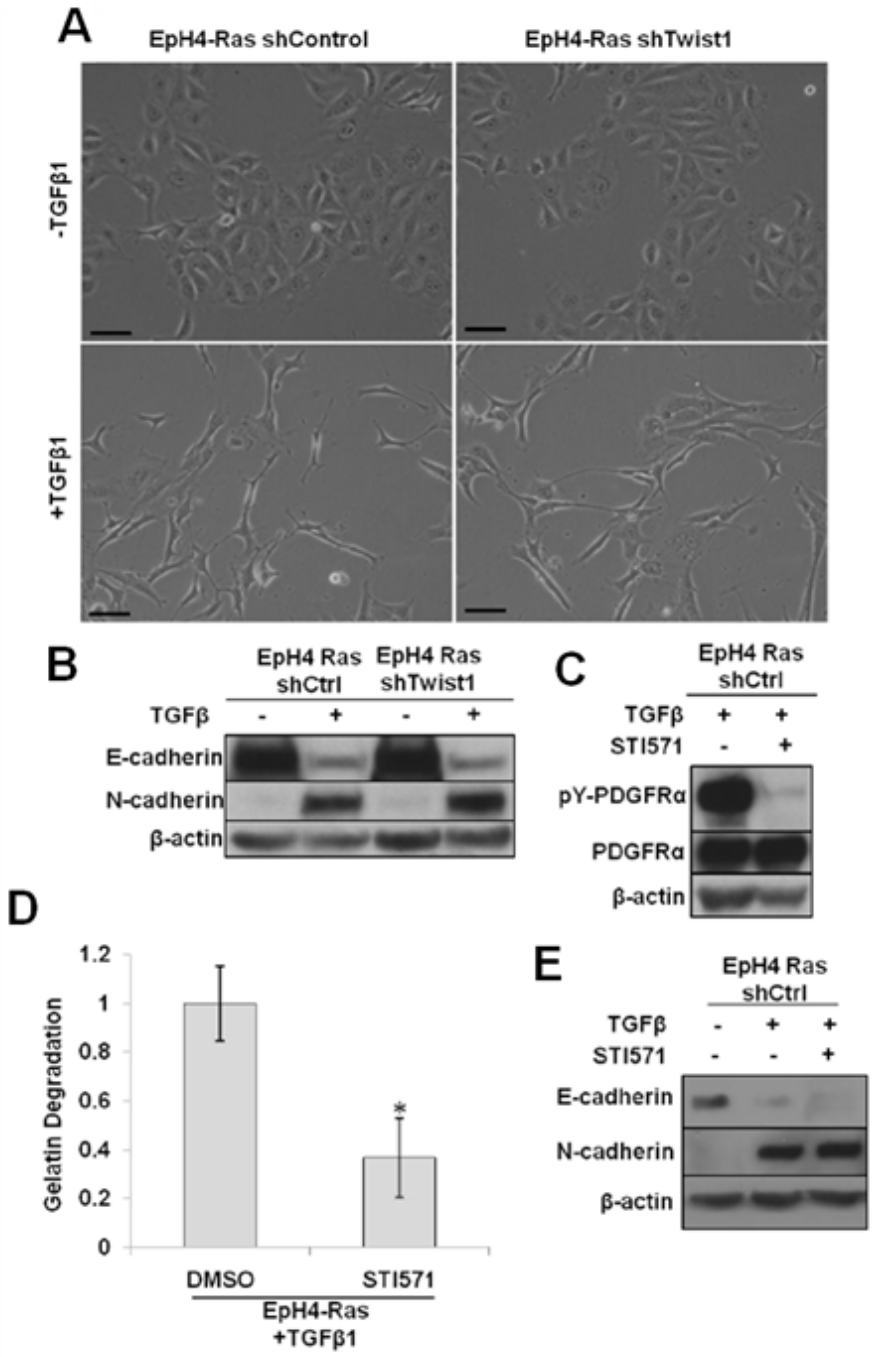
A
EpH4-Ras shControl
EpH4-Ras shTwist1
-TGFβ1
+TGFβ1
B
EpH4 Ras shCtrl
EpH4 Ras shTwist1
TGFβ - + - +
E-cadherin
N-cadherin
β-actin
C
EpH4 Ras shCtrl
TGFβ + +
STI571 - +
pY-PDGFRα
PDGFRα
β-actin
D
Gelatin Degradation
1.2
1
0.8
0.6
0.4
0.2
0
*
DMSO
STI571
EpH4-Ras +TGFβ1
E
EpH4 Ras shCtrl
TGFβ - + +
STI571 - - +
E-cadherin
N-cadherin
β-actin

inhibited by shRNAs, invadopodia formation and matrix degradation were significantly reduced in 2D and 3D cultures (Figure 2.10 A-C and E). Importantly, knocking down Twist1 abolished induction of PDGFRα in EpH4-Ras cells treated with TGFβ (Figure 2.10 D), but did not prevent induction of EMT morphogenesis and loss of E-cadherin (Figure 2.11 A-B), similar to knockdown of Twist1 in HMLE-Snail cells. Furthermore, treating EpH4-Ras cells with the PDGFRα inhibitor ST1571 significantly suppressed their ability to degrade FITC-gelatin in response to TGFβ treatment (Figure 2.11 C-D). Importantly, treatment with STI571 did not revert the EMT phenotype (Figure 2.11 E). Together, these results support our conclusion that Twist1 is a central mediator of invadopodia formation and matrix degradation via induction of PDGFRα in response to EMT-inducing signals.

Invadopodia are necessary for Twist1-induced metastasis. Twist1 is required for mammary tumor cells to metastasize from the mammary gland to the lung. We then tested whether PDGFRα and invadopodia are required for the ability of Twist1 to promote tumor metastasis *in vivo*. To do so, we generated HMLE-Twist1 cells that were transformed with oncogenic Ras (HMLER-Twist1) and expressed shRNAs against either PDGFRα or a control shRNA. These cells also expressed GFP to allow identification of tumor cells in mice. Individual cell lines were injected subcutaneously into nude mice. Suppression of PDGFRα did not affect cell proliferation in culture or tumor growth rate *in vivo* (Figure 2.12 A-B). Six weeks after tumor implantation, we sacrificed the mice and examined primary tumors for histology and invadopodia. Since HMLER-Twist1 tumors expressing large T antigen, we used an antibody against large T antigen to stain implanted tumor cells. Interestingly, HMLER-Twist1 tumor cells

invaded into surrounding stroma and adjacent adipose tissue, while PDGFRa knockdown inhibited local invasion and tumor cells remained encapsulated (Figure 2.13 A). Staining for invadopodia using cortactin and Tks5 in sections of primary tumor tissue revealed that HMLER-Twist1 tumor cells contained abundant invadopodia, while knocking down PDGFRα significantly reduced their occurance (Figure 2.13 B-C). To test whether PDGFRα is required for distant metastasis, examination of lung lobes and sections revealed clusters of HMLER-Twist1 shControl cells throughout the lungs (Figure 2.13 E-F). Significantly, suppression of PDGFRα expression significantly reduced the number of disseminated tumor cells in the lung (Figure 2.13 D). These results strongly indicate that induction of PDGFRα is required for the ability of Twist1 to form invadopodia and promote tumor metastasis without affecting primary tumor growth *in vivo*.

To demonstrate that invadopodia are required for the ability of Twist1 to metastasize *in vivo*, we expressed shRNAs against Tks5 to inhibit invadopodia formation in HMLER-Twist1 cells. Knockdown of Tks5 did not affect cell growth rate *in vitro* (Figure 2.12 C). These cells were implanted subcutaneously into nude mice to follow primary tumor growth and lung metastasis. Consistent with the results from the PDGFRα knockdown experiments, Tks5 knockdown inhibited local tumor invasion and significantly reduced the numbers of tumor cells that disseminated into the lung, while primary tumor growth was not affected (Figure 2.12 D, Figure 2.13 A, D and E). Together, these data demonstrate that induction of invadopodia formation via PDGFRα activation is essential for the ability of Twist1 to promote tumor metastasis *in vivo*.

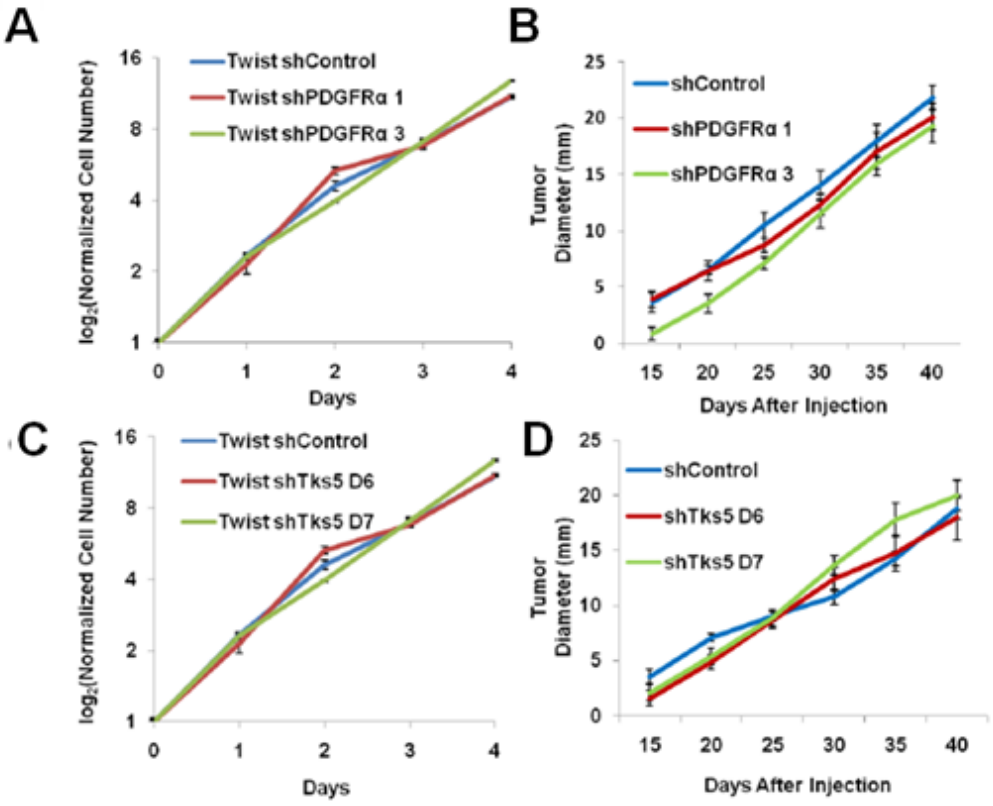

Figure 2.12: Knockdown of Tks5 and PDGFRα do not affect proliferation or tumor growth. (A) HMLE-Twist1 cells expressing control or PDGFRα shRNAs in triplicates were counted every 24 hours to establish growth curve. (B) Nude mice were injected with 1.5 million HMLER-Twist1 cells expressing control or PDGFRα shRNAs. Tumor diameters were measured every 5 days starting 15 days after injection until tumors reached 20 mm in diameter. N=5 mice per group. (C) HMLE-Twist1 cells expressing control or Tks5 shRNAs in triplicates were counted every 24 hours to establish growth curve. (D) Nude mice were injected with 1.5 million HMLER-Twist1 cells expressing control or Tks5 shRNAs. Tumor diameters were measured every 5 days starting 15 days after injection until tumors reached 20 mm in diameter. N=5 mice per group. Error bars are SEM.

Figure 2.13: Twist1-induced metastasis is mediated by invadopodia *in vivo* and requires PDGFRα. (A) Representative images of primary tumor paraffin tissue sections stained with SV40 Large-T antigen IHC and counterstained with hematoxylin. Tumor margin is indicated with dashed line when apparent. Closed triangles indicate invasive, Large-T positive tumor cells. Asterisks indicate adjacent adipose tissue. Scale bars are 100 μm. (B) Images of sections of primary tumors stained with cortactin (green), Tks5 (red), and DAPI (blue). Scale bars are 1 μm for insets, 5 μm for full images. (C) Quantification of number of invadopodia (cortactin/Tks5 colocalization) per cell. N=3 tumors, n=150 cells/sample. *$p<0.02$. (D) Quantification of total number of GFP positive tumor cells (HMLER-Twist1 cells expressing indicated shRNAs) in individual lungs. N=5 mice per group. (E) Representative images of lungs from mice injected with HMLER-Twist1 cells expressing indicated shRNAs show a decrease in dissemination of GFP positive tumor cells (green) to the lungs upon knockdown of PDGFRα or Tks5. (F) Representative images of GFP-positive (green) cells within lung tissue (indicated by GFP-negative, DAPI-positive cells). Cells disseminated as groups of 1-5 cells, with some larger nodules occasionally found. Scale bars are 5 μm. Error bars are SEM. *$p<0.05$.

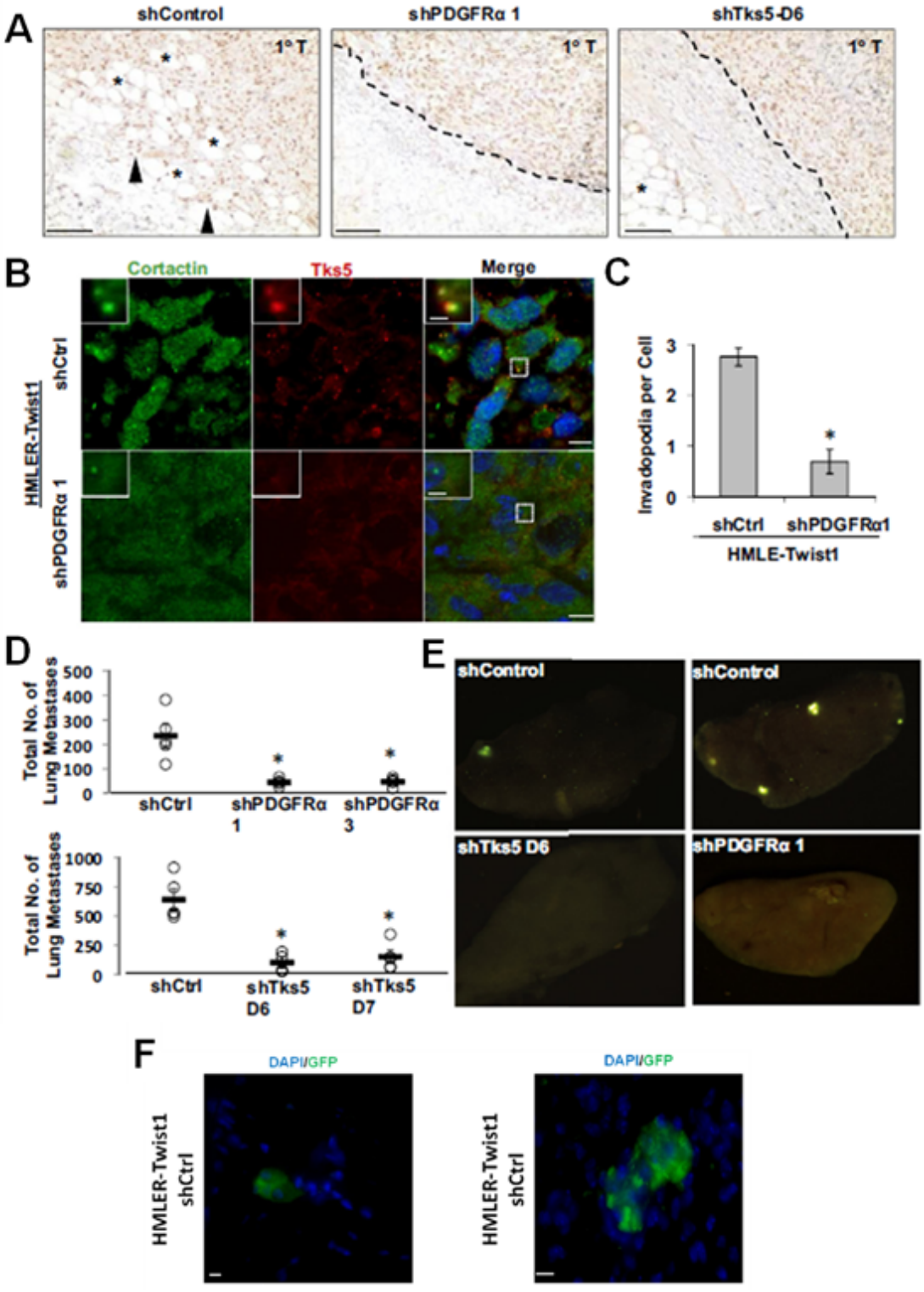
A
shControl
shPDGFRα 1
shTks5-D6
1° T
B
Cortactin
Tks5
Merge
HMLER-Twist1
shCtrl
shPDGFRα 1
C
Invadopodia per Cell
shCtrl
shPDGFRα1
HMLE-Twist1
D
Total No. of Lung Metastases
shCtrl
shPDGFRα 1
shPDGFRα 3
shTks5 D6
shTks5 D7
E
shControl
shTks5 D6
shPDGFRα 1
F
DAPI/GFP
HMLER-Twist1 shCtrl

Twist1 and PDGFRα in human breast cancer patients. Given the immediate induction of PDGFRα by Twist1 and their tight association in various tumor cells, we set out to determine whether PDGFRα is a direct transcriptional target of Twist1. We examined the human PDGFRα promoter for potential Twist1-binding E-box sequences (CANNTG). We designed three sets of primers on the putative promoter: primer sets 1 and 2 target the identified E-box, and primer set 3 targets an adjacent region lacking the putative E-box (Figure 2.14 A). By chromatin immunoprecipitation, we found that Twist1 directly bound to the E-box on the putative PDGFRα promoter (Figure 2.14 B). Twist1 was able to activate the isolated human PDGFRa promoter in an E-box-dependent fashion in a luciferase reporter assay (Figure 2.14 C-D). Furthermore, this consensus E-box sequence is highly conserved between all mammalian species examined and chickens (Figure 2.14 E), indicating that induction of PDGFRα by Twist1 is direct and evolutionally conserved.

To more directly probe the *in vivo* association between Twist1 and PDGFRα in human breast tumor samples, we analyzed four published large human breast tumor gene expression datasets summarizing 860 primary breast cancers (Pawitan et al., 2005; Sotiriou et al., 2006; Wang et al., 2005; Miller et al., 2005). In each data set, we calculated the rank-based Spearman correlation coefficient between Twist1 and all 22282 genes on the array, including PDGFRα. PDGFRα was consistently among the top ranked genes associated with Twist1 (4th, 17th, 47th, and 54th out of 22282 genes) in all four breast cancer datasets (Figure 2.15 A-B). Expression of Twist1 and PDGFRα were positively correlated with correlation coefficients ranging from 0.56 to 0.70

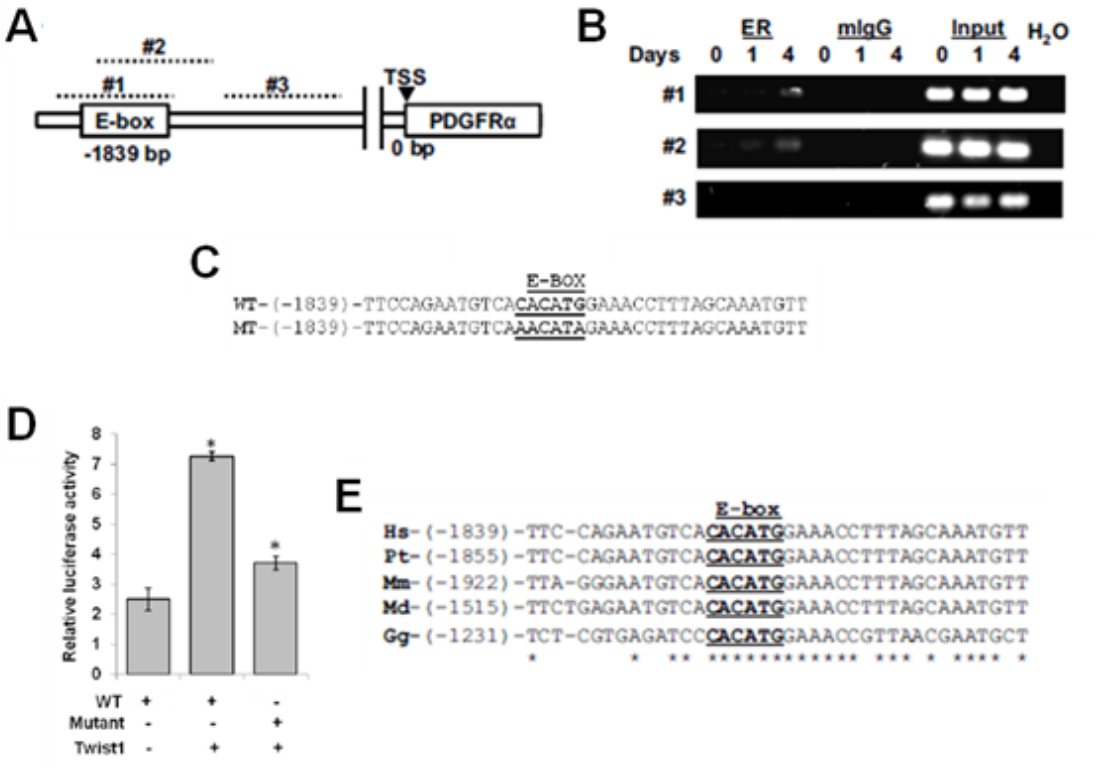

Figure 2.14: PDGFRα is a direct target of Twist1. (A) Schematic of the human PDGFRα gene promoter region with conserved E-box element 1839 bp upstream of transcriptional start site (TSS), and regions targeted by three primer pairs (#1–3, dashed lines). Primer pairs #1 and #2 target the putative E-box while primer pair #3 targets a downstream region lacking a conserved E-box. (B) HMLE-Twist1-ER cells were treated with 20 nM 4-hydroxytamoxifen for 0, 1, or 4 hours. Chromatin was immunoprecipitated using estrogen receptor antibody and PCR was performed on the ChIP product using three primer pairs. (C) Region of promoter mutated for assay, WT=wild-type promoter, MT=mutated, E-box null promoter. (D) Relative luciferase activity of MCF7 cells transfected with indicated plasmids. (E) Alignment of conserved E-box (underlined) in PDGFRα promoter. Number in parenthesis indicates distance upstream from transcription start site. Hs=*Homo sapiens*, Pt=*Pan troglodytes*, Mm=*Mus musculus*, Md=*Monodelphus domesticus*, Gg=*Gallus gallus*. N=3 experiments. Error bars are SEM. * $p<0.05$.

Figure 2.15: Twist1 and PDGFRα are correlated with reduced survival in human patients. (A) Correlation between Twist1 and PDGFRα expression in four human breast cancer gene expression datasets. Microarray measurements of PDGFRa (y-axis) are plotted against the measurements of Twist1 (x-axis). Each dot is a pair of probeset-level aggregated values for the corresponding gene. The regression line between two genes is drawn as a solid line. The Spearman correlation coefficient, p-value, and the number of patient samples in each study are listed for each dataset. (B) Histogram of rank of correlation between all genes and Twist1 in four human breast cancer gene expression datasets. Location of PDGFRα correlation is indicated with blue line and label. (C) Representative images of normal human breast tissue or human breast cancer samples stained for Twist1 and PDGFRα. Scale bar is 5 μm for inset, 100 μm for full images. (D) Kaplan-Meier survival curve for samples classified as high PDGFRα/high Twist1 expression and low PDGFRα/low Twist1 by IHC analysis. Censored data are indicated with X.

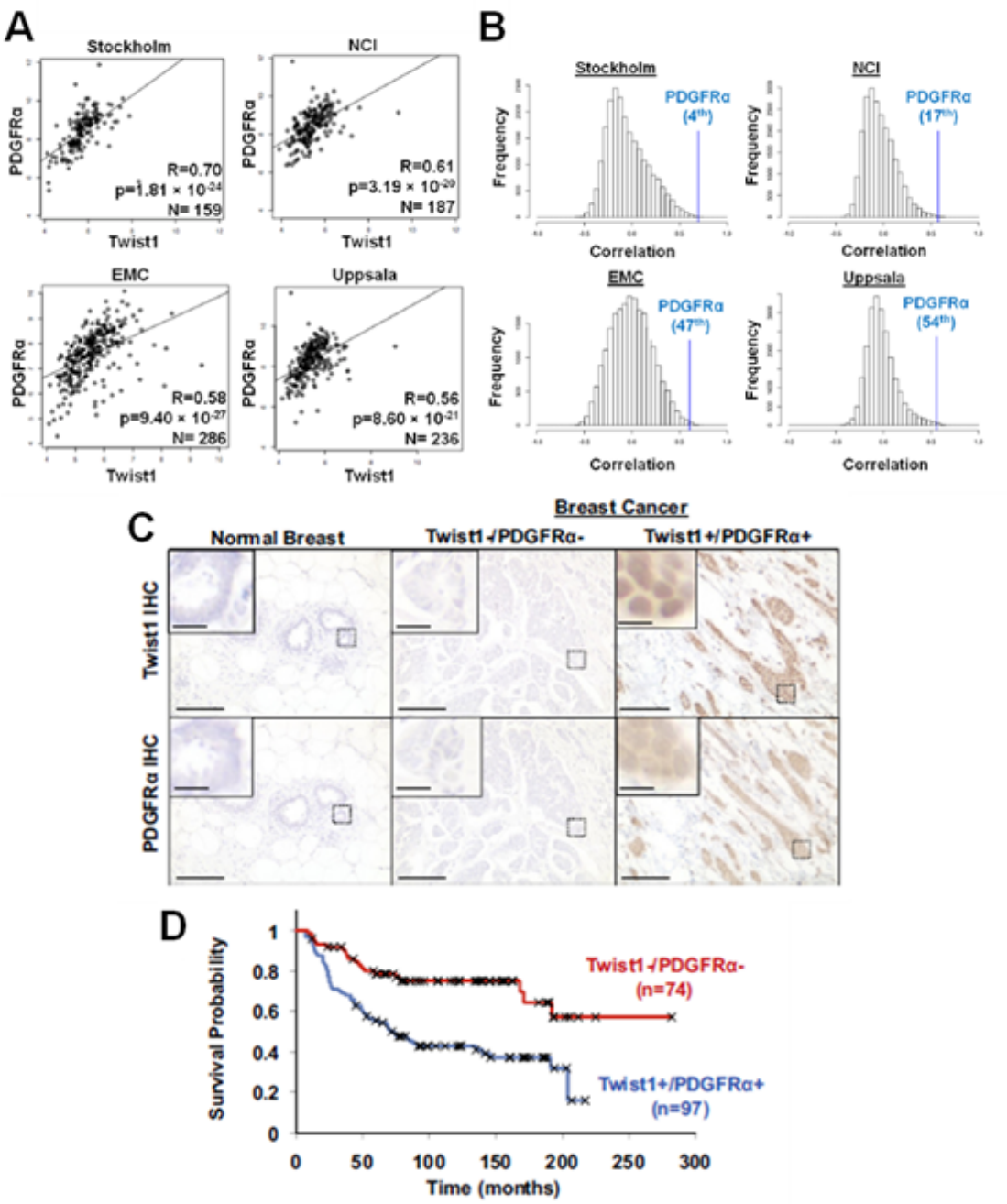
A
Stockholm
NCI
EMC
Uppsala
PDGFRα
Twist1
R=0.70
p=1.81 × 10-24
N= 159
R=0.61
p=3.19 × 10-20
N= 187
R=0.58
p=9.40 × 10-27
N= 286
R=0.56
p=8.60 × 10-21
N= 236
B
Stockholm
NCI
EMC
Uppsala
PDGFRα (4th)
PDGFRα (17th)
PDGFRα (47th)
PDGFRα (54th)
Frequency
Correlation
C
Breast Cancer
Normal Breast
Twist1-/PDGFRα-
Twist1+/PDGFRα+
Twist1 IHC
PDGFRα IHC
D
Survival Probability
Time (months)
Twist1-/PDGFRα- (n=74)
Twist1+/PDGFRα+ (n=97)

(Figure 2.15 A-B). Furthermore, in all four data sets, PDGF ligand expression correlated with PDGFRα and Twist1 expression in over 95% of tumor samples, indicating that PDGFRα could be active in these samples. To further assess whether coexpression of Twist1 and PDGFRα could affect survival in breast tumor patients, we stained Twist1 and PDGFRα in a set of human invasive breast tumor tissue array samples and found that co-expression of Twist1 and PDGFRα was negatively associated with long-term survival (Figure 2.15 C-D). Together, these data provides further support for a direct and functional association between Twist1 and PDGFRα in human breast cancers and suggests that regulation of invadopodia by Twist1 and PDGFRα contributes to human breast cancer progression.

DISCUSSION

Our study has identified a unique function of the Twist1 transcription factor in promoting invadopodia formation and matrix degradation during tumor metastasis. We demonstrate that transcriptional induction of PDGFRα and activation of Src by Twist1 are essential for invadopodia formation and matrix degradation. Induction of PDGFRα and invadopodia formation is also essential for the ability of Twist1 to promote metastasis *in vivo*. Twist1 and PDGFRα are central mediators of invadopodia in response to several EMT-inducing signals. Finally, we provide evidence for a tight association between Twist1 and PDGFRα in human breast tumor samples.

ECM degradation is considered a key step promoting tumor invasion and metastasis. Extensive studies have largely focused on secreted MMPs as key proteases in tumor invasion. More recent studies suggest a role for invadopodia and their associated proteases in localized matrix degradation during cell invasion. Conceptually,

invadopodia provide an elegant solution to restrict protease activity to areas of the cell in direct contact with ECM, thus precisely controlling cell invasion *in vivo*. In this study, we show that Twist1, a key transcription factor in tumor metastasis, is both necessary and sufficient to promote invadopodia formation. Importantly, invadopodia formation is required for the ability of Twist1 to promote tumor metastasis *in vivo*. Together, these results demonstrate an essential role for invadopodia in tumor invasion and metastasis *in vivo*.

How invadopodia formation is regulated at the molecular level is still not well understood. Our current study indicates that Twist1 directly induces the expression and activation of PDGFRα, thus promoting Src kinase activation and invadopodia formation. Although we did not detect induction of several important invadopodia proteins, including cortactin, Tks4, Tks5, and MT1-MMP, by Twist1 (data not shown), we are actively exploring additional mechanisms by which Twist1 regulates invadopodia.

Another question arising from our study is whether invadopodia function is required for the EMT process. Epithelial cells sit on top of a layer of basement membrane. For the EMT program to occur *in vivo*, these cells must breach the underlying basement membrane to dissociate (Nakaya et al., 2008). Little is known about the functional relationship between basement membrane integrity and the EMT program. In HMLE-Snail cells and EpH4-Ras cells treated with TGFβ, knockdown of Twist1 inhibited invadopodia formation, while these cells underwent the morphological changes associated with EMT and lost E-cadherin expression. Additionally, knockdown of Tks5, a required component of invadopodia, did not revert the EMT phenotype in

HMLE-Twist1 cells. These results indicate that invadopodia function is not essential for EMT to occur in 2D cultures. However, it is plausible that the EMT program requires activation of Twist1 and invadopodia formation to allow degradation of the basement membrane *in vivo*. Studies *in vivo* or in 3D cultures with intact basement membrane are required to fully answer this question.

The EMT program is considered a key event promoting carcinoma cell dissociation, invasion, and metastasis. Several transcription factors, including Snail, Slug, ZEB1, ZEB2, and Twist1, promote EMT in epithelial cells (Peinado et al., 2007). During mesoderm formation and neural crest development, these transcription factors are activated to allow the dissociation and migration of epithelial cells. A major unsolved question is to determine the distinct cellular functions and molecular targets of individual EMT-inducing transcription factors. Extensive studies in recent years have demonstrated that Snail (Batlle et al., 2000; Cano et al., 2000), Slug (Hajra et al, 2002), and ZEB2 (Comijin et al., 2001), all zinc-finger-containing transcriptional repressors, directly bind to the E-boxes on the E-cadherin promoter and suppress its transcription. In this study, we identified a unique function of Twist1 in promoting matrix degradation via invadopodia. We show that Twist1 functions as a transcriptional activator to directly induce the expression of PDGFRα, in contrast to the EMT-inducing Zn-finger transcription factors.

Vertebrate Twist1 lacks a transcription activation domain and requires dimerization with other bHLH transcription factors to activate transcription. Previous studies have shown Twist1 heterodimers with MyoD function as transcriptional repressors (Hamamori et al., 1997). In contrast, heterodimerization with E12 enables

Twist1 to activate FGF2 transcription (Laursen et al, 2007). Here we demonstrate that Twist1 functions as a transcriptional activator to directly induce the transcription of PDGFRα. Twist1 might function as an activator or repressor of transcription based on dimerization partners under different physiological and cellular environments. The factors that heterodimerize with Twist1 to activate PDGFRα transcription remain unknown, although the E12/E47 proteins could perform this function.

The pathway linking Twist1, PDGFR, and invadopodia is likely to play a conserved role in matrix degradation during both tumor metastasis and embryonic morphogenesis

Twist1 has been associated with increased metastasis in both experimental tumor metastasis models and in many types of human cancers. Interestingly, PDGFRα overexpression and activation have also been observed in aggressive human breast tumors (Seymour and Bezwoda, 1994; Jechlinger et al, 2006). Activation of PDGFRs was first observed in TGFβ-induced EMT and shown to be involved in cell survival during EMT and experimental metastasis in mice (Jechlinger et al., 2006). Here, we demonstrated a role of PDGFRα in invadopodia formation and matrix degradation during tumor metastasis. Interestingly, suppression of PDGFRα had no significant effects on cell proliferation or survival *in vitro* and *in vivo*. These results could be due to the greater specificity of shRNAs compared to chemical inhibition as well as differences in cellular and signaling contexts. Indeed, we found that STI571 (Gleevec), a c-ABL and c-Kit inhibitor that also inhibits PDGFR at a higher concentration, suppressed Twist1-induced invadopodia formation and matrix degradation. However,

long-term (four days) treatment with STI571 resulted in cell toxicity in HMLE-Twist1 cells (data not shown).

Our analyses identified Twist1 as a transcription inducer of PDGFRα and demonstrate a tight correlation between the expression level of Twist1 and PDGFRα in four large human breast tumor gene expression studies. Interestingly, PDGF ligand was also present in over 95% of tumor samples that expressed Twist1 and PDGFRα, indicating PDGFRα is activated in these tumors. Although these two genes alone are not sufficient to predict survival with statistical significance in these studies, these data, together with our metastasis data in mice and human breast cancer tissue array data, strongly suggest their involvement in breast cancer progression. Twist1, as a transcription factor, is difficult to target therapeutically. As a downstream target of Twist1 with roles in tumor invasion, PDGFRα might be a potentially valuable target for future therapeutics against metastasis.

Although our study focuses on the role of Twist1-induced invadopodia in metastasis, it also has important implications in development. Twist1 null mice and PDGFRα null mice both show defects in cranial neural crest development (Chen and Behringer, 1995, Sun et al., 2000). In addition, the expression pattern of Twist1 and PDGFRα are similar along the developing neural crest and craniofacial region in developing mouse embryos (Gitelman, 1997, Takakura et al., 1997). Our identification of PDGFRα as a highly conserved transcriptional target of Twist1 suggests that the pathway linking Twist1, PDGFRα, and invadopodia might play a key role in regulating neural crest development. Reactivation of this developmental machinery in tumor

metastasis is another example of an important developmental pathway regulating tumor progression.

METHODS

Cell Lines: 67NR, 168FARN, 4T1 cells and the human mammary epithelial cell lines HMLE and HMLER were cultured as previously described (Yang et al., 2004). EpH4Ras cells were maintained in mammary epithelial growth media (MEGM; Lonza; Basel, Switzerland) mixed 1:1 with Dulbecco's modification of Eagle's Media (DMEM, Mediatech, Manassas, VA)/F12 (Mediatech) supplemented with human EGF (Sigma-Aldrich, Saint Louis, MO), insulin (Sigma Aldrich), and hydrocortisone (Sigma Aldrich).

Antibodies: Antibodies were used at the following concentrations: B-actin (Abcam, ab8226, 1:20000 WB), Cortactin (Upstate, 05-180, 1:1000 WB, 1:1000 IF), Cortactin (Santa Cruz, sc-11408, 1:2000 WB), E-cadherin (BD Laboratories, 610182, 1:1000 WB), Fyn (Alexis Biochemicals, 804-564-C100, 1:1000 WB), N-cadherin (Santa Cruz, H-63, 1:1000 WB), GFP (Abcam, ab6556-25, 1:100 IF), PDGFRα (Cell Signaling, 3174, 1:2000 WB, 1:200 IHC), PDGFRB (Cell Signaling, 3169, 1:2000 WB), pY^{754}PDGFRα (Cell Signaling, 2992, 1:2000 WB), pY^{1009}PDGFRB (Cell Signaling, 3124, 1:2000 WB), Phosphotyrosine (Millipore, 05-0321, 1:1000 WB, 1:500 IF), Phosphotyrosine (Chemicon, AB1599, 1:1000 WB), Src (Cell Signaling, 2109, 1:1000 WB), Src (Cell Signaling, 2110, 1:500 IP), pY^{416}Src (Cell Signaling, 2101, 1:1000 WB), SV40LargeT (Santa Cruz , sc-147, 1:100 IHC), Tks5 (Generous gift from Dr. Sara Courtneidge, 1:1000 WB, 1:250 IF), Twist1 (Generous gift from Dr. Gitelman,

1:500 WB), Yes (BD Laboratories, BD610376, 1:1000 WB). Western blot, WB; Immunofluorescence, IF; Immunohistochemistry, IHC; Immunoprecipitation, IP)

Viral Production and Infection: Stable cell lines were created via infection of target cells using either lentiviruses or Moloney viruses. 293T cells were seeded at 1×10^6 cells per 6 cm dish in DMEM supplemented with 10%FBS (Biopioneer, San Diego, CA). After 18 hr, cells were transfected as follows: 6 µl TransIT-LT1 (Mirus Bio, USA) was added to 150 µl DMEM and incubated 20 min. One microgram of viral vector along with 0.9 µg of the appropriate gag/pol expression vector (pUMCV3 for pBabe or pWZL or pCMVΔ8.2R for lentiviral vectors) and 0.1 µg VSV-G expression vector were then added to the DMEM/LT-1 mixture. The mixture was incubated 30 min and then added to 293T cells overnight. The next day fresh media was added to the transfected 293T cells. Viral supernatant was harvested at 48 and 72 hr posttransfection, passed through a 0.45 micron syringe filter, and added to the recipient cell lines with 6 µg/ml protamine sulfate for a 4 hr infection. HMLE and EpH4Ras cells were then selected with 2 µg/ml puromycin (EMD Biosciences, USA), or 10 µg/ml blasticidin (Invitrogen, Carlsbad, CA).

Plasmids: The Twist1 and Snail cDNAs and the Twist1-ER and Snail-ER in the pWZL-Blast vector were described in Mani et al., 2009. The three shRNA lentiviral constructs against Twist1 in the pSP108 vector were described in Yang et al. (2004). The shRNA lentiviral constructs against Tks5 in the pLKO vector were provided by Dr. Sara Courtneidge (Sanford-Burnham Institute for Biomedical Research, La Jolla, CA). The shRNAmir lentiviral constructs against PDGFRα in the pGIPZ vector were

purchased from Open Biosystems. The oncogenic Ras (V12) was cloned into the pRRL lentiviral vector.

Real-Time PCR: Total RNAs were extracted from cells at 80%–90% confluency using RNeasy Mini Kit coupled with DNase treatment (QIAGEN, Venlo, Netherlands) and reverse transcribed with High Capacity cDNA Reverse Transcription Kit (Applied Biosystems, Foster City, CA). Resulting cDNAs were analyzed in triplicates using SYBR-Green Master PCR mix (Applied Biosystems) using an Applied Biosystems 7500 Fast Real Time PCR System with SDS Software. Relative mRNA concentrations were determined by $2^{-(Ct-Cc)}$ where Ct and Cc are the mean threshold cycle differences after normalizing to GAPDH values. Primer pairs used for RT-PCR are as follows:

GAPDH: 5'-GAGAGACCCTCACTGCTG, 5'-GATGGTACATGACAAGGTGC

PDGFRα: 5'-CCTGGTCTTAGGCTGTCTTCT,5'-GCCAGCTCACTTCACTCTCC

PDGFRB: 5'-AGACACGGGAGAATACTTTTGC,5'-AGTTCCTCGGCATCATGGG

Twist1: 5'-TCCGCGTCCCACTAGCA,5'-GTTATCCAGCTCCAGAGTCTCTAGAC

Src: 5'-GAGACGTGCTCACCATTGTG, 5'-GCTTCTGGACGTAGTTGGCT

Fyn: 5'-TCTGCTGCCGCCTAGTAGTT-3',5'-ACAGACAGATCGGTAAGCCTT

Yes: 5'-CTCCAGAGCCTGTCAGTACAA,5'-CTGCTGAAATTAACTGCTGTTCC

PDGF-A: 5'-CCAGCGACTCCTGGAGATAGA,5'-CTTCTCGGGCACATGCTTAGT

PDGF-B: 5'-TCTCTGCTGCTACCTGCGT, 5'-CAAAGGAGCGGATCGAGTGG

PDGF-C: 5'-ATTCACAGCCAAGGTTTCCT, 5'-GGGTCTTCAAGCCCAAATCTTT

PDGF-D: 5'-AAACGGCTACGTGCAGAGTC, 5'-CCGTGTATTCTCCGAGAGTGA

Immunoprecipitation: Cells at 80%–90% confluence were washed with PBS containing 100 μM Na_3VO_4 and lysed in lysis buffer (50 mM Tris-HCL [pH 7.5], 150 mM NaCl, 1% Triton X-100, 10 mM NaF, 100 μM Na_3VO_4, 2 mM DTT) containing 1:50 dilution Protease Inhibitor Cocktail Set III (Calbiochem, San Diego, CA). For immunoprecipitations, lysates were incubated with antibodies overnight at 4°C. Fifty microliters Protein G-Sepharose 4B conjugated beads (Invitrogen) were added for 12 hr at 4°C. Beads were washed in lysis buffer and in PBS containing 100 μM Na_3VO_4. Proteins were eluted from beads using SDS sample buffer and analyzed on 4%–12% precast SDS gels (PAGEgel, San Diego, CA).

In Situ Zymography: This protocol is adapted from Artym et al. (2009). In brief, 12 mm coverslips were incubated in 20% nitric acid for 2 hr and washed in H_2O for 4 hr. Coverslips were incubated with 50 μg/ml poly-L-lysine diluted in PBS for 15 min followed by PBS washes before 0.15% gluteraldehyde in PBS was added for 10 min, followed by PBS washes. Coverslips were inverted onto 20 μl droplets of 1:9 0.1% fluorescein isothiocyante (FITC)-gelatin (Invitrogen): 0.2% porcine gelatin (Sigma-Aldrich) for 10 min. Coverslips were washed in PBS and then incubated 15 min in 5 mg/ml $NaBH_4$. Coverslips were rinsed in PBS and incubated at 37° in 10% calf serum (Hyclone, USA) in DMEM for 2 hr. Twenty thousand cells were seeded on each coverslip, incubated for 8 hr, and processed for immunofluorescence. Each experiment was performed in triplicate. Images were taken at ten fields per sample for a total of approximately 150 cells per sample with a Deltavision RT Deconvolution Microscope with MetaMorph software. Gelatin degradation was quantified using ImageJ software. To measure the percentage of degraded area in each field, identical signal threshold for

the FITC-gelatin fluorescence are set for all images in an experiment and the degraded area with FITC signal below the set threshold was measured by ImageJ. The resulting percentage of degradation area was further normalized to total cell number (counted by DAPI staining for nuclei) in each field. The final gel degradation index is the average percentage degradation per cell obtained from all ten fields. Each experiment was repeated at least three times.

Immunofluorescence: Matrix substrates were prepared using 0.2% porcine gelatin as for in situ zymography. Cells were fixed at 37°C in 4% paraformaldehyde (PFA)/PBS with 50 μM $CaCl_2$ for 15 min, permeabilized with 0.1% Triton X-100/PBS for 10 min, and blocked with 5% goat serum. Samples were incubated with primary antibodies overnight at 4°C and with secondary antibodies and/or phalloidin for 2 hr. After washing, coverslips were mounted with VectaShield HardSet (Vector Laboratories, Burlingame, CA). Images were collected with a Deltavision RT Deconvolution Microscope with MetaMorph software.

Chromatin Immunoprecipitation: Cells at 80% confluence were crosslinked with 4% PFA, lysed, and sonicated. Nuclear lysates were incubated with Protein G Dynabeads (Invitrogen) preconjugated with antiestrogen receptor antibody overnight. DNA was reverse crosslinked and purified by phenol-chloroform and ethanol precipitation.

Subcutaneous Tumor Implantation and Metastasis Assay: All animal care and experiments were approved by the Institutional Animal Care and Use Committee (IACUC) of the University of California, San Diego. Cells (1.5 million) resuspended in 50% Matrigel (BD Biosciences, USA) were injected into the left and right flanks of

nude mice and allowed to grow to about 2 cm in diameter before mice were sacrificed. Primary tumor size was measured every 5 days. Lungs were harvested and imaged for GFP positive tumor cells with a Leica MZ16F with ImagePro MC6.1 software. Tissues were embedded in paraffin, sectioned, stained with hematoxylin and eosin, and imaged to identify GFP positive tumor cells.

Three-Dimensional Cell Culture: Equal volumes of neutralized collagen I (Millipore, USA) and Matrigel were mixed on ice and 20 µl added to the bottom of each well of an eight chamber coverglass slide. Cells of interest were mixed with the Matrigel:collagen mix to give a final concentration of 200,000 cells per ml and 100 cells µl of the cell:matrix mixture added to each well. Media was changed every other day until establishment of spherical colonies. TGFβ1 (R&D Systems, Minneapolis, MN) was added at 5 ng/ml every other day for up to 2 weeks. Cells were fixed with 4% PFA and processed as described above for immunofluorescence.

Immunohistochemistry: Paraffin sections of human or mouse samples were rehydrated through xylene and graded alcohols. Antigen retrieval was accomplished using a pressure cooker in 10 mM sodium citrate with 0.05% Tween. Samples were incubated with 3% H_2O_2 for 30 min followed by 5 hr blocking in 20% goat serum in PBS. Endogenous biotin and avidin were blocked using a Vector Avidin/Biotin blocking kit (Vector Laboratories). Primary antibodies were incubated overnight at 4°C in 20% goat serum. Biotinylated secondary antibody and Vectorstain ABC kit (Vector Laboratories) were used as indicated by manufacturer. Samples were developed with diaminobenzidine (DAB) (Vector Laboratories) and samples counterstained with hematoxylin (Vector Laboratories) and mounted with Permount.

Gelatin Zymography: Conditioned media were collected from cells at 80-90% confluency for 2 days. SDS loading buffer without DTT was added to samples of conditioned media and incubated at room temperature for 15 min. Samples were analyzed using 10% gelatin zymogram gels (Invitrogen). Gels were first incubated in Zymogram Renaturing Buffer (Invitrogen) for one hour and then incubated in Zymogram Developing Buffer (Invitrogen) overnight at 37^{o}C. Gels were stained in hot 0.1% Coomassie R-250 (EMD)/40% ethanol/10% acetic acid for 30 min and destained in 10% ethanol/7.5% acetic acid for 30 min.

Invasion and Migration Assays: For invasion assays, 50 μg of Matrigel was overlayed on Transwell permeable supports, dried overnight, and reconstituted with mammary epithelial growth media lacking recombinant epidermal growth factor. 40,000 cells were plated onto each well in triplicate and incubated for 72 hours. Cells were fixed with 4% PFA in PBS, washed extensively with PBS, stained with 0.1% crystal violet, washed extensively with PBS, and dried. Crystal violet was released with 50 μL 10% acetic acid and absorbency measured at 520 nm with an IMPLEN Nanophotometer. Identical protocols were used for migration assays using Transwells without Matrigel. All assays were performed in triplicates.

Luciferase Reporter Assay: MCF7 cells were transfected with PDGFRα prom-Luc reporter plasmid, pGL4[Rluc] plasmid, Twist1 and its dimerization partner E47. 24 hours later, the cell lysates were assayed using dual-luciferase assay kit (Promega, USA) with an EG&G Berthold AutoLumat LB953. The firefly luciferase activity was normalized to that of Renilla luciferase to control transfection efficiency between samples.

Bioinformatics and Statistical Analysis: Four published microarray datasets were downloaded from NCBI's Gene Expression Omnibus (GEO), a public repository of microarray data. Obtained GEO identifiers (Study name, sample size) were GSE1456 (STOCKHOLM, n=159), GSE2034 (EMC, n=286), GSE2990 (NCI, n=187), and GSE3494 (UPPSALA, n=236). All samples were from breast cancer patients. Quantile-normalization was performed on an integrated dataset of .CEL files from individual patients to achieve the same distribution of signals across samples within a study (Bolstad et al., 2005). Multiple measurement values were aggregated at the probeset-level per patient with the Median-Polish technique (Irrizary et al., 2003). Measurement values of the two probesets were plotted in Figure S8C with a linear regression model fit. The rank-based Spearman correlation coefficient is displayed in the figure.

Spurious probesets were removed from the data analysis after a custom annotation process based on the probe sequences. In Affymetrix arrays, a gene is represented by multiple probesets composed of 11-20 probes. However, some probe sequences did not align to an exon and therefore produced off-target measurement values (as opposed to the manufacturer's probeset-to-gene annotation). For example, none of the 11 probes of the probeset '211533_at' in HG-133A platform aligned to the gene/transcript region (chr4:54790021-54841682) of the gene PDGFRα that was the suggested target by the manufacturer's original annotation. This erroneous annotation of probesets has been previously pointed out by other investigators (Dai et al., 2005; Ferrari et al., 2007). Previously, our group has also shown that re-annotation of microarray probes using their sequence is a crucial step in cross-platform studies of

microarray data (Kuo et al., 2006). The same filtering technique was applied to the four breast cancer studies above.

Once each probe was aligned to genome using BLAT (Kent et al., 2002), its genomic position was matched against AceView gene models to obtain the target gene, as AceView provides a comprehensive evidence-based gene/transcript annotation (Thierry-Mieg et al., 2006). Our selection criteria for a "good" probeset was that it needed to have all its member probes perfectly aligned within exons of a given gene using the AceView gene model. Therefore, probeset '213943_at' was chosen for TWIST1 and '203131_at' for PDGFRα. Two probesets '211533_at' and '215305_at' supposedly targeting PDGFRα in the original annotation were removed. Follow-up RT-PCR results supported our findings.

ACKNOWLEDGMENTS

This chapter was reproduced with permission from co-authors, modified from the publication: Mark A. Eckert, Thinzar M. Lwin, Andrew T. Chang, Jihoon Kim, Etienne Danis, Lucila Ohno-Machado, and Jing Yang. "Twist1-induced invadopodia formation promotes tumor metastasis." Cancer Cell. Vol. 19, Issue 3, 372-386, March 8, 2011.

We are grateful to Dr. Sara Courtneidge and the members of her laboratory, especially Begoňa Diaz and Danielle Murphy, for their suggestions and for providing the antibody and shRNA constructs for Tks5. We thank Drs. Robert A. Weinberg, Alexandra Newton, Kun-Liang Guan, and other members of the Yang lab for their suggestions to the manuscript. We thank Dr. David Cheresh for providing Yes and Fyn

antibodies. We thank Dr. Cornelis Murre for providing the E47 expression construct. We thank the NCI Cancer Diagnosis Program (CDP) for providing breast tumor tissue microarray slides. We thank the Shared Microscope Facility and UCSD Cancer Center Specialized Support Grant P30 CA23100. This work was supported by grants to J. Y. from NIH (DP2 OD002420-01), Kimmel Scholar Award, and California Breast Cancer Research Program (12IB-0065), by a NIH Molecular Pathology of Cancer Predoctoral Training grant and a DOD Breast Cancer Predoctoral fellowship (M.A.E), by an NIH Pharmacological Science Predoctoral Training grant (A.T.C), by a DOD Breast Cancer Era of Hope Postdoctoral Fellowship (E.D.), and by the Susan G. Komen Foundation grant FAS0703850 (J.K. and L.O.).

REFERENCES

Abram, C. L., Seals, D. F., Pass, I., Salinsky, D., Maurer, L., Roth, T. M., and Courtneidge, S. A. (2003). The adaptor protein fish associates with members of the ADAMs family and localizes to podosomes of Src-transformed cells. J Biol Chem *278*, 16844–16851.

Artym, V. V., Yamada, K. M., and Mueller, S. C. (2009). ECM degradation assays for analyzing local cell invasion. Methods Mol Biol *522*, 211–219.

Ayala, I., Baldassarre, M., and Giacchetti, G. (2008). Multiple regulatory inputs converge on cortactin to control invadopodia biogenesis and extracellular matrix degradation. J Cell Sci *121*, 369–378.

Batlle, E., Sancho, E., Franci, C., Dominguez, D., Monfar, M., Baulida, J., and Garcia De Herreros, A. (2000). The transcription factor snail is a repressor of Ecadherin gene expression in epithelial tumour cells. Nat Cell Biol *2*, 84–89.

Blake, R. A., Broome, M. A., Liu, X., Wu, J., Gishizky, M., Sun, L., and Courtneidge, S. A. (2000). SU6656, a selective Src family kinase inhibitor, used to probe growth factor signaling. Mol Cell Biol *20*, 9018–9027.

Blouw, B., Seals, D. F., Pass, I., Diaz, B., and Courtneidge, S. A. (2008). A role for the podosome/invadopodia scaffold protein Tks5 in tumor growth *in vivo*. Eur J Cell Biol *87*, 555–567.

Bolstad, B. M., Irizarry, R. A., Astrand, M., Speed, T. P. (2003). A comparison of normalization methods for high density oligonucleotide array data based on variance and bias. Bioinformatics *19*, 185-93.

Bowden, E. T., Onikoyi, E., Slack, R., Myoui, A., Yoneda, T., Yamada, K. M., and Mueller, S. C. (2006). Co-localization of cortactin and phosphotyrosine identifies active invadopodia in human breast cancer cells. Exp Cell Res *312*, 1240–1253.

Boyer, B., and Thiery, J. P. (1993). Epithelium-mesenchyme interconversion as example of epithelial plasticity. APMIS *101*, 257–268.

Buschman, M. D., Bromann, P. A., Cejudo-Martin, P., Wen, F., Pass, I., and Courtneidge, S. A. (2009). The novel adaptor protein Tks4 (SH3PXD2B) is required for functional podosome formation. Mol Biol Cell *20*, 1302–1311.

Cano, A., Perez-Moreno, M. A., Rodrigo, I., Locascio, A., Blanco, M. J., del Barrio, M. G., Portillo, F., and Nieto, M. A. (2000). The transcription factor snail controls epithelial-mesenchymal transitions by repressing E-cadherin expression. Nat Cell Biol *2*, 76–83.

Chen, W.T. (1989). Proteolytic activity of specialized surface protrusions formed at rosette contact sites of transformed cells. J Exp Zool *251*, 167–185.

Chen, Z. F., and Behringer, R. R. (1995). Twist is required in head mesenchyme for cranial neural tube morphogenesis. Genes Dev *9*, 686–699.

Comijn, J., Berx, G., Vermassen, P., Verschueren, K., van Grunsven, L., Bruyneel, E., Mareel, M., Huylebroeck, D., and van Roy, F. (2001). The twohanded E box binding zinc finger protein SIP1 downregulates E-cadherin and induces invasion. Mol Cell *7*, 1267–1278.

Dai, M., Wang, P., Boyd, A.D., Kostov, G., Athey, B., Jones, E.G., Bunney, W. E., Myers, R. M., Speed, T. P., and Akil, H. (2005). Evolving gene/transcript definitions significantly alter the interpretation of GeneChip data. Nucleic Acids Res *33*, e175.

Ferrari, F., Bortoluzzi, S., Coppe, A., Sirota, A., Safran, M., Shmoish, M., Ferrari, S., Lancet, D., Danieli, G. A., Bicciato, S. (2007). Novel definition files for human GeneChips based on GeneAnnot. BMC Bioinformatics *8*, 446.

Gitelman, I. (1997). Twist protein in mouse embryogenesis. Dev Biol *189*, 205–214.

Hajra, K. M., Chen, D. Y., and Fearon, E. R. (2002). The SLUG zinc-finger protein represses E-cadherin in breast cancer. Cancer Res *62*, 1613–1618.

Hamamori, Y., Wu, H. Y., Sartorelli, V., and Kedes, L. (1997). The basic domain of myogenic basic helix-loop-helix (bHLH) proteins is the novel target for direct inhibition by another bHLH protein Twist. Mol Cell Biol *17*, 6563–6573.

Hay, E. D. (1995). An overview of epithelio-mesenchymal transformation. Acta Anat. (Basel) *154*, 8–20.

Irizarry, R. A., Bolstad, B. M., Collin, F., Cope, L. M., Hobbs, B., Speed, T. P. (2003). Summaries of Affymetrix GeneChip probe level data. Nucleic Acids Res *31*, e15.

Jechlinger, M., Grunert, S., Tamir, I.H., Janda, E., Ludemann, S., Waerner, T., Seither, P., Weith, A., Beugh, H., and Kraut, N. (2003). Expression profiling of epithelial plasticity in tumor progression. Oncogene *16*, 7155–7169.

Jechlinger, M., Sommer, A., Moriggl, R., Seither, P., Kraut, N., Capodiecci, P., Donovan, M., Cordon-Cardo, C., Beug, H., and Grunert, S. (2006). Autocrine PDGFR signaling promotes mammary cancer metastasis. J Clin Invest *116*, 1561–1570.

Kent, W. J. (2002). BLAT—the BLAST-like alignment tool. Genome Res *12*, 656-64.

Kuo, W. P., Liu, F., Trimarchi, J., Punzo, C., Lombardi, M., Sarang, J., Whipple, M. E., Maysuria, M., Serikawa, K., and Lee, S. Y. (2006). A sequence-oriented comparison of gene expression measurements across different hybridization-based technologies. Nat Biotechnol *24*, 832-40.

Kypta, R. M., Goldberg, Y., Ulug, E. T., and Courtneidge, S. A. (1990). Association between the PDGF receptor and members of the src family of tyrosine kinases. Cell *62*, 481–492.

Laursen, K. B., Mielke, E., Iannaccone, P., and Fuchtbauer, E. M. (2007). Mechanism of transcriptional activation by the proto-oncogene Twist1. J Biol Chem *282*, 34623–34633.

Linder, S. (2007). The matrix corroded: podosomes and invadopodia in extracellular matrix degradation. Trends Cell Biol. *17*, 107–117.

Mani, S. A., Yang, J., Brooks, M., Schwaninger, G., Zhou, A., Miura, N., Kutok, J. L., Hartwell, K., Richardson, A. L., and Weinberg, R. A. (2007). Mesenchyme Forkhead 1 (FOXC2) plays a key role in metastasis and is associated with aggressive basal-like breast cancers. Proc Natl Acad Sci USA *104*, 10069–10074.

Mani, S. A., Guo, W., Liao, M. J., Eaton, E. N., Ayyanan, A., Zhou, A. Y., Brooks, M., Reinhard, F., Zhang, C. C., and Shipitsin, M. (2008). The epithelial-mesenchymal transition generates cells with properties of stem cells. Cell *133*, 704–715.

Miller, L. D., Smeds, J., George, J., Vega, V. B., Vergara, L., Ploner, A., Pawitan, Y., Hall, P., Klaar, S., and Liu, E. T. (2005). An expression signature for p53 status in human breast cancer predicts mutation status, transcriptional effects, and patient survival. Proc Natl Acad Sci USA *102*, 13550–13555.

Nakaya, Y., Sukowati, E. W., Wu, Y., and Sheng, G. (2008). RhoA and microtubule dynamics control cell-basement membrane interaction in EMT during gastrulation. Nat Cell Biol *10*, 765–775.

Pawitan, Y., Bjohle, J., Amler, L., Borg, A. L., Egyhazi, S., Hall, P., Han, X., Holmberg, L., Huang, F., and Klaar, S. (2005). Gene expression profiling spares early breast cancer patients from adjuvant therapy: derived and validated in two population-based cohorts. Breast Cancer Res *7*, R953–R964.

Peinado, H., Olmeda, D., and Cano, A. (2007). Snail, Zeb and bHLH factors in tumour progression: an alliance against the epithelial phenotype? Nat Rev Cancer *7*, 415–428.

Seals, D. F., Azucena, E. F., Jr., Pass, I., Tesfay, L., Gordon, R., Woodrow, M., Resau, J. H., and Courtneidge, S. A. (2005). The adaptor protein Tks5/fish is required for podosome formation and function, and for the protease-driven invasion of cancer cells. Cancer Cell *7*, 155–165.

Seymour, L., and Bezwoda, W. R. (1994). Positive immunostaining for platelet derived growth factor is an adverse prognostic factor in patients with advanced breast cancer. Breast Cancer Res Treat *32*, 229–233.

Sotiriou, C., Wirapati, P., Loi, S., Harris, A., Fox, S., Smeds, J., Nordgren, H., Farmer, P., Praz, V., and Haibe-Kains, B. (2006). Gene expression profiling in breast cancer: understanding the molecular basis of histologic grade to improve prognosis. J Natl Cancer Inst *98*, 262–272.

Sun, T., Jayatilake, D., Afink, G. B., Ataliotis, P., Nister, M., Richardson, W. D., and Smith, H. K. (2000). A human YAC transgene rescues craniofacial and neural tube development in PDGFRalpha knockout mice and uncovers a role for PDGFRalpha in prenatal lung growth. Development *127*, 4519–4529.

Takakura, N., Yoshida, H., Ogura, Y., Kataoka, H., Nishikawa, S., and Nishikawa, S. I. (1997). PDGFRa expression during mouse embryogenesis: immunolocalization analyzed by whole-mount immunohistostaining using the monoclonal anti-mouse PDGFRa antibody APA5. J Histochem Cytochem *45*, 883–893.

Tarone, G., Cirillo, D., Giancotti, F. G., Comoglio, P. M., and Marchisio, P. C. (1985). Rous sarcoma virus-transformed fibroblasts adhere primarily at discrete protrusions of the ventral membrane called podosomes. Exp Cell Res *159*, 141–157.

Thierry-Mieg, D., Thierry-Mieg, J. (2006). AceView: a comprehensive cDNA-supported gene and transcripts annotation. Genome Biol *7*, S12.

Wang, Y., Klijn, J. G., Zhang, Y., Sieuwerts, A. M., Look, M. P., Yang, F., Talantov, D., Timmermans, M., Meijer-van Gelder, M. E., and Yu, J. (2005). Gene-expression profiles to predict distant metastasis of lymph-node-negative primary breast cancer. Lancet *365*, 671–679.

Yang, J., Mani, S. A., Donaher, J. L., Ramaswamy, S., Itzykson, R. A., Come, C., Savagner, P., Gitelman, I., Richardson, A., and Weinberg, R. A. (2004). Twist, a master regulator of morphogenesis, plays an essential role in tumor metastasis. Cell *117*, 927–939.

Chapter III:

ADAM12 is Required for Twist1-Induced Motility and Invadopodia Formation

ABSTRACT

Invadopodia play a central role in mediating local invasion and metastasis downstream of Twist1. Although PDGFRα plays an essential role in inducing invadopodia formation regulated by Twist1, other genes involved in invadopodia are also regulated by Twist1. Here we find that Twist1 strongly induces expression of a disintegrin and metalloprotease 12 (ADAM12). Knockdown of ADAM12 leads to a decrease in motility and invasion independent of any effects on the epithelial-mesenchymal transition (EMT) in multiple cell lines. In addition, we find that knockdown of ADAM12 increases focal adhesion number and increases overall cell adhesion to the ECM. ADAM12 is also involved in regulation of invadopodia formation: knockdown of ADAM12 significantly decreases invadopodia formation and associated gelatin degradation. In a series of mutagenesis rescue experiments, we find that the disintegrin domain of ADAM12 is involved in both regulation of focal adhesions and invadopodia formation while the metalloprotease domain is also required for efficient invadopodia formation. Finally, we demonstrate a role for ADAM12 in local invasion in a 3D organoid model of local invasion and in metastasis in a mouse model of breast cancer metastasis.

INTRODUCTION

Understanding how cells gain the ability to invade during the metastatic process is essential in not only elucidating the mechanisms of cancer invasiveness, but also in designing new therapeutics targeting conserved pathways. Invadopodia are hypothesized to be essential mediators of local invasion and eventual metastasis in cancer by increasing proteolytic activity at areas of the cell in contact with the extracellular matrix (Linder, 2009; Gimona et al., 2008; Murphy and Courtneidge, 2011). Identifying invadopodia components essential for the formation and function of invadopodia has great potential to discover new pathways and regulatory components necessary for metastasis. The transmembrane metalloprotease a disintegrin and metalloprotease 12 (ADAM12) is an exciting target with interesting roles in metastasis and invadopodia formation.

ADAM12 is a member of the adamlysin family of zinc-dependent metalloproteases united by the common feature of possessing both a metalloprotease and a disintegrin domain (Kveiborg et al., 2008). Immediately C-terminal to the disintegrin domain are a cysteine-rich domain, an epidermal growth factor (EGF)-like domain, and a short (33 amino acid), unique cytoplasmic tail. ADAM12 is embedded in the membrane via a transmembrane domain (Figure 3.1). In addition to the full-length ADAM12 protein, there is an additional splice variant of ADAM12, ADAM12S, that lacks the transmembrane and cytoplasmic domains, replacing them with a short, unique peptide sequence (Gilpin et al., 1998).

The metalloprotease domain of ADAM12 is typical of metzyncins with a conserved HEXXHXXGXXH zinc-binding consensus sequence (Jacobsen et al., 2008).

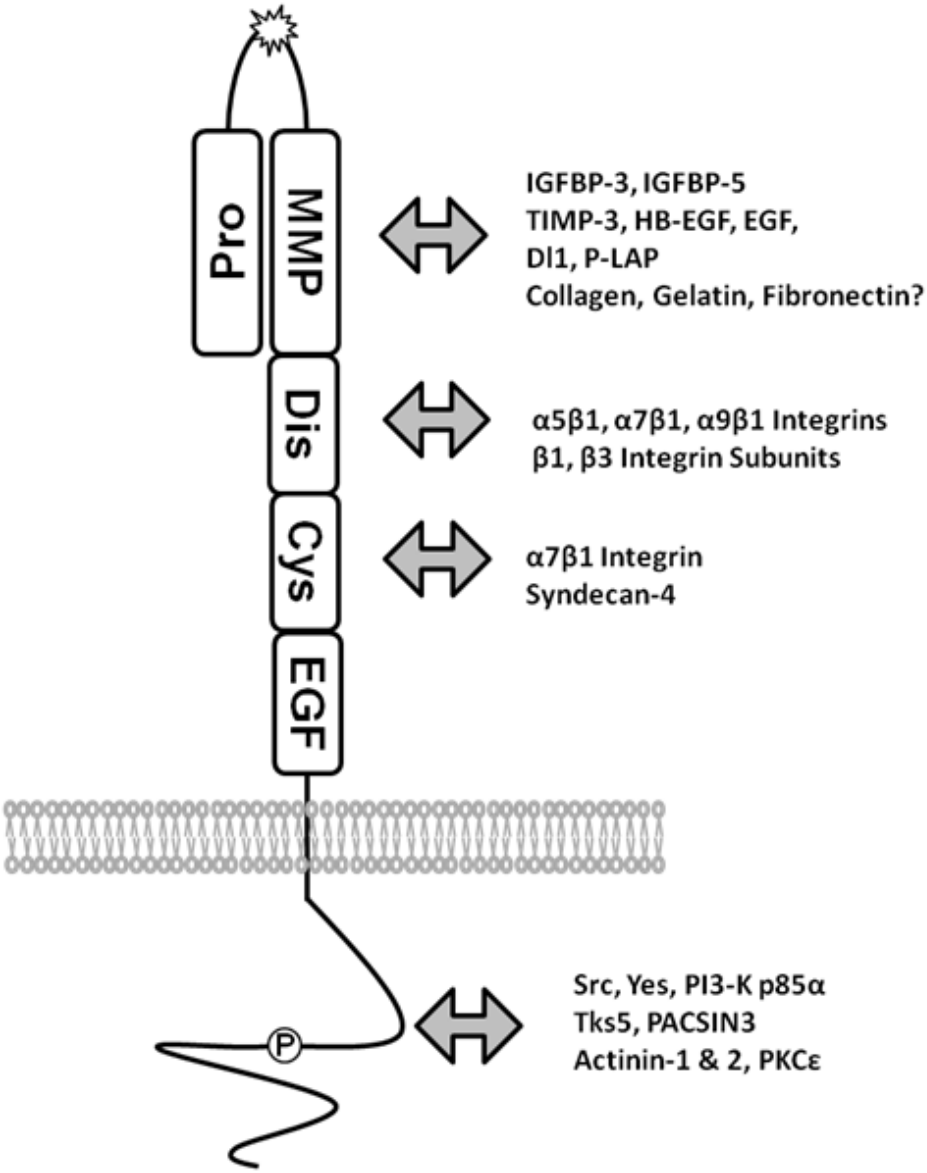

Figure 3.1: ADAM12 Structure. Schematic of ADAM12 domain architecture. Domains, from amine to carboxy terminus: PRO, propeptidase; MMP, zinc metalloprotease; DIS, disintegrin; CYS, cysteine-rich; EGF, EGF-like. Following the transmembrane domain is a C-terminal cytoplasmic tail that can be tyrosine phosphorylated (P). Proteins that have been shown to directly interact with specific domains of ADAM12 are indicated by the double-headed arrow (Kveiborg et al., 2008)

The catalytic activity of the enzyme remains latent until processed in the Golgi by a furin-like proprotein convertase (Wewer et al. 2006). The prodomain also contains a short signal sequence to direct ADAM12 to the secretory pathway for eventual delivery to the membrane (Loechel et al., 1999). The propeptidase domain remains associated with ADAM12 after cleavage and may be required for its trafficking to the membrane (Wewer et al. 2006).

As a transmembrane protease, ADAM12 acts as a sheddase capable of releasing membrane-bound ligands from the cell surface (Seals and Courtneidge, 2003). The most well-characterized substrates for ADAM12 in this regard are heparin-binding EGF (HB-EGF), delta-like 1 (Dl1), and phospholipase A2-activating protein (P-LAP) (Ito et al., 2004; Dyczynska et al., 2007; Asakura et al., 2002). HB-EGF and Dl1 cleavage leads to activation of the EGF and Notch pathways, respectively, while cleavage of P-LAP releases a placental oxytocinase (Ito et al., 2004; Dyczynska et al., 2007; Asakura et al., 2002). In addition, ADAM12S is capable of proteolytically processing insulin-like growth factor binding protein 3 (IGFBP-3) and IGFBP-5 (Loechel et al., 2000). Cleavage of IGFBPs by ADAM12 may have contradictory effects that depend on cell context, as IGFBPs may either potentiate IGFR signaling or sequester IGF ligands (Clemmons, 1998).

ADAM12 was initially described as capable of *in vitro* cleavage of ECM components, including fibronectin, collagen, and gelatin, but more recent reports have been unable to duplicate these observations (Jacobsen et al., 2008; Roy et al., 2004). The metalloprotease activity of ADAM12 is attenuated at the cell surface via interactions with tissue inhibitor of metalloprotease 2 (TIMP-2) and TIMP-3 (Loechel

et al., 2000). No commercially-available small-molecule inhibitors specific to ADAM12 exist, although its activity is strongly attenuated by hydroxamate metalloprotease inhibitors such as GM6001 (Oh et al., 2004). A synthetic peptide derived from TIMP-2 shows strong promise as a specific inhibitor of ADAM12 metalloprotease activity with nanomolar affinities for ADAM12 (Kveiborg et al., 2010).

Directly C-terminal to the metalloprotease domain of ADAM12 is a disintegrin domain (Kveiborg et al., 2008). Initially discovered in snake venom metalloproteases, the disintegrin domain usually contains an integrin-interacting sequence such as an RGD motif that is suspected to disrupt integrin-ECM interactions through competitive inhibition (Gutiérrez et al., 2005). ADAM12 lacks such an RGD motif, instead possessing an RX6DEVF motif that can interact with α9β1 integrin (Zolkiewska 1999). In addition, ADAM12 has been reported to directly interact with α7β1 and α5β1 integrin heterodimers and individually with β1 and β3 subunits (Thodeti et al. 2005; Zhao et al. 2004; Huang, Bridges, and White 2005). ADAM12 preferentially interacts with β1 integrin in the presence of both β1 and β3 integrin, but interactions with β3 integrin do occur in the abscence of β1 integrin (Thodeti et al., 2005). Direct interactions with β1 integrin attenuate attachment and integrin-linked signaling (Kawaguchi et al., 2003).

Functional studies on the role of the disintegrin domain of ADAM12 in mediating integrin activation and signaling have reached contradictory conclusions. When cells were plated on a substrate coated with recombinant peptides derived from the disintegrin domain of ADAM12, overall cell attachment was increased (Thodeti et al., 2005). In contrast, expression of ADAM12 in adipocytes led to a loss of focal

adhesions and an increase in integrin solubility, indicative of a decrease in cell attachment strength (Kawaguchi et al., 2003; Kveiborg et al., 2008). These results imply that cell-bound ADAM12 is capable of disrupting cell-ECM integrin interactions, while use of ADAM12 as a substrate for cell attachment enhances integrin-mediated adhesion via direct interactions between exogenous ADAM12 and cell-anchored integrins.

The cysteine-rich domain of ADAM12 immediately follows the disintegrin domain and has roles in mediating cellular-adhesion and interactions with ECM. The mechanism of the interaction with the ECM through this domain is primarily through binding of proteoglycans such as syndecan-4 (Thodeti et al., 2003). Interactions with syndecan-4 promotes cell adhesion and spreading and require the cysteine-rich domain. In addition, the cysteine-rich region of ADAM12 also cooperates with the disintegrin domain to mediate interactions with α7β1 integrin (Zhao et al., 2004). Interestingly, a hydrophobic region within the cysteine-rich region bears strong similarities to a viral fusion protein sequence (Blobel et al., 1992). This has led to proposals that ADAM12, which is highly expressed in developing muscles, is involved in myoblast fusion during muscle development (Kveiborg et al., 2008; Yagami-Hiromasa et al., 1995). The cysteine-rich domain of ADAM12 remains relatively uncharacterized, however, and is clearly an interesting target for future research.

The EGF-like domain of ADAM12 has not been studied by mutagenesis or with any functional assays. EGF-like domains in other proteins contribute to the 3D structure and topology of membrane-bound proteins through formation of dual beta-sheets formed via the interactions of six conserved cysteine residues within the domain (Bork et al., 1996). It is likely the EGF-like domain in ADAM12 plays a similar role.

ADAM12 has a unique 179 amino acid cytoplasmic tail that may play roles in the subcellular localization of ADAM12 or in recruitment of other proteins. The cytoplasmic tail possesses proline-rich PxxP regions that are classic Src homology 3 (SH3)-binding domains (Abram et al., 2003; Kang et al., 2001). In addition, ADAM12 is tyrosine phosphorylated in response to constitutive Src activity, creating potential sites for interaction with proteins that contain SH2 domains (Stautz et al., 2010). The cytoplasmic tail also directly interacts with the nonreceptor tyrosine kinases Src and Yes, the p85α subunit of phosphoinositide 3-kinase (PI3-K), the adaptor protein Grb2, and the invadopodia-specific scaffolding protein Tks5 (Kang et al., 2001; Kang et al., 2000; Suzuki et al., 2000; Abram et al., 2003). Unknown regions of the cytoplasmic tail also mediate interactions with both actinin 1 and 2 (Galliano et al., 2000; Cao et al., 2001). Both actinins are involved in linkage of the actin cytoskeleton to focal adhesions, suggesting a role for ADAM12 in focal adhesion biogenesis or regulation (Sjöblom et al., 2008). The cytoplasmic tail of ADAM12 additionally serves as a subcellular retention signal, preventing translocation of the protein to the membrane until phosphorylation by protein kinase C ε (PKCε) (Sundberg et al., 2004).

Under non-pathological conditions, ADAM12 expression is highest in muscle and adipose tissue during development and was initially thought to play an essential role in myogenesis and muscle formation (Yagami-Hiromasa et al., 1995). ADAM12 knockout mice are viable and fertile, however (Kurisaki et al., 2003). In fact, in ADAM9-ADAM12-ADAM15 triple knockout mice, the only overt defects were a slight reduction in skeletal muscle in the upper trunk and a lack of brown fat tissue (Sahin et al., 2004). As there are over twenty adamalysins, many of them poorly characterized,

compensation by other members of the family is a clear possibility (Kveiborg et al., 2008).

ADAM12 is associated with disease stage in both breast and bladder cancer (Narita et al., 2012; Fröhlich et al., 2006). In addition, expression of ADAM12 has been reported in liver, lung, stomach, and colon cancer, as well as glioblastoma (Kveiborg et al., 2008). Soluble ADAM12, either ADAM12S or a cleaved form of full-length ADAM12, is found at high levels in the urine of breast cancer patients and is associated with cancer progression (Roy et al., 2004). Expression of ADAM12 under the control of a mammary-gland specific promoter was not sufficient for tumorigenesis is a transgenic mouse model (Kveiborg et al., 2005). Induction of mammary cancer by crossing this mouse into a mouse mammary tumor virus (MMTV)-polyoma middle T (pYMT) background led to a significant increase in tumor growth rate and metastasis to the lung with an additional expansion of the stromal compartment in the primary tumor (Kveiborg et al., 2005). Similarly, in a mouse model of prostate cancer, ADAM12 was found to be essential for prostate tumor growth (Peduto et al., 2006). Combined, these models demonstrate a clear role for ADAM12 in tumor growth and progression, but do not address the potential mechanism by which ADAM12 induces these phenotypes. Interestingly, these results are reminiscent of those obtained when Tks5 was knocked down in xenotransplantation experiments (Blouw et al., 2008). These results may suggest an important role for invadopodia in mediating tumor growth through release of growth factors from the cell surface or surrounding ECM.

Interestingly, ADAM12 localizes to invadopodia in Hs578t cells (Courtneidge et al., 2005). In addition, both ADAM12 and the highly-related ADAM19 directly interact

with the vital invadopodia scaffolding protein Tks5 (Abram et al., 2003). Albrechtsen et al. developed an antibody directed against ADAM12 that induces clustering of ADAM12 and subsequent invadopodia formation at sites of clustering. The mechanism is dependent on the metalloprotease activity of ADAM12 and is hypothesized to induce localized shedding of EGF ligand at invadopodia (Albrechtsen et al., 2011). In light of the critical role for Src activity in invadopodia formation, the observation that ADAM12 expression increases Src activation via an unknown mechanism when expressed in C2C12 cells provides a potential role for ADAM12 in inducing localized activation of Src kinases at invadopodia (Kang et al., 2001). The ability of ADAM12 to interact with integrins through the disintegrin domain suggests a possible role for ADAM12 in modulating integrin interactions at invadopodia (Kawaguchi et al., 2003).

Based on the roles of ADAM12 in invadopodia formation and interesting ability to act as a robust biomarker for progression, we were therefore interested in determining the functions of ADAM12 in Twist1-induced invasion and invadopodia formation.

RESULTS

Twist1-induced ADAM12 is necessary for efficient migration. Due to the possible role for ADAM12 in invadopodia formation and the robust induction of invadopodia observed following Twist1 expression, we first sought to determine if ADAM12 was in fact upregulated following Twist1 activation. To these ends, we first utilized a Twist1-estrogen receptor (Twist1-ER) fusion protein construct (Yang et al., 2004). In the absence of 4-hydroxytamoxifen (4-OHT), the Twist1-ER protein is sequestered in the cytoplasm due to interactions with heat shock proteins (HSPs). Upon addition of 4-OHT, the interaction between Twist1-ER and HSPs is disrupted, allowing the fusion

protein to translocate to the nucleus (Whelan and Miller, 1996). We induced Twist1-ER activation (nuclear translocation) by addition of 4-OHT and collected mRNA at time points from 0 days to 14 days. A robust induction of ADAM12 expression in response to Twist1 expression was observed, beginning 24 to 48 hours after addition of 4-OHT (Figure 3.2 A). These results implied that ADAM12 is a downstream target of Twist1.

We next verified that Twist1 mRNA was translated and expressed at the protein level. Overexpression of Twist1 in human mammary epithelial cells (HMLEs) was sufficient to induce a strong upregulation of ADAM12 protein (Figure 3.2 B); the two bands likely correspond to pro-ADAM12 and the activated, cleaved form of ADAM12 (Wewer et al., 2006). To determine if Twist1 was necessary for invadopodia formation we made use of the Hs578t cell line. This breast cancer cell line is ideal due to both forming large numbers of ADAM12-positive invadopodia and expressing Twist1 (Figure 3.2 B) (Courtneidge et al., 2005). We virally transduced the Hs578t cells with constructs containing control (shCtrl) or knockdown (shTwist) shRNAs against Twist1 (Yang et al., 2004). Both were effective at knocking down expression of Twist1 and also reduced expression of ADAM12 (Figure 3.2 C). We therefore concluded that Twist1 is both necessary and sufficient for induction of ADAM12 expression.

To investigate more fully the effects of ADAM12 on Twist1-induced invasion and metastasis, we virally transduced HMLE-Twist1 and Hs578t cell populations with two shRNA constructs against ADAM12 (shADAM12.1 and shADAM12.4). Both constructs were stable and efficient at knocking down ADAM12 expression at the protein level in both HMLE-Twist1 (Figure 3.2 B) and Hs578t cells

Figure 3.2: Twist1 is necessary and sufficient for ADAM12 expression. (A) RT-PCR for ADAM12 normalized to GAPDH in HMLE cells expressing either Twist1-ER or Myc-ER (Control) at the indicated time points following treatment with 4-hydroxytamoxifen. Y-axis is $\log_2$ scale. (B) Immunoblot for ADAM12 and β-actin of SDS-PAGE of HMLE or HMLE-Twist1 cells expressing the indicated constructs. (C) Immunoblot for ADAM12, Twist1, and B-actin of SDS-PAGE of Hs578t cells expressing the indicated constructs. (D) Immunoblot for ADAM12 and β-actin of SDS-PAGE of Hs578t cells expressing the indicated constructs. (E) Brightfield images of HMLE-Twist1 cells expressing the indicated constructs. (F) Immunoblot for N-cadherin, E-cadherin, MT1-MMP, and β-actin of SDS-PAGE of HMLE or HMLE-Twist1 cells expressing the indicated constructs.

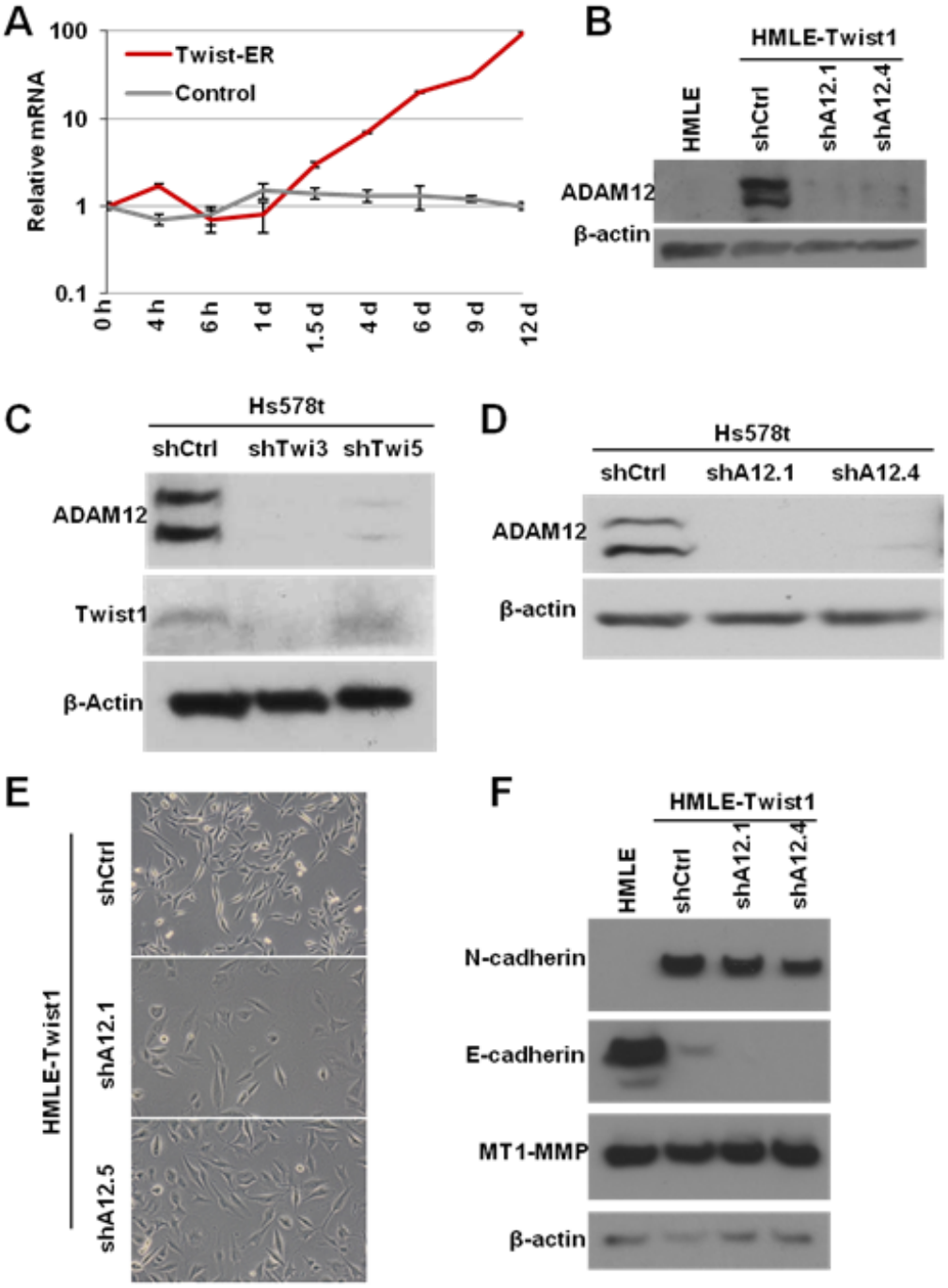
A
100
10
1
0.1
Relative mRNA
Twist-ER
Control
0 h
4 h
6 h
1 d
1.5 d
4 d
6 d
9 d
12 d
B
HMLE-Twist1
HMLE
shCtrl
shA12.1
shA12.4
ADAM12
β-actin
C
Hs578t
shCtrl
shTwi3
shTwi5
ADAM12
Twist1
β-Actin
D
Hs578t
shCtrl
shA12.1
shA12.4
ADAM12
β-actin
E
HMLE-Twist1
shCtrl
shA12.1
shA12.5
F
HMLE-Twist1
HMLE
shCtrl
shA12.1
shA12.4
N-cadherin
E-cadherin
MT1-MMP
β-actin

(Figure 3.2 D). At the cellular level, knockdown of ADAM12 did not prevent or revert the EMT process in HMLE-Twist1 cells. Although the shADAM12 cells lost cell-cell junctions, they were less elongated and spindle shaped than shCtrl cells (Figure 3.2 E). In spite of this change in morphology, HMLE-Twist1 cells expressing shADAM12 constructs still upregulated mesenchymal markers such as neuronal-cadherin (N-cadherin) and downregulated epithelial markers such as E-cadherin (Figure 3.2 F). Importantly, knockdown of ADAM12 did not affect levels MT1-MMP (Figure 3.2 F).

Upregulation of Twist1 has multiple effects that promote cancer progression. During the EMT process, cells not only gain the ability to invade and metastasize, but also become more intrinsically motile (Kalluri and Weinberg, 2009). We therefore tested if ADAM12 was essential for Twist1-induced migration in both HMLE cells overexpressing Twist1 (HMLE-Twist1 cells) and in Hs578t cells. In both HMLE-Twist1 and Hs578t cells, knockdown of ADAM12 was sufficient to induce a decrease in motility in Transwell migration assays (Figure 3.3 A-B).

To further assay defects in cell motility we also performed scratch assays with the same cell lines used above. In this assay, the wells were first coated with a layer of collagen I to mimic endogenous ECM. A significant decrease in motility upon knockdown of ADAM12 was observed over all time points collected (Figure 3.3 C-D).

Knockdown of ADAM12 increases focal adhesion number. In the course of performing experiments, an obvious defect in apparent cell size was observed. Both HMLE-Twist1 and Hs578t cells expressing shADAM12 constructs appeared significantly larger than shCtrl-expressing cells (Figure 3.4 A). When quantified by measuring the relative surface area of each cell, a significant difference in

Figure 3.3: ADAM12 is necessary for efficient migration. (A) Representative brightfield images of Transwell migration assay inserts following two hour incubation of HMLE-Twist1 or Hs578t cells expressing the indicated constructs. Cells are stained with crystal violet. (B) Relative migration of HMLE-Twist1 and Hs578t cells expressing the indicated constructs normalized to HMLE-Twist1-shCtrl migration. Error bars are standard error of the mean (SEM). * $p < 0.05$. (C) Representative brightfield images of scatch assay at indicated time points for HMLE-Twist1 and Hs578t cells expressing the indicated constructs. Dashed red line delineates edge of scratch. (D) Quantification of relative migration in the scratch assay following six hour incubation for HMLE-Twist1 and Hs578t cells expressing the indicated constructs normalized to HMLE-Twist1-shCtrl migration. Error bars are SEM. * $p < 0.05$.

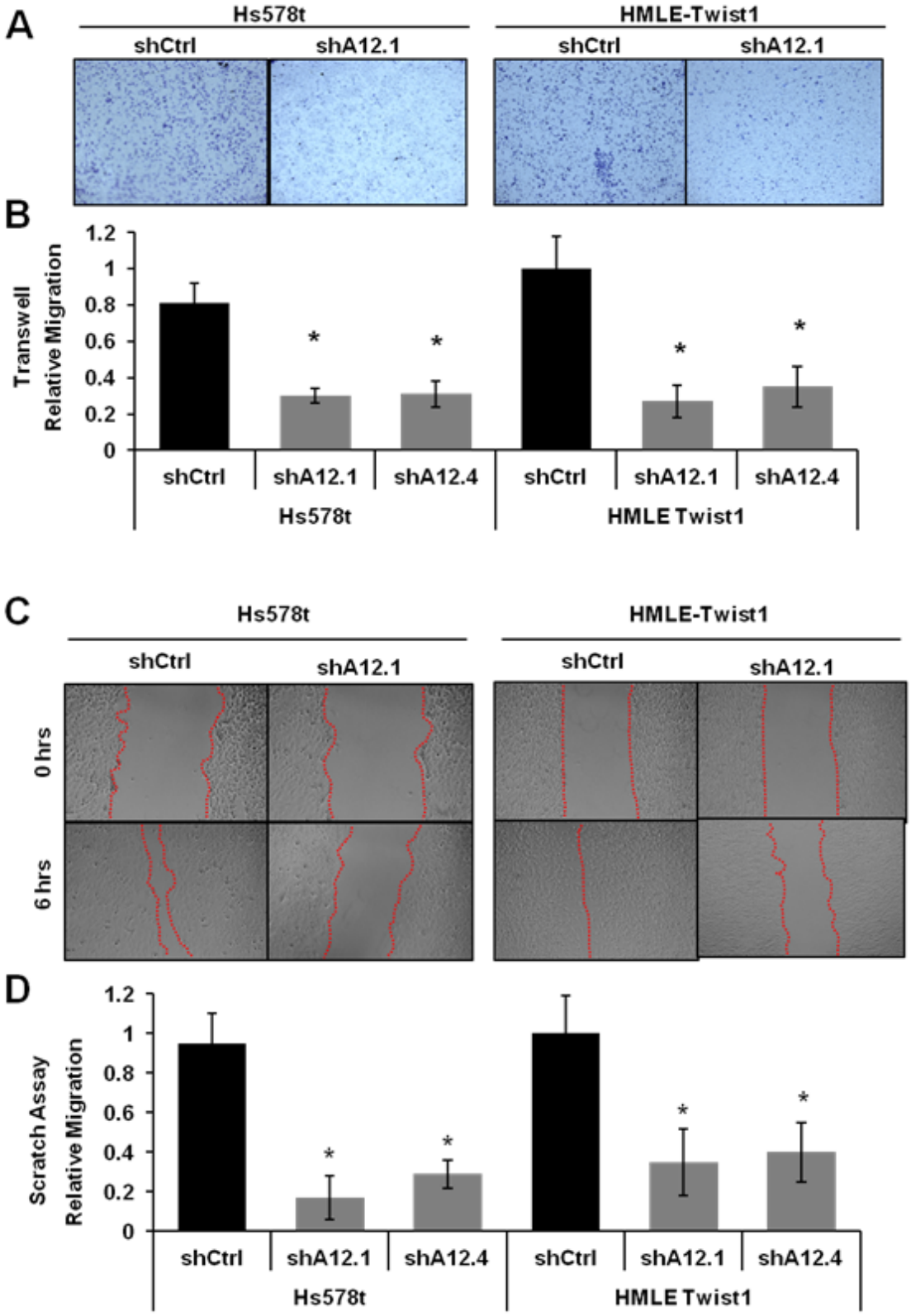
A
Hs578t
HMLE-Twist1
shCtrl
shA12.1
shCtrl
shA12.1
B
Transwell
Relative Migration
1.2
1
0.8
0.6
0.4
0.2
0
*
*
*
*
shCtrl
shA12.1
shA12.4
shCtrl
shA12.1
shA12.4
Hs578t
HMLE Twist1
C
Hs578t
HMLE-Twist1
shCtrl
shA12.1
shCtrl
shA12.1
0 hrs
6 hrs
D
Scratch Assay
Relative Migration
1.2
1
0.8
0.6
0.4
0.2
0
*
*
*
*
shCtrl
shA12.1
shA12.4
shCtrl
shA12.1
shA12.4
Hs578t
HMLE Twist1

Figure 3.4: Knockdown of ADAM12 increases cell spreading. (A) Representative brightfield images of HMLE-Twist1 and Hs578t cells expressing the indicated constructs plated on 0.1% collagen matrix. Cell borders are outlined with dashed red line. Images are taken at same magnification. (B) Quantification of relative cell area in HMLE-Twist1 and Hs578t cells expressing the indicated constructs normalized to Hs578t-shCtrl cells. Error bars are SEM. * $p < 0.05$. (C) Representative brightfield images of HMLE-Twist1 and Hs578t cells in suspension expressing the indicated constructs. Images are taken at same magnification. (D) Quantification of relative cell volume of HMLE-Twist1 and Hs578t cells expressing the indicated constructs normalized to Hs578t-shA12.1 cells. Error bars are SEM. NS = Not significant, * $p > 0.05$. (E) Immunofluorescence for ADAM12 (green), F-actin (red), and vinculin (blue) in Hs578t cells plated on 0.1% collagen matrix. White line within inset is analyzed for pixel intensity across a single focal adhesion. Colors of the plot correspond to those in the fluorescence image. Y-axis is arbitrary intensity. Scale bar = 5 μm.

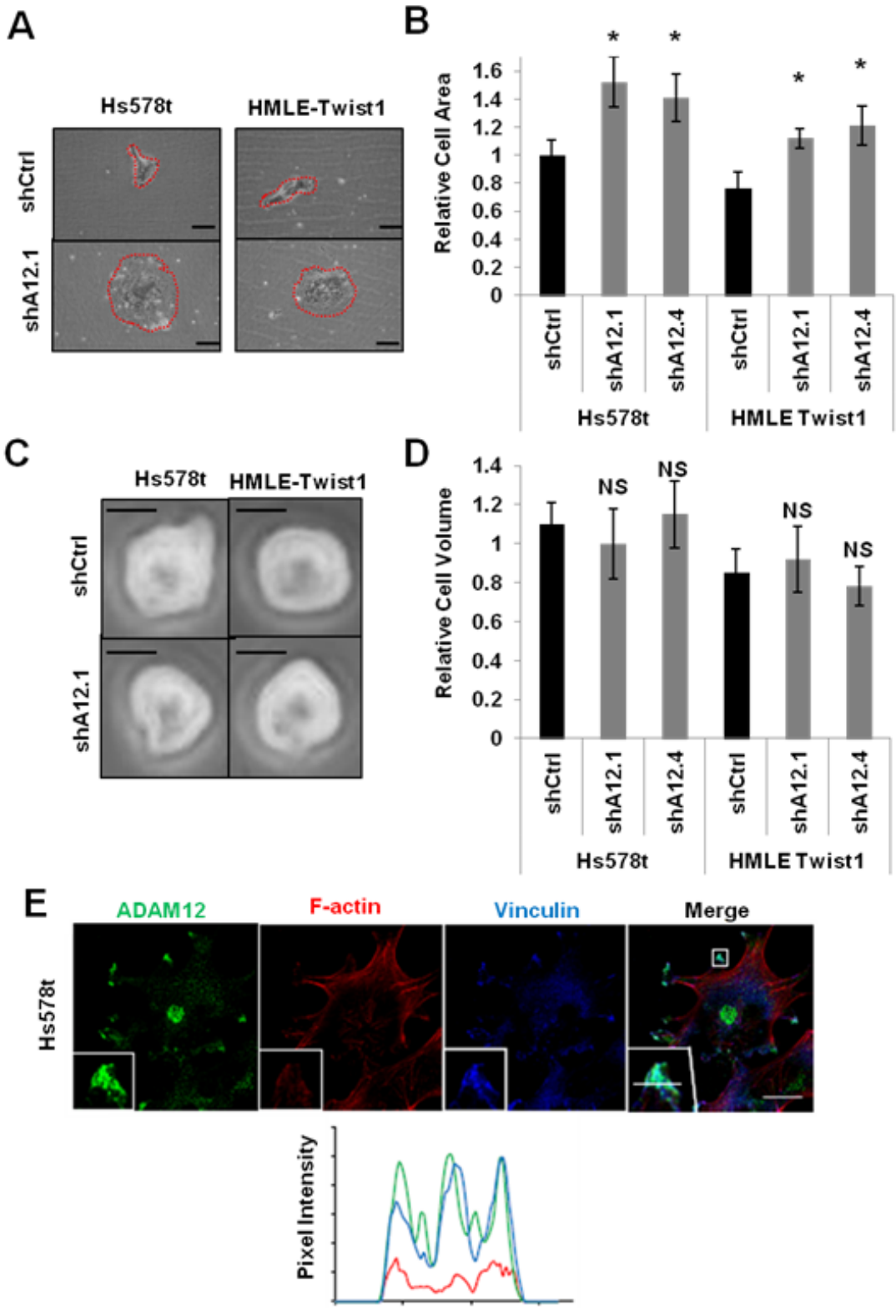
A
Hs578t
HMLE-Twist1
shCtrl
shA12.1
B
Relative Cell Area
1.6
1.4
1.2
1
0.8
0.6
0.4
0.2
0
*
*
*
*
shCtrl
shA12.1
shA12.4
shCtrl
shA12.1
shA12.4
Hs578t
HMLE Twist1
C
Hs578t
HMLE-Twist1
shCtrl
shA12.1
D
Relative Cell Volume
1.4
1.2
1
0.8
0.6
0.4
0.2
0
NS
NS
NS
NS
shCtrl
shA12.1
shA12.4
shCtrl
shA12.1
shA12.4
Hs578t
HMLE Twist1
E
ADAM12
F-actin
Vinculin
Merge
Hs578t
Pixel Intensity

apparent cell size was noted (Figure 3.4 B). Increased cell size in two dimensions can be due to either an intrinsic increase in cell volume or an increase in cell spreading (Xiong et al., 2010). We therefore measured cell size in suspension by trypsinizing the cells and measuring the relative volume of HMLE-Twist1 and Hs578t cells expressing shCtrl and shADAM12 constructs in suspension using a hemocytometer. We observed no significant difference in cell volume upon knockdown of ADAM12 (Figure 3.4 C-D), implying that the apparent increase in cell size is due to an increase in cell spreading rather than an actual increase in cell size.

Increased cell spreading directly correlates with increased focal adhesion number (Tamura et al., 1998). This was particularly interesting in light of the fact that ADAM12 is capable of interaction with integrins involved in focal adhesions (Kveiborg et al., 2008). Indeed, when Hs578t cells were stained with for ADAM12 and the focal adhesion protein vinculin, ADAM12 localized to focal adhesions on the periphery of the cell (Figure 3.4 E). This is consistent with previous reports that ADAM12 localizes to both invadopodia and peripheral areas of the cell (Abram et al., 2003; Kawaguchi et al., 2003).

We therefore went on to assay focal adhesion formation by staining both Hs578t and HMLE-Twist1 cells expressing control and shADAM12 vectors for focal adhesion formation on collagen I. A clear increase in focal adhesion formation (elongated ellipsoid vinculin staining adjacent to F-actin stress fibers) was observed with an associated increase in stress fiber formation upon ADAM12 knockdown (Figure 3.5 A). Stress fiber formation requires focal adhesion formation and is a surrogate marker for focal adhesion formation in many cell lines. Quantification of both

Figure 3.5: Knockdown of ADAM12 increases focal adhesion number. (A) Representative immunofluorescence images of HMLE-Twist1 and Hs578t cells expressing the indicated constructs stained for vinculin (green), F-actin (red), and nuclei (blue). Scale bar = 5 μm. (B) Quantification of total number of vinculin-positive focal adhesions per cell in HMLE-Twist1 and Hs578t cells expressing the indicated constructs. Error bars are SEM. * $p < 0.05$. (C) Quantification of total number of F-actin-positive stress fibers per cell in HMLE-Twist1 and Hs578t cells expressing the indicated constructs. Error bars are SEM. * $p < 0.05$.

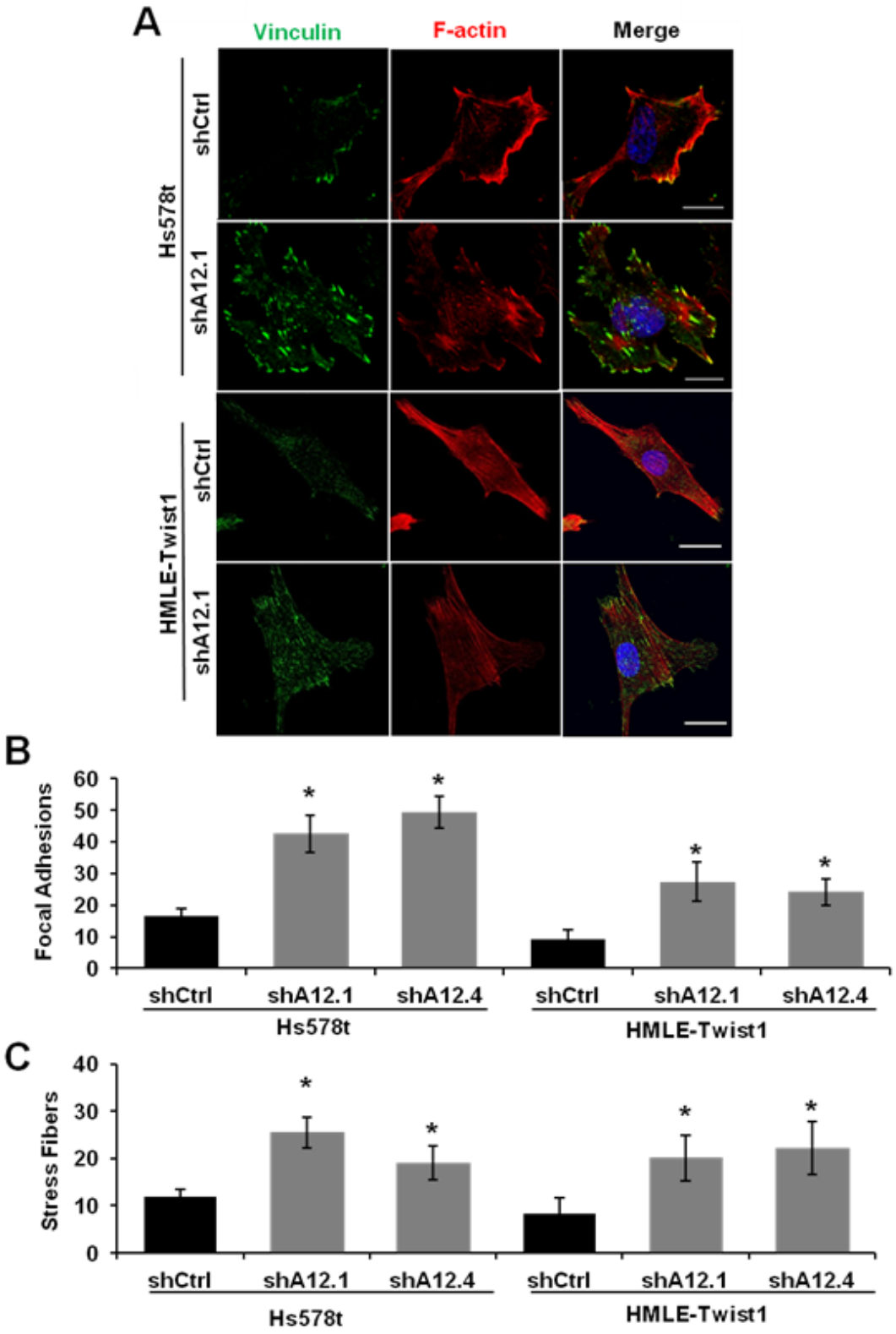
A
Vinculin
F-actin
Merge
Hs578t
shCtrl
shA12.1
HMLE-Twist1
shCtrl
shA12.1
B
Focal Adhesions
60
50
40
30
20
10
0
shCtrl
shA12.1
shA12.4
shCtrl
shA12.1
shA12.4
Hs578t
HMLE-Twist1
C
Stress Fibers
40
30
20
10
0
shCtrl
shA12.1
shA12.4
shCtrl
shA12.1
shA12.4
Hs578t
HMLE-Twist1

focal adhesions (vinculin-positive elongated puncta) and stress fiber formation indicated a significant increase in both adhesive and cytoskeletal structures upon knockdown of ADAM12 (Figure 3.5 B-C).

Increased attachment strength is associated with focal adhesions and increased interactions with the surrounding matrix (Elineni and Gallant, 2011). We therefore sought to determine the relative strength of integrin binding between the shCtrl and shADAM12 cell line. Live cells were briefly washed with 0.01% TritonX-100 to extract integrins not bound to matrix or in focal adhesions. Cells were then fixed and stained for β1-integrin with immunofluorescence. Relative levels of β1-integrin were quantified by calculating the integrated pixel intensity of staining before and after extraction to measure the strength of integrin interactions (Kawaguchi et al., 2003). We observed a significant decrease in soluble integrins in those cells expressing the shADAM12 construct (Figure 3.6A), implying that a larger proportion of integrins were interacting with matrix molecules in the knockdown cells. This was consistent with our hypothesis that integrin-mediated focal adhesions are more numerous and stronger upon knockdown of ADAM12.

To determine if the increase in focal adhesion number upon ADAM12 knockdown affected the adhesive properties of the cells, we performed a cell detachment assay. Briefly, subconfluent Hs578t cells expressing shCtrl or shADAM12 constructs were treated with 0.05% trypsin for the indicated amount of time before washing, fixing, and staining with crystal violet. Crystal violet was extracted with dilute acetic acid and relative percentage of cells remaining attached quantified. A significant difference in detachment between the shCtrl and shADAM12 cell lines was observed

Figure 3.6: Knockdown of ADAM12 increases adhesion and focal adhesion signaling. (A) Percentage of integrins remaining following 5 minute extraction with 0.01% TritonX-100 as measured with fluorescence microscopy. Error bars are SEM. * $p < 0.05$. (B) Fraction of Hs578t cells remaining following treatment with 0.05% Trypsin for indicated amount of time followed by washing to remove non-adherent cells. Error bars are SEM. (C) Immunoblot for total FAK and FAK phosphorylated at tyrosine 397 (pY^{397}FAK) in Hs578t cells expressing the indicated constructs. Ctrl = empty vector control; A12FL = ADAM12 expression construct. Tyrosine phosphorylation of Y^{397}FAK relative to total FAK quantified below blots, normalized to Hs578t-shCtrl or Hs578t-Ctrl. (D) Quantification of F-actin-positive stress fibers per cell in Hs578t cells expressing the indicated constructs treated with control mouse immunoglobin G (IgG) antibody (Ctrl) or with 1:50 dilution of AIIB2 β1-integrin inhibitory antibody (AIIB2) for 12 hours. Error bars are SEM. * $p < 0.05$. (E) Quantification of relative cell area in Hs578t cells expressing the indicated constructs treated with control mouse IgG antibody (Ctrl) or with 1:50 dilution of AIIB2 β1-integrin inhibitory antibody (AIIB2) for 12 hours. Error bars are SEM. * $p < 0.05$.

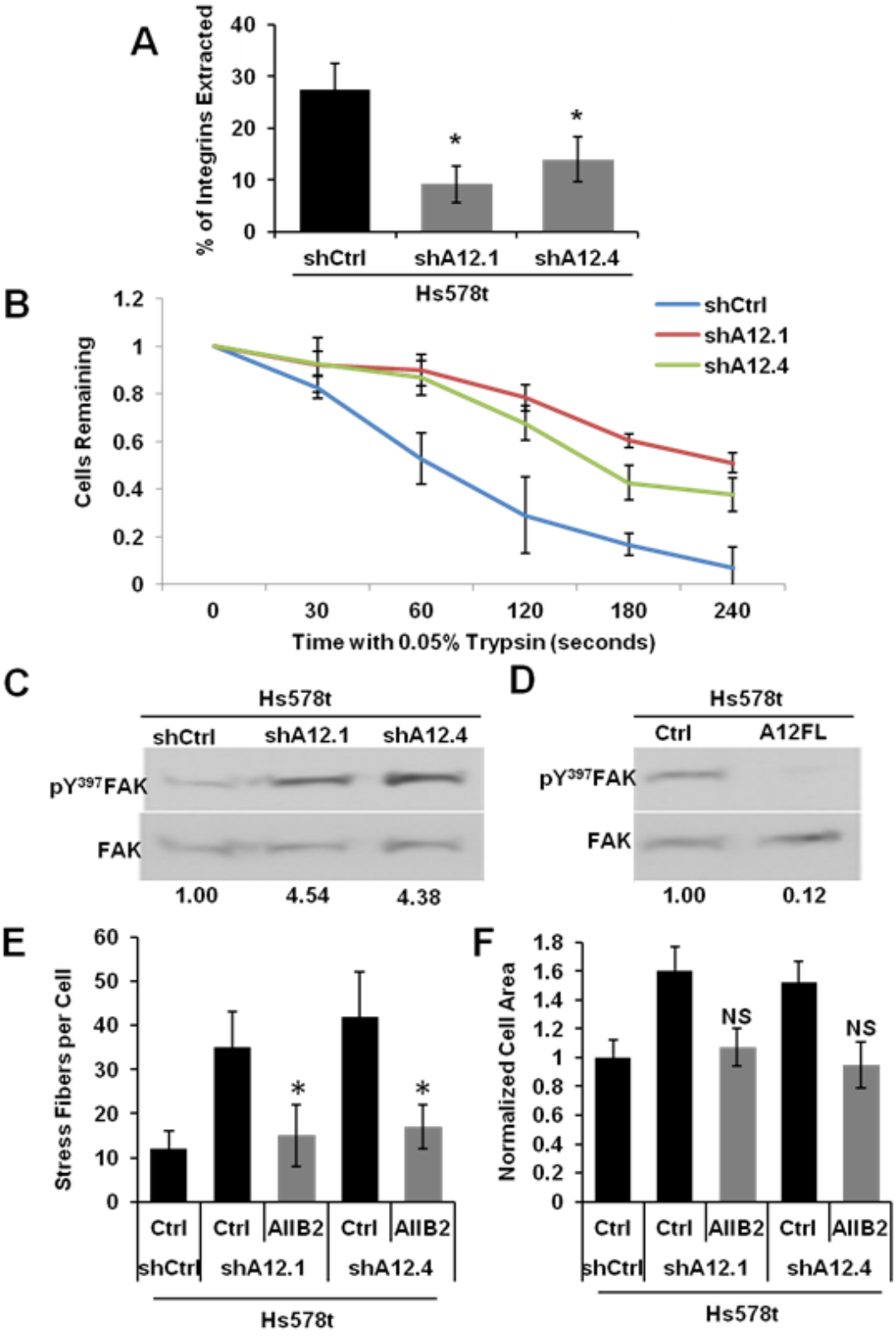
A
% of Integrins Extracted
40
30
20
10
0
*
*
shCtrl
shA12.1
shA12.4
Hs578t
B
Cells Remaining
1.2
1
0.8
0.6
0.4
0.2
0
shCtrl
shA12.1
shA12.4
0
30
60
120
180
240
Time with 0.05% Trypsin (seconds)
C
Hs578t
shCtrl
shA12.1
shA12.4
pY397FAK
FAK
1.00
4.54
4.38
D
Hs578t
Ctrl
A12FL
pY397FAK
FAK
1.00
0.12
E
Stress Fibers per Cell
60
50
40
30
20
10
0
*
*
Ctrl
Ctrl
AIIB2
Ctrl
AIIB2
shCtrl
shA12.1
shA12.4
Hs578t
F
Normalized Cell Area
1.8
1.6
1.4
1.2
1
0.8
0.6
0.4
0.2
0
NS
NS
Ctrl
Ctrl
AIIB2
Ctrl
AIIB2
shCtrl
shA12.1
shA12.4
Hs578t

with shADAM12 expressing cells being more resistant to trypsin-mediated detachment (Figure 3.6 B).

Focal adhesion kinase (FAK) is a downstream effector of focal adhesion activation (Schlaepfer et al., 1999). Autophosphorylation of FAK at tyrosine 397 is an early event in focal adhesion formation and is required for subsequent signaling through Src kinase and PI3-K (Schlaepfer and Hunter, 1997). We therefore investigated the status of FAK phosphorylation upon knockdown of ADAM12 in Hs578t cells. Both knockdowns induced a greater than four-fold increase in Y397FAK phosphorylation (Figure 3.6 C). Conversely, overexpression of full-length ADAM12 in Hs578t led to an almost 10-fold reduction in FAK tyrosine phosphorylation (Figure 3.6 D). Overexpression of ADAM12 in both Hs578t and HMLE-Twist1 cells was associated with large amounts of cell death making maintaining cell lines difficult.

To determine if the effects of ADAM12 knockdown were dependent on β1-integrin, we used a mouse monoclonal blocking antibody against β1-integrin, AIIB2 (Park et al., 2006). Concentrations of AIIB2 hybridoma supernatant were empirically determined that reduced, but did not eliminate FAK tyrosine phosphorylation. Treatment of Hs578t cells expressing shADAM12 constructs with AIIB2 led to a decrease in stress fiber formation (Figure 3.6 E) and a reduction in cell spreading on collagen matrices (Figure 3.6 F). This implied that the increase in stress fibers and cell spreading was associated with β1 integrins.

ADAM12 is required for invadopodia formation. In addition to impairing cell motility, knockdown of ADAM12 caused an even more severe defect of invasion in the Transwell invasion assay (Figure 3.7 A). ADAM12 has been described as localized to

invadopodia and directly interacts with the invadopodia-specific scaffolding protein Tks5 (Abram et al., 2003). We therefore suspected that ADAM12 could be playing additional roles in invadopodia formation.

First, we verified that ADAM12 localized to invadopodia in Hs578t cells grown on collagen by costaining for cortactin, F-actin, and ADAM12 with immunofluorescence. Robust colocalization of ADAM12 with puncta of F-actin and cortactin corresponding to invadopodia was observed in Hs578t cells (Figure 3.7 B). When ADAM12 was knocked down in both Hs578t and HMLE-Twist1 cells, however, we observed a significant decrease in F-actin/cortactin positive invadopodia formation on collagen matrices with most of the cortactin associated with cortical actin in shADAM12 cells (Figure 3.7 C-F).

As it appeared that ADAM12 was essential for invadopodia formation in Hs578t and HMLE-Twist1 cells, we went on to test the ability of the cells to degrade ECM with the FITC-gelatin degradation assay. In these assays, areas of gelatin degradation or proteolysis are visualized as dark areas beneath the cell as the fluorescent FITC-labeled gelatin is degraded by the action of invadopodia. As expected, a significant decrease in gelatin degradation was observed upon knockdown of ADAM12, indicating that invadopodia are required for gelatin degradation in our system (Figure 3.8 A-B).

The disintegrin and MMP domains of ADAM12 have distinct roles. ADAM12 has multiple functional domains, including a metalloprotease domain that cleaves other proteins, a disintegrin domain that interacts with integrins, and a cytoplasmic tail that may act as a scaffold for signaling or a physical linkage to the cytoskeleton (Kveiborg et al., 2008). To determine what domains of ADAM12 were

Figure 3.7: ADAM12 is necessary for Twist1-induced invasion and invadopodia formation. (A) Relative invasion of HMLE-Twist1 and Hs578t cells expressing the indicated constructs normalized to HMLE-Twist1-shCtrl invasion after 36 hour incubation. Error bars are standard error of the mean (SEM). * $p < 0.05$. (B) Representative immunofluorescence for ADAM12 (green), F-actin (red), and cortactin (blue) in Hs578t cells plated on 0.1% collagen. Inset corresponds to white box and corresponds to cluster of ADAM12, F-actin, and cortactin positive puncta indicative of invadopodia. Graph is plot of pixel intensity across single invadopodia in inset. Y-axis is arbitrary intensity. Scale bar = 5 μm. (C) Representative immunofluorescence for cortactin (green), F-actin (red), and nuclei (blue) in Hs578t cells expressing the indicated constructs. Inset corresponds to white box in full-size image. Scale bar = 5 μm. (D) Quantification of percentage of Hs578t cells expressing indicated construct with invadopodia (cortactin and F-actin positive puncta). Error bars are SEM. * $p < 0.05$. (E) Representative immunofluorescence for cortactin (green), F-actin (red), and nuclei (blue) in HMLE-Twist1 cells expressing the indicated constructs. Inset corresponds to white box in full-size image. Scale bar = 5 μm. (F) Quantification of percentage of HMLE-Twist1 cells expressing indicated construct with invadopodia (cortactin and F-actin positive puncta). Error bars are SEM. * $p < 0.05$.

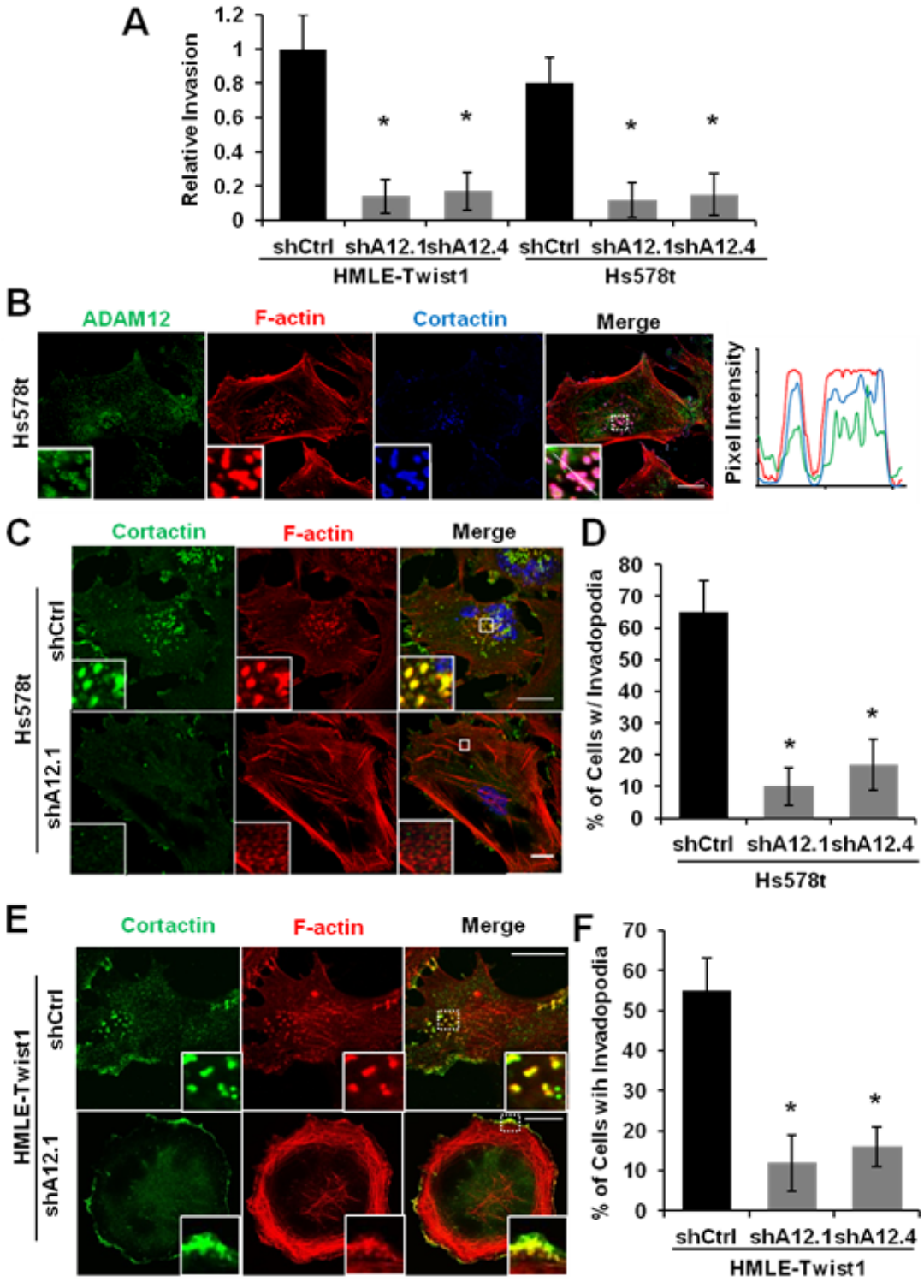
A
Relative Invasion
1.2
1
0.8
0.6
0.4
0.2
0
shCtrl shA12.1shA12.4 shCtrl shA12.1shA12.4
HMLE-Twist1
Hs578t
B
ADAM12
F-actin
Cortactin
Merge
Hs578t
Pixel Intensity
C
Cortactin
F-actin
Merge
Hs578t
shCtrl
shA12.1
D
% of Cells w/ Invadopodia
80
70
60
50
40
30
20
10
0
shCtrl shA12.1shA12.4
Hs578t
E
Cortactin
F-actin
Merge
HMLE-Twist1
shCtrl
shA12.1
F
% of Cells wih Invadopodia
70
60
50
40
30
20
10
0
shCtrl shA12.1shA12.4
HMLE-Twist1

Figure 3.8: ADAM12 is required for Twist1-induced gelatin degradation. (A) Representative fluorescence images for F-actin (red), FITC-gelatin (green), and nuclei (blue) in Hs578t and HMLE-Twist1 cells expressing the indicated constructs following incubation for 12 hours on matrix. Areas of degradation appear as black areas beneath the cells. Scale bar = 5 μm. (B) Quantification of relative gelatin degradation of Hs578t and HMLE-Twist1 cells expressing the indicated constructs normalized to HMLE-Twist1 level following 12 hour incubation. Error bars are SEM. * $p < 0.05$.

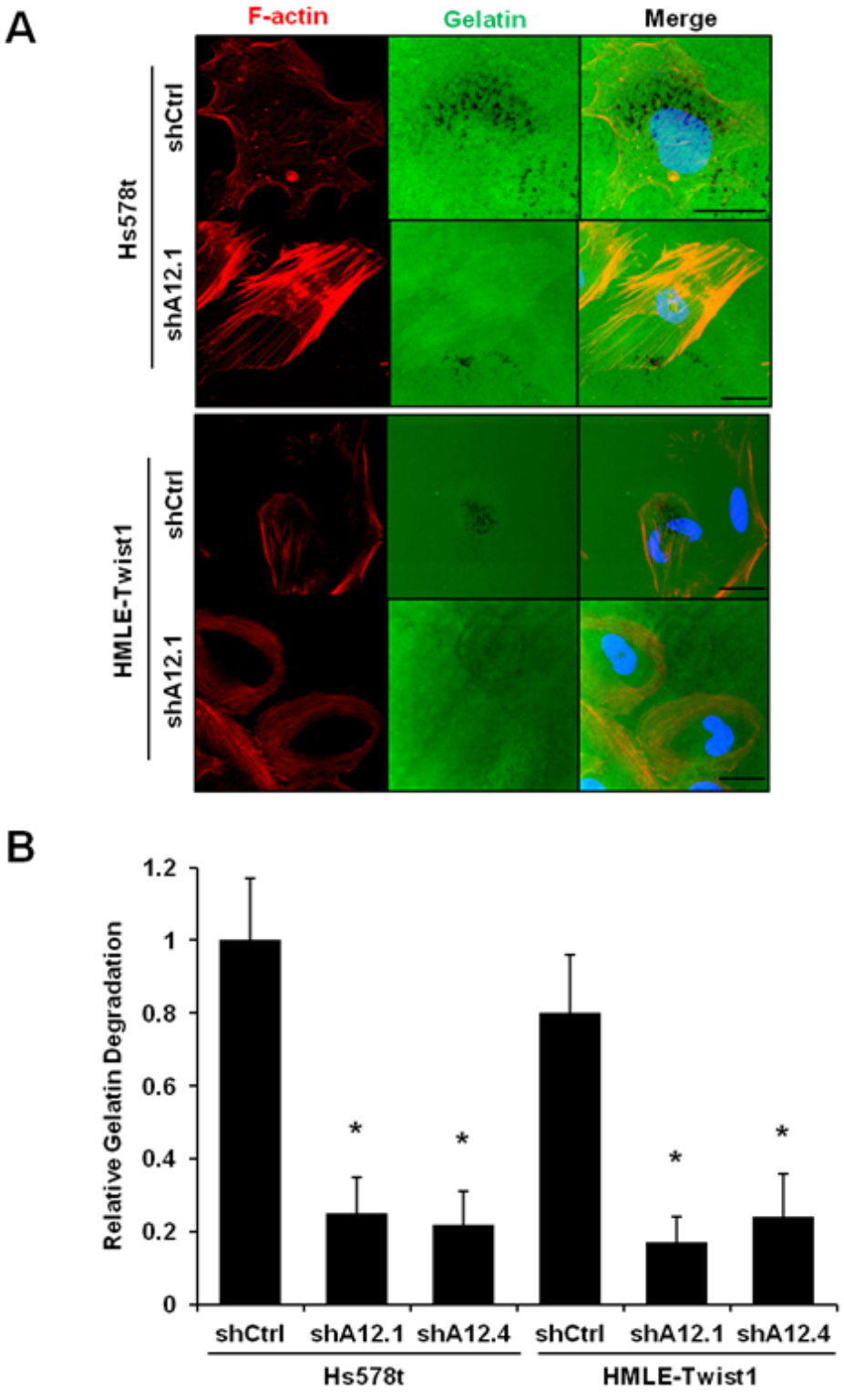
A
F-actin
Gelatin
Merge
Hs578t
shCtrl
shA12.1
HMLE-Twist1
shCtrl
shA12.1
B
Relative Gelatin Degradation
1.2
1
0.8
0.6
0.4
0.2
0
*
*
*
*
shCtrl
shA12.1
shA12.4
shCtrl
shA12.1
shA12.4
Hs578t
HMLE-Twist1

necessary for its roles in focal adhesion and invadopodia regulation, we performed a series of rescue experiments with mutant ADAM12 proteins. Mutant constructs were designed using site-directed mutagenesis to generate a metalloprotease-null ADAM12 (E351Q, A12ΔMMP) and a disintegrin domain mutant ADAM12 (D488A, A12ΔDis). The metalloprotease mutation disrupts a critical catalytic glutamate while the disintegrin mutation replaces a critical charged aspartate with an uncharged alanine residue (Jacobsen et al., 2008; Huang et al., 2005). An additional truncation mutation was generated in which the protein is terminated following the transmembrane domain at amino acid 727 (A12ΔCyt) to remove the ADAM12 cytoplasmic tail (Kang et al., 2001). Unfortunately, the cytoplasmic truncation mutation construct was consistently expressed at a much higher level than the other mutants (Figure 3.9 A).

Hs578t-shADAM12 cells transiently transfected with ADAM12 constructs on 0.1% collagen were stained for vinculin and F-actin to visualize focal adhesions. All constructs reduced focal adhesion number to approximately control levels except for A12ΔDis (Figure 3.9 B). Interpretation of the cytoplasmic truncation mutation is difficult, as it is expressed at a much higher level when transiently transfected (Figure 3.9 A). This may be due to more efficient translocation to the membrane due to a lack of a retention signal. Invadopodia formation was assayed identically, except cells were stained with cortactin and F-actin and cells positive for punctuate colocalization of F-actin and cortactin were quantified as invadopodia positive. In this case, only the A12FL and A12ΔCyt constructs were able to increase invadopodia formation to levels comparable to Hs578t-shCtrl cells with A12ΔMMP and A12ΔDis mutation constructs failing to increase invadopodia number to Hs578t-shCtrl levels (Figure 3.9 C).

Figure 3.9: The disintegrin and MMP domains of ADAM12 have different roles in regulation of focal adhesions and invadopodia. (A) Immunoblot for ADAM12 and β-actin in Hs578t-shADAM12.1 cells transfected with control vector (Ctrl), A12FL (FL), A12ΔMMP (MMP), A12ΔDis (Dis), and A12ΔCyt (Cyt) constructs. (B) Quantification of total number of vinculin-positive focal adhesions per cell in Hs578t-shADAM12 cells transfected with the indicated constructs. Error bars are SEM. NS = Not significant, $p > 0.1$. * $p < 0.1$. P-value based on combination of both knockdowns transfected with indicated construct compared to Hs578t-shADAM12 cells transfected with control vector (B) Quantification of percentage of cells with cortactin/F-actin positive invadopodia in Hs578t-shADAM12 cells transfected with the indicated constructs. Error bars are SEM. NS = Not significant, $p > 0.1$. * $p < 0.1$. P-value based on combination of both knockdowns transfected with indicated construct compared to Hs578t-shADAM12 cells transfected with control vector (C) Quantification of percentage of Hs578t-shADAM12 cells treated with the indicated compounds that are positive for F-actin/cortactin positive invadopodia. AIIB2 is β1 integrin blocking antibody (1:50 dilution hybridoma supernatant, 12 hours); PF-228 is FAK inhibitor (10 μM, 12 hours). Error bars are SEM. * $p < 0.05$.

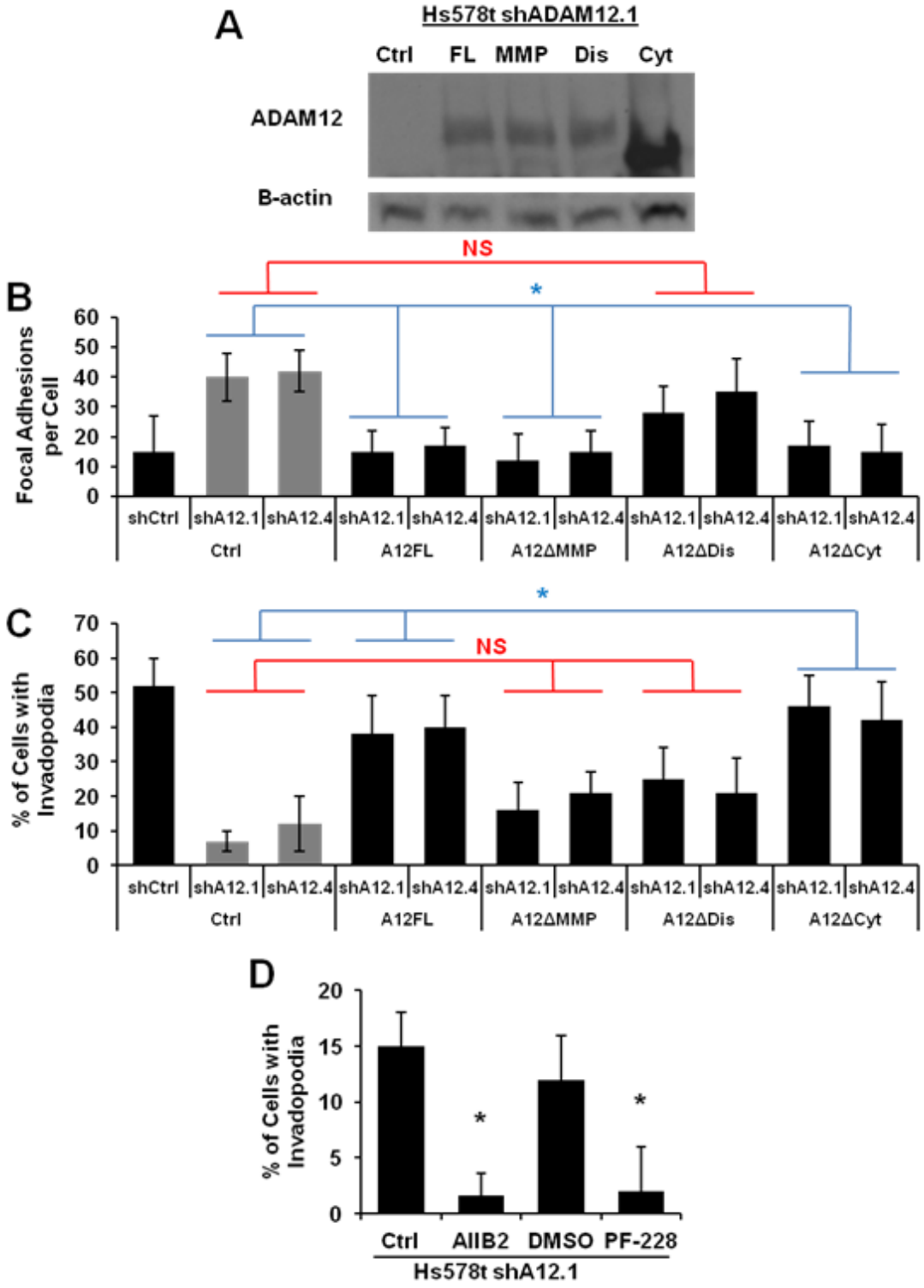
A
Hs578t shADAM12.1
Ctrl
FL
MMP
Dis
Cyt
ADAM12
B-actin
B
NS
*
Focal Adhesions per Cell
60
50
40
30
20
10
0
shCtrl
shA12.1
shA12.4
Ctrl
A12FL
A12ΔMMP
A12ΔDis
A12ΔCyt
C
*
NS
% of Cells with Invadopodia
70
60
50
40
30
20
10
0
D
% of Cells with Invadopodia
20
15
10
5
0
Ctrl
AIIB2
DMSO
PF-228
Hs578t shA12.1

Previous reports have suggested that focal adhesions inherently antagonize invadopodia formation by sequestering signaling molecules necessary for invadopodia formation, particularly Src (Chan et al., 2009). As other reports have suggested integral roles for focal adhesions and FAK in invadopodia formation, we were eager to determine the role of focal adhesions in regulating invadopodia in our cell lines (Alexander et al., 2008; Hauck et al., 2002). To test this hypothesis, we treated Hs578t-shADAM12 cells with AIIB2 blocking antibody or the FAK-specific tyrosine kinase inhibitor PF-228 at concentrations sufficient to significantly reduce FAK tyrosine phosphorylation (Slack-Davis et al., 2007). Following incubation, we then performed an invadopodia formation assay by quantifying the percentage of cells with cortactin/F-actin positive invadopodia under the different treatment conditions. If focal adhesions intrinsically inhibit invadopodia formation, we hypothesized that inhibition of focal adhesions should increase invadopodia formation. At these concentrations, however, we observed an almost complete elimination of invadopodia formation suggesting that focal adhesions are essential for invadopodia formation in our system (Figure 3.9 C).

ADAM12 is necessary for efficient metastasis to the lungs. Due to the role of invadopodia in regulating directed proteolysis of the ECM, we were interested if ADAM12 was also required for invasion in a 3D culture system. To test this hypothesis, we embedded HMLE-Twist1 cells expressing control or shADAM12 constructs in a Matrigel culture system. In this culture system, cells are plated as single cells embedded in Matrigel. Structure growth was monitored over time by bright field microscopy. After one week in 3D Matrigel culture, cells expressing the control knockdown had projected into the surrounding matrix. HMLE-Twist1-shADAM12 cells remained

largely rounded with few projections into the surrounding ECM (Figure 3.10 A). When quantified, a significant decrease in 3D invasiveness of HMLE-Twist1-shADAM12 cells was observed (Figure 3.10 B).

Due to the clear role of ADAM12 in regulating both motility and invasion *in vitro*, we were curious if ADAM12 was also required for *in vivo* metastasis. Before going on to a mouse model, we verified that there was no growth defect in HMLE-Twist1 cells upon knockdown of ADAM12 *in vitro* by performing a growth curve analysis. There was no significant difference in growth rate (Figure 3.10 C). To determine if ADAM12 promotes metastatic dissemination we utilized a xenotransplantation model in which we first transformed the HMLE-Twist1 cells expressing shCtrl or shADAM12 constructs by infection with constitutively active Ras. Cells were then fluorescently labeled by infection with a lentiviral GFP construct. Following transformation and labeling, we subcutaneously injected cells along with Matrigel into the flanks of nude mice. Approximately 40 days later, when tumors reached 1.5 cm in diameter, we sacrificed the mice and collected lung and primary tumor tissue for further analysis.

As HMLE cells are immortalized with SV40 Large T Antigen, we could conveniently use IHC to identify tumor cells as positive for SV40. When examined with brightfield microscopy, the periphery of those tumors expressing shADAM12 constructs remained largely encapsulated in a layer of connective tissue and fibroblasts. In contrast, those cells expressing control shRNA constructs had a poorly defined border and projected into the surrounding tissue, often as single cells (Figure 3.10 D). When we examined the lungs for GFP-positive disseminated tumor cells, we

Figure 3.10: ADAM12 is required for efficient metastasis to the lung. (A) Representative brightfield images of HMLE-Twist1 cells expressing indicated constructs grown in Matrigel for one week. Images were taken at same magnification. (B) Quantification of percentage of organoid structures with projections greater than half the diameter of the structure. Error bars are SEM. * $p < 0.05$. (C) Relative cell number of HMLE-Twist1 cells expressing the indicated constructs at the indicated time points normalized to starting cell number. Error bars are SEM. (D) Representative immunohistochemistry for SV40 Large-T antigen in tumor sections collected from mice injected with HMLER-Twist1 cells expressing the indicated constructs. Primary tumors are labeled $1^{o}T$ and tumor margins are represented by dashed line. Note invasion of surrounding ECM by single cells in control knockdown (black arrows) (E) Fluorescence image of GFP-positive puncta of disseminated HMLER-Twist1 cells expressing the indicated constructs in lungs of nude mice (indicated by yellow triangles). Lung is in grayscale. Scale bar = 1 mm (F) Quantification of total number of GFP-positive lung metastases (sum of all five lobes) in mice injected with HMLER-Twist1 cells expressing the indicated constructs. * $p < 0.05$.

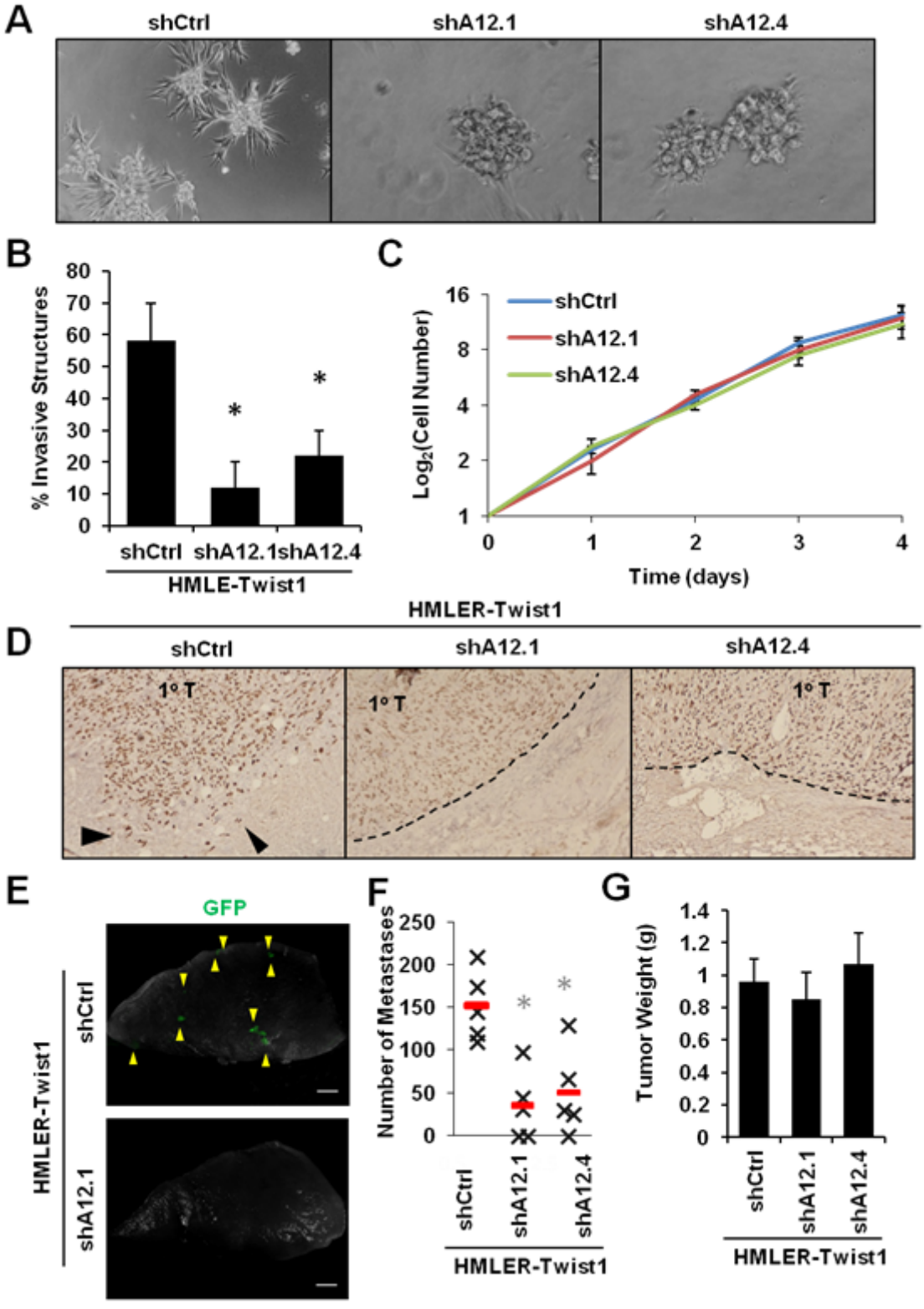
A
shCtrl
shA12.1
shA12.4
B
% Invasive Structures
80
70
60
50
40
30
20
10
0
*
*
shCtrl
shA12.1
shA12.4
HMLE-Twist1
C
Log2(Cell Number)
16
8
4
2
1
shCtrl
shA12.1
shA12.4
0
1
2
3
4
Time (days)
HMLER-Twist1
D
shCtrl
shA12.1
shA12.4
1° T
1° T
1° T
E
GFP
HMLER-Twist1
shCtrl
shA12.1
F
Number of Metastases
250
200
150
100
50
0
*
*
shCtrl
shA12.1
shA12.4
HMLER-Twist1
G
Tumor Weight (g)
1.4
1.2
1
0.8
0.6
0.4
0.2
0
shCtrl
shA12.1
shA12.4
HMLER-Twist1

observed a large and significant increase in disseminated cells in the HMLER-Twist1-shControl cells compared to those cells expressing the shADAM12 construct (Figure 3.11 E-F). We thus concluded that ADAM12 is necessary for metastasis in a xenotransplantation model of cancer dissemination.

DISCUSSION

ADAM12 is a multifunctional protein with roles in regulating cell signaling, adhesion, and invadopodia formation. Due to our observation that Twist1 induces invadopodia formation, we were curious to understand the possible role of ADAM12 in mediating Twist1-induced invadopodia formation and local invasion. Despite numerous investigations into the role of ADAM12 in both cancer cells and normal tissues, ADAM12 had not previously been associated with the EMT process. We characterized ADAM12 as an essential regulator of migration, focal adhesions, and invadopodia during Twist1-induced EMT with important roles in regulation of invasion and metastasis.

In order to characterize the function of ADAM12 in regulating Twist1-mediated invasion, we used two model cell lines: Hs578t breast carcinoma cells and HMLE cells overexpresssing Twist1. The Hs578t cell line was selected due to the observations that it forms numerous invadopodia that colocalize with ADAM12 and that they express high levels of Twist1. HMLE-Twist1 cells exogenously express Twist1 and form numerous invadopodia that are essential for metastasis. In addition HMLE cells are amenable to many experimental techniques.

In both HMLE-Twist1 and Hs578t cells we observed a tight correlation between ADAM12 expression and Twist1. Overexpression of Twist1 led to an increase in

ADAM12 expression in HMLE cells while stable knockdown of Twist1 led to a decrease in ADAM12 levels in Hs578t cells. We were able to generate two different shRNAs targeting ADAM12 that strongly reduced protein levels of ADAM12. This is the first report of an association of ADAM12 expression with EMT or Twist1. The only previous report on transcriptional regulation of ADAM12 implicated NFK-B as a direct regulator of ADAM12 gene expression (Ray et al., 2010). It is important to note, however, that ADAM12 is unlikely to be a direct target of Twist1 as the promoter for ADAM12 lacks E-box elements essential for Twist1-mediated transcriptional regulation. Importantly, however, knockdown of ADAM12 did not affect the EMT process. As loss of E-cadherin is necessary, but not sufficient, for metastasis it was important to demonstrate that E-cadherin was still downregulated in response to Twist1 (Yang et al., 2004). The role we demonstrate for ADAM12 downstream of Twist1 in inducing invasion and metastasis is therefore an active process regulated by Twist1.

In order to characterize the effects of ADAM12 on Twist1-mediated invasion, we first examined the effects of ADAM12 on cell motility. ADAM12 expression has previously been both positively and negatively correlated with cell migration in different cell lines (Rao et al., 2011; Roy et al., 2011). Characterizing the specific effects of ADAM12 in Twist1-mediated migration was therefore a priority. Upon knockdown of ADAM12, we observed a significant decrease in migration in both Transwell migration and scratch assays in both HMLE-Twist1 and Hs578t cells. This implies that for Twist1-induced EMT processes, ADAM12 positively regulates migration. It will be interesting to characterize the roles of ADAM12 in regulation of motility in EMT induced by transforming growth factor β (TGF-β) or other

transcriptional regulators of EMT such as Snail to determine the generalizability of our findings.

We also observed a dramatic and significant increase in cell spreading independent of cell size in response to knockdown of ADAM12. Cell spreading has previously been associated with increases in focal adhesion number and we observed strong colocalization of ADAM12 at focal adhesions in Hs578t cells (Xiong et al., 2010). This led us to examine focal adhesions in both HMLE-Twist1 and Hs578t cell lines. Using immunofluorescence techniques, we observed significant increases in focal adhesion and stress fiber number in both cell lines upon knockdown of ADAM12. Previous experiments utilizing substrates coated in recombinant ADAM12 fragments have indicated a role for ADAM12 in mediating B1 integrin-dependent attachment and focal adhesion formation (Thodeti et al., 2005). These experiments are inherently artificial, however, and may reflect the relative binding affinity of ADAM12 for integrins rather than a real role in adhesion. Sundberg et al. found that PKC-induced translocation of ADAM12 to the membrane led to attenuation of focal adhesion number and strength (Sundberg et al., 2004). The most direct evidence for an inhibitory role of ADAM12 in focal adhesions was described in adipocytes, however. Overexression of ADAM12 led to a dramatic decrease in both stress fiber and vinculin-positive focal adhesion formation (Kawaguchi et al., 2003). This suggests that transmembrane ADAM12 is capable of disrupting focal adhesion formation and adhesion.

Our data suggested that ADAM12 was regulating focal adhesion number downstream of Twist1. To further characterize the effects of ADAM12, we examined the effects of knockdown on measurements of integrin binding and cell adhesion. In an

integrin extraction assay, more integrins were solubilized in control cells than those expressing shADAM12 constructs. As integrins not participating in interactions with the ECM are more easily solubilized, this implies that a larger pool of β1 integrins were engaged in interactions with the ECM in knockdown cells than controls. This is consistent with a model in which ADAM12 disrupts integrin-mediated interactions with ECM components. Knockdown cells also took significantly longer to trypsinize than control cells, indicating a stronger attachment with the ECM upon knockdown of ADAM12. Tyrosine phosphorylation of FAK, a marker of focal adhesion formation and signaling, was significantly increased in ADAM12 knockdown cells and almost eliminated when ADAM12 was overexpressed in Hs578t cells (Mitra and Schlaepfer, 2006). This suggests that knockdown of ADAM12 induces an increase in the formation of functional focal adhesions. Significantly, stress fiber formation and cell spreading in Hs578t-shADAM12 cells were reduced when treated with the β1 integrin blocking antibody AIIB2 (Park et al., 2006). This suggests that the mechanism by which ADAM12 knockdown increases focal adhesions is primarily through β1 integrin-mediated interactions with the ECM.

Due to the tight association of ADAM12 with invadopodia and previous associations with increased invasiveness, we went on to characterize the roles of ADAM12 in mediating invasion downstream of Twist1 (Albrechtsen et al., 2011; Abram et al., 2003). In a Transwell invasion assay, ADAM12 was necessary for invasion through a Matrigel-derived ECM. Additionally, ADAM12 both localized to invadopodia and was required for efficient invadopodia formation and gelatin degradation. Although ADAM12 has previously been described as localized to

invadopodia where it directly interacts with Tks5, relatively few studies have investigated the functional role of ADAM12 at invadopodia (Abram et al., 2003). Ligation of ADAM12 with a monoclonal antibody led to clustering of ADAM12 at the cell surface and localized shedding of EGF that induced invadopodia formation. This phenotype required the metalloprotease domain of ADAM12 and is hypothesized to lead to localized activation of Src kinases necessary for invadopodia formation (Albrechtsen et al., 2011). We therefore attempted to understand the dual roles of ADAM12 in focal adhesion and invadopodia regulation with a series of mutagenesis rescue experiments.

We generated three mutant forms of ADAM12: ADAM12ΔMMP, with an inactivating mutation in the metalloprotease domain (Jacobsen et al., 2008); ADAM12ΔDis, with a mutation that disrupts interactions with β1 integrin (Huang et al., 2005); and ADAM12ΔCyt, a truncation mutation that eliminates the cytoplasmic tail C-terminal to the transmembrane domain (Kang et al., 2001). Hs578t cells transiently transfected with either mutant or wild-type ADAM12 were assayed for both invadopodia formation and focal adhesion formation. Focal adhesion formation was rescued by all constructs except for ADAM12ΔDis. This suggests that ADAM12 is capable of negatively regulating focal adhesion formation via interactions with the disintegrin domain. This is consistent with reports that the disintegrin domain of ADAM12 directly interacts with β1 and β3 integrins (Thodeti et al., 2005). We hypothesize that the interaction is most likely through β1 integrin, due to the fact that treatment of Hs578t-shADAM12 cells with AIIB2 β1 integrin blocking antibody decreased stress fiber formation and cell spreading.

Interestingly, both the metalloprotease and disintegrin domains of ADAM12 were required for efficient rescue of the defect in invadopodia formation. This suggests that ADAM12 plays multiple roles in the regulation of invadopodia formation. Consistent with previously published data, the MMP domain may in fact play a role in the localized shedding of growth factors at invadopodia (Albrechtsen et al., 2011). Recently, it was found that the related ADAM family protease ADAM10 cleaves PDGFRβ to induce constitutive PDGFR signaling (Mendelson et al., 2010). Building on the observation of the important role of PDGFR signaling in invadopodia formation, it would be interesting to explore the possibility that PDGFR shedding is regulated by ADAM12. Probing for the presence of cleaved PDGFR in conditioned media in cells expressing control and ADAM12 knockdown constructs would allow initial verification of this hypothesis.

The observation that the disintegrin domain of ADAM12 is required for invadopodia formation can be explained by either an inhibitory role for focal adhesions in invadopodia formation or an intrinsic role for ADAM12 disintegrin activity at invadopodia. Previous publications have suggested that focal adhesions inhibit invadopodia formation via a mechanism involving sequestering of Src kinase activity at focal adhesions (Vitale et al., 2008; Chan et al., 2009). This conflicts with multiple other reports that FAK localizes to invadopodia and is required for invadopodia formation (Hauck et al., 2002; Alexander et al., 2008). In addition, some models of invadopodia formation suggest that they result from conversion of nascent focal adhesions to invadopodia (T. Oikawa et al., 2009).

To determine if focal adhesions intrinsically inhibit invadopodia formation, we treated Hs578t-shADAM12 cells with the β1 integrin blocking antibody AIIB2 or the FAK inhibitor PF-228 at concentrations sufficient to significantly reduce FAK tyrosine phosphorylation (Slack-Davis et al., 2007). We hypothesized that if focal adhesions inhibit invadopodia formation, inhibition of focal adhesions would lead to a rescue of invadopodia formation. Treatment with both AIIB2 and PF-228 led to a virtually complete elimination of invadopodia in Hs578t-shADAM12, however. This suggests that focal adhesions do not negatively regulate invadopodia formation in our system. The fact that the ADAM12ΔDis mutation fails to rescue invadopodia formation still suggests a role for ADAM12 in regulating focal adhesions or integrin-mediated interactions in invadopodia formation, however.

We hypothesize that dynamic interaction of integrins and focal adhesions with the ECM are required for efficient invadopodia formation. This is consistent with a model in which the increase in number of focal adhesions associated with ADAM12 knockdown is due to an increase in the stability of focal adhesions rather than an intrinsic increase in focal adhesion formation. This may also explain the migratory phenotype: knockdown of ADAM12 inhibits migration by inhibiting the turnover of focal adhesions required for cell motility (Owen et al., 2007; Urra et al., 2012). To test this hypothesis, it would be interesting to perform live-cell imaging experiments using fluorescently labeled paxillin and LifeAct to investigate the dynamics of these processes. LifeAct is a 17 amino acid fluorescently-tagged peptide that binds F-actin for use in live-cell imaging (Riedl et al., 2010). Use of total internal reflectance fluorescence (TIRF) microscopy will allow us to detect and quantify the dynamics of

both invadopodia and focal adhesions. If our hypotheses regarding focal adhesion dynamics are correct, we expect to observe decreased focal adhesion turnover in cells expressing ADAM12 knockdown constructs. Manipulating the dynamics of focal adhesions and invadopodia with inhibitors that regulate the turnover and formation of focal adhesions will be critical to understand any potential link between focal adhesions and invadopodia. These experiments will be essential in building a model of the role of ADAM12 in the regulation of both of these subcellular structures.

Further complicating any exploration of potential crosstalk between invadopodia and focal adhesions, however, is the recent report that focal adhesions are capable of degrading ECM components via recruitment of MT1-MMP to focal adhesions (Wang and McNiven, 2012). In light of this observation, it is vitally important to discriminate between invadopodia and focal adhesion-mediated degradation in any assays. Wang et al. report that focal adhesion-mediated degradation appears at the edges of the cell as oblong areas of degradation similar to the morphology of focal adhesions (Wang and McNiven, 2012). Due to the large increase in focal adhesions we observed upon knockdown of ADAM12, we therefore propose to analyze the relative contribution of invadopodia-mediated and focal adhesion-mediated degradation upon ADAM12 knockdown by grouping areas of degradation by morphology and location. Use of this technique at multiple time points will also allow us to characterize the relative kinetics of the two modes of ECM proteolysis, an area that remains unexplored. Correlating degradation ability with invasion assays will allow us to better understand the relative contributions of focal adhesions and invadopodia in mediating Twist1-induced invasion.

As both focal adhesions and invadopodia are capable of degrading the ECM and knockdown of ADAM12 leads to robust focal adhesion formation, this suggests the defect in ADAM12 mediated metastasis may be related to the migration defect. Performing invasion and migration rescue experiments with the mutant ADAM12 constructs are a priority in understanding what domains of ADAM12 are responsible for regulating these more complex processes. Future experiments characterizing the relative contributions of focal adhesions and invadopodia to metastasis in *in vivo* systems will be essential in understanding the most relevant targets for both future experiments and future therapeutic interventions.

METHODS

Cell Lines: HMLE cells were cultured as previously described (Yang et al., 2004). Hs578t breast carcinoma cells were maintained in Dulbecco's modification of Eagle's Media (DMEM, Mediatech, Manassas, VA) supplemented with 10% fetal bovine serum (Clontech), insulin (Sigma-Aldrich), and penicillin/streptomycin. All cells were maintained at 37^{o}C with 5% CO_2.

Antibodies: Antibodies were used at the following concentrations: ADAM12 (GeneTex, GTX11536, 1:2000 WB, 1:500 IF), β-actin (Abcam, ab8226, 1:20000 WB), β1 integrin (P4C10, a kind gift from Dr. David Cheresh, 1:500 IF), Cortactin (Upstate, 05-180, 1:1000 IF), Cortactin (Santa Cruz, sc-11408, 1:2000 WB), E-cadherin (BD Laboratories, 610182, 1:1000 WB), MT1-MMP (GeneTex, EP1264Y, 1:500), N-cadherin (Santa Cruz, H-63, 1:1000 WB), SV40LargeT (Santa Cruz , sc-147, 1:100 IHC, Twist1 (Generous gift from Dr. Gitelman, 1:500 WB), Vinculin (GeneTex,

SPM227, 1:500 IF). Western blot, WB; Immunofluorescence, IF; Immunohistochemistry, IHC.

Viral Production and Infection: Stable shADAM12 cell lines were created via infection of target cells using either lentiviruses or Moloney viruses. 293T cells were seeded at 1×10^6 cells per 6 cm dish in DMEM supplemented with 10% FBS (Biopioneer, San Diego, CA). After 18 hr, cells were transfected as follows: 6 µl TransIT-LT1 (Mirus Bio, USA) was added to 150 µl DMEM and incubated 20 min. One microgram of viral vector along with 0.9 µg of the appropriate gag/pol expression vector (pUMCV3 for pBabe or pWZL or pCMVΔ8.2R for lentiviral vectors) and 0.1 µg VSV-G expression vector were then added to the DMEM/LT-1 mixture. The mixture was incubated 30 min and then added to 293T cells overnight. The next day fresh media was added to the transfected 293T cells. Viral supernatant was harvested at 48 and 72 hr posttransfection, passed through a 0.45 micron syringe filter, and added to the recipient cell lines with 6 µg/ml protamine sulfate for a 4 hr infection. HMLE and Hs578t cells were then selected with 2 µg/ml puromycin (EMD Biosciences, USA), or 10 µg/ml blasticidin (Invitrogen, Carlsbad, CA).

Plasmids: The three shRNA lentiviral constructs against Twist1 in the pSP108 vector were described in Yang et al. (2004). ADAM12-Myc construct in pcDNA3.1 was a kind gift from Dr. Sara Courtneidge (Sanford-Burnham Institute for Biomedical Research, La Jolla, CA). ADAM12 was subcloned into pWb expression construct from pcDNA3.1 by ligation into pWZL-Blast mammalian expression vector after cutting with XhoI/SalI restriction enzymes. The shRNA constructs against ADAM12 were created using the Invitrogen Blockit RNAi Designer. Candidate shRNAs were screened

with NCBI BLAST to ensure specificity. Oligos were synthesized by Integrated DNA Technologies and were cloned into pSp81 vector with BstBI and BamHI restriction digestion followed by ligation. The shRNA constructs with associated U6 lentiviral promoter cassette and construct were cloned into pSp108 transfer vector with BamHI and SalI cuts followed by ligation.

Site-Directed Mutagenesis: Primers were generated for mutagenesis using PrimerX software to target the described residues in ADAM12. Primers were synthesized by Integrated DNA Technologies. Mutagenesis was performed using the QuikChange PCR protocol with Phusion DNA polymerase (New England Biolabs) using the ADAM12-myc construct as the template for mutagenesis. Following 30 cycles of synthesis, the template plasmid was digested with DpnI. DH5α cells were directly transformed with the product of the reaction. Colonies were screened by ampicillin resistance. Mutagenesis of final product was verified by sequencing by Retrogen (San Diego, CA) to verify sequence. The cytoplasmic tail truncation mutant was generated by PCR cloning of the extracellular and transmembrane domains from the pWZL-Blast construct, restriction digest with XhoI/SalI, and relegation into pWZL-Blast vector.

Real-Time PCR: Total RNAs were extracted from cells at 80%–90% confluency using RNeasy Mini Kit coupled with DNase treatment (QIAGEN, Venlo, Netherlands) and reverse transcribed with High Capacity cDNA Reverse Transcription Kit (Applied Biosystems, Foster City, CA). Resulting cDNAs were analyzed in triplicates using SYBR-Green Master PCR mix (Applied Biosystems) using an Applied Biosystems 7500 Fast Real Time PCR System with SDS Software. Relative mRNA concentrations were determined by $2^{-(Ct-Cc)}$ where Ct and Cc are the mean threshold

cycle differences after normalizing to GAPDH values. Primer pairs used for RT-PCR are as follows:

GAPDH: 5'- GAGAGACCCTCACTGCTG, 5'-GATGGTACATGACAAGGTGC

ADAM12:5'-TCAAAAGCCCCTGTAGAGAA, 5'-TCTGTGTGCACGAGCAAAAG

In Situ Zymography: This protocol is adapted from Artym et al. (2009). In brief, 12 mm coverslips were incubated in 20% nitric acid for 2 hr and washed in H_2O for 4 hr. Coverslips were incubated with 50 μg/ml poly-L-lysine diluted in PBS for 15 min followed by PBS washes before 0.15% gluteraldehyde in PBS was added for 10 min, followed by PBS washes. Coverslips were inverted onto 20 μl droplets of 1:9 0.1% fluorescein isothiocyante (FITC)-gelatin (Invitrogen): 0.2% porcine gelatin (Sigma-Aldrich) for 10 min. Coverslips were washed in PBS and then incubated 15 min in 5 mg/ml $NaBH_4$. Coverslips were rinsed in PBS and incubated at 37° in 10% calf serum (Hyclone, USA) in DMEM for 2 hr. Twenty thousand cells were seeded on each coverslip, incubated for 8 hr, and processed for immunofluorescence. Each experiment was performed in triplicate. Images were taken at ten fields per sample for a total of approximately 150 cells per sample with an Olympus FV1000 confocal microscope. Gelatin degradation was quantified using ImageJ software. To measure the percentage of degraded area in each field, identical signal threshold for the FITC-gelatin fluorescence are set for all images in an experiment and the degraded area with FITC signal below the set threshold was measured by ImageJ. The resulting percentage of degradation area was further normalized to total cell number (counted by DAPI staining for nuclei) in each field. The final gel degradation index is the average percentage

degradation per cell obtained from all ten fields. Each experiment was repeated at least three times.

Immunofluorescence: Matrix substrates were prepared by coating glass coverslips with 0.1% rat tail collagen I in DMEM for one hour. 20,000 cells were seeded onto coverslips in a 24 well plate and collected following three days of incubation. Cells were fixed at 37°C in 4% paraformaldehyde (PFA)/PBS with 50 μM $CaCl_2$ for 15 min, permeabilized with 0.1% Triton X-100/PBS for 10 min, and blocked with 5% goat serum. Samples were incubated with primary antibodies overnight at 4°C and with secondary antibodies and/or phalloidin (Invitrogen) for 2 hr. After washing, coverslips were mounted with VectaShield HardSet (Vector Laboratories, Burlingame, CA). Images were collected with an Olympus FV1000 confocal microscope.

Quantification of Cell Size: Images of cells on 0.1% collagen coated 24 well plates or in suspension were collected and identical thresholds applied to all images to isolate area of cell. Total area of cells was calculated using ImageJ. Relative areas were calculated by normalization to cells expressing shCtrl constructs.

Integrin Extraction Assay: Adapted from Kawaguchi et al., 2003. Cells were plated on 0.1% rat tail collagen I matrix in a 24 well plate. After incubation for 48 hours, media was aspirated and replaced with 0.01% TritonX-100 diluted in DMEM for 5 min at $4^{o}C$ with gentle agitation. Following incubation, media was quickly aspirated, rinsed once with PBS, and fixed with 4% PFA/PBS. Cells were processed for immunofluorescence for B1 integerin without additional permeabilization. Images were collected at random of the basal surface of cells stained for β1 integrin with an Olympus FV1000 confocal microscope. Total integrated pixel intensity normalized to cell

number was calculated for each sample with ImageJ. Fifty fields were analyzed and experiment was repeated in triplicate. Samples were normalized to samples not extracted with TritonX-100 to normalize the percentage of integrins lost by detergent extraction.

Trypsin Release Assay: 24 well plates were coated with 0.1% rat tail collagen I diluted in DMEM for one hour. Cells were plated on 0.1% rat tail collagen I matrix in a 24 well plate and allowed to sit for 48 hours. 0.05% trypsin was added into each well for the indicated amounts of time. Trypsin was inactivated by addition of an equal volume of 10% calf serum in DMEM. Wells were rinsed with PBS, fixed with 4% PFA, and stained with 0.1% crystal violet. Acetic acid was used to extract crystal violet from cells and the amount of crystal violet extracted quantified with an IMPLEN Nanophotometer. Relative cell number, normalized to un-trypsinized samples, was quantified for each time point.

Quantification of Focal Adhesion and Stress Fibers: Cells cultured for 48 hours on 0.1% rat tail collagen substrates were fixed and stained for F-actin and vinculin. Stress fibers were quantified by counting visually at 60x magnification on an Olympus FV1000 confocal microscope. Cortical actin was not counted; only stress fibers crossing the entire cell body were included in the count. Images of vinculin immunofluorescence were processed by applying identical threshold to all cells. Focal adhesions were quantified by setting minimum and maximum sizes limits for analysis. Settings were calibrated by quantification of positive and negative standards: Hs578t cells treated with $MnCl_2$ (increase in focal adhesions) or AIIB2 integrin blocking

antibody (decrease in focal adhesions) to ensure that changes in focal adhesion number were captured with the algorithm.

Three-Dimensional Cell Culture: Equal volumes and concentrations of NaOH-neutralized collagen I (Millipore, USA) and Matrigel were mixed on ice and 20 µl added to the bottom of each well of an eight chamber coverglass slide. Cells of interest were mixed with the Matrigel:collagen mixture to give a final concentration of 200,000 cells per ml and 100 cells µl of the cell:matrix mixture added to each well. Media supplemented with 5% Matrigel was changed every other day throughout assays.

Quantification of Invasive Spheroids: After one week in 3D culture (described above), images were collected of spheroid structures. Structures were counted as invasive if they had projections from the main spheroid body that extended farther than half the diameter of the spheroid. Structures that did not have a well defined spheroid structure were not quantified. Images were analyzed with ImageJ software.

Subcutaneous Tumor Implantation and Metastasis Assay: All animal care and experiments were approved by the Institutional Animal Care and Use Committee (IACUC) of the University of California, San Diego. Cells (1.5 million) resuspended in 50% Matrigel (BD Biosciences, USA) were injected into the left and right flanks of nude mice and allowed to grow to 1.5 cm in diameter before mice were sacrificed. Primary tumor size was measured every 5 days. Lungs were harvested and imaged for GFP positive tumor cells with a Leica MZ16F with ImagePro MC6.1 software. Tissues were embedded in paraffin, sectioned, stained with hematoxylin and eosin, and imaged to identify GFP positive tumor cells.

Immunohistochemistry: Paraffin sections of mouse samples were rehydrated through xylene and graded alcohols. Antigen retrieval was accomplished using a pressure cooker in 10 mM sodium citrate with 0.05% Tween. Samples were incubated with 3% H_2O_2 for 30 min followed by 5 hr blocking in 20% goat serum in PBS. Endogenous biotin and avidin were blocked using a Vector Avidin/Biotin blocking kit (Vector Laboratories). Primary antibodies were incubated overnight at 4°C in 20% goat serum. Biotinylated secondary antibody and Vectorstain ABC kit (Vector Laboratories) were used as indicated by manufacturer. Samples were developed with diaminobenzidine (DAB) (Vector Laboratories) and samples counterstained with hematoxylin (Vector Laboratories) and mounted with Permount.

Invasion and Migration Assays: For invasion assays, 50 μg of Matrigel was overlayed on Transwell permeable supports, dried overnight, and reconstituted with mammary epithelial growth media lacking recombinant epidermal growth factor. 40,000 cells were plated onto each well in triplicate and incubated for 72 hours. Cells were fixed with 4% PFA in PBS, washed extensively with PBS, stained with 0.1% crystal violet, washed extensively with PBS, and dried. Crystal violet was released with 50 μL 10% acetic acid and absorbency measured at 520 nm with an IMPLEN Nanophotometer. Identical protocols were used for migration assays using Transwells without Matrigel. All assays were performed in triplicates.

ACKNOWLEDGEMENTS

I would like to thank Dr. Sara Courtneidge and members of the lab for their helpful discussions regarding the project and their willingness to provide us with essential reagents. In particular, Dr. Begoňa Diaz and Dr. Danielle Murphy made

essential contribution to this project. Dr. David Cheresh and members of his lab were very generous in supplying us with antibodies against integrins that were instrumental in this project. I would also like to thank members of the Yang lab for their helpful suggestions and questions regarding the project. Helmi Lwin was particularly instrumental in beginning this project by designing shRNAs against ADAM12. Dr. Jeff Tsai also provided essential assistance in completing animal experiments involved in this project.

REFERENCES

Abram, C. L., Seals, D. F., Pass, I., Salinsky, D., Maurer, L., Roth, T. M., and Courtneidge, S. A. (2003). The adaptor protein fish associates with members of the ADAMs family and localizes to podosomes of Src-transformed cells. J Biol Chem *278*, 16844–16851.

Albrechtsen, R., Stautz, D., Sanjay, A., Kveiborg, M., and Wewer, U. M. (2011). Extracellular engagement of ADAM12 induces clusters of invadopodia with localized ectodomain shedding activity. Exp Cell Res *317*, 195–209.

Alexander, N. R., Branch, K. M., Parekh, A., Clark, E. S., Iwueke, I. C., Guelcher, S. A., and Weaver, A. M. (2008). Extracellular matrix rigidity promotes invadopodia activity. Current biology : CB 18, 1295–1299.

Artym, V. V., Yamada, K. M., and Mueller, S. C. (2009). ECM degradation assays for analyzing local cell invasion. Methods Mol Biol *522*, 211–219.

Asakura, M., Kitakaze, M., Takashima, S., Liao, Y., Ishikura, F., Yoshinaka, T., Ohmoto, H., Node, K., Yoshino, K., Ishiguro, H., et al. (2002). Cardiac hypertrophy is inhibited by antagonism of ADAM12 processing of HB-EGF: metalloproteinase inhibitors as a new therapy. Nat Med *8*, 35–40.

Blouw, B., Seals, D., Pass, I., Diaz, B., and Courtneidge, S. (2008). A role for the podosome/invadopodia scaffold protein Tks5 in tumor growth *in vivo*. Eur J Cell Biol *87*, 555–567.

Blobel, C. P., Wolfsberg, T. G., Turck, C. W., Myles, D. G., Primakoff, P., and White, J. M. (1992). A potential fusion peptide and an integrin ligand domain in a protein active in sperm–egg fusion. Nature *356*, 248–252.

Bork, P., Downing, A. K., Kieffer, B., and Campbell, I. D. (1996). Structure and distribution of modules in extracellular proteins. Qt Rev Biophys *29*, 119–167.

Courtneidge, S. A., Azucena, E. F., Pass, I., Seals, D. F., and Tesfay, L. (2005). The Src Substrate Tks5, Podosomes (Invadopodia), and Cancer Cell Invasion. Cold Spring Harbor Symposia on Quantitative Biology *70*, 167–171.

Cao, Y., Kang, Q., and Zolkiewska, A. (2001). Metalloprotease-disintegrin ADAM 12 interacts with alpha-actinin-1. Biochem J *357*, 353–361.

Chan, K. T., Cortesio, C. L., and Huttenlocher, A. (2009). FAK alters invadopodia and focal adhesion composition and dynamics to regulate breast cancer invasion. J Cell Biol *185*, 357–370.

Clemmons, D. R. (1998). Role of insulin-like growth factor binding proteins in controlling IGF actions. Mol Cell Endocrinol *140*, 19–24.

Dyczynska, E., Sun, D., Yi, H., Sehara-Fujisawa, A., Blobel, C. P., and Zolkiewska, A. (2007). Proteolytic processing of delta-like 1 by ADAM proteases. J Biol Chem *282*, 436–444.

Elineni, K. K., and Gallant, N. D. (2011). Regulation of cell adhesion strength by peripheral focal adhesion distribution. Biophys J *101*, 2903–2911.

Fröhlich, C., Albrechtsen, R., Dyrskjøt, L., Rudkjaer, L., Ørntoft, T. F., and Wewer, U. M. (2006). Molecular profiling of ADAM12 in human bladder cancer. Clin Cancer Res *12*, 7359–7368.

Galliano, M.-F. (2000). Binding of ADAM12, a marker of skeletal muscle regeneration, to the muscle-specific actin-binding protein, alpha-actinin-2, is required for myoblast fusion. J Biol Chem *275*, 13933–13939.

Gilpin, B. J., Loechel, F., Mattei, M. G., Engvall, E., Albrechtsen, R., and Wewer, U. M. (1998). A novel, secreted form of human ADAM 12 (meltrin alpha) provokes myogenesis *in vivo*. J Biol Chem *273*, 157–166.

Gimona, M., Buccione, R., Courtneidge, S. A., and Linder, S. (2008). Assembly and biological role of podosomes and invadopodia. Curr Opin Cell Biol *20*, 235–241.

Gutiérrez, J. M., Rucavado, A., Escalante, T., and Díaz, C. (2005). Hemorrhage induced by snake venom metalloproteinases: biochemical and biophysical mechanisms involved in microvessel damage. Toxicon *45*, 997–1011.

Hauck, C. R. Hsia, D. A. Ilic, D. Schlaepfer, D. D. (2002). v-Src SH3-enhanced interaction with focal adhesion kinase at beta 1 integrin-containing invadopodia promotes cell invasion. J Biol Chem *277*, 12487–12490.

Huang, J., Bridges, L. C., and White, J. M. (2005). Selective modulation of integrin-mediated cell migration by distinct ADAM family members. Mol Biol Cell *16*, 4982–4991.

Ito, N., Nomura, S., Iwase, A., Ito, T., Kikkawa, F., Tsujimoto, M., Ishiura, S., and Mizutani, S. (2004). ADAMs, a disintegrin and metalloproteinases, mediate shedding of oxytocinase. Biochem Biophys Res Commun *314*, 1008–1013.

Jacobsen, J., Visse, R., Sørensen, H. P., Enghild, J. J., Brew, K., Wewer, U. M., and Nagase, H. (2008). Catalytic properties of ADAM12 and its domain deletion mutants. Biochem *47*, 537–547.

Kalluri, R., and Weinberg, R. A. (2009). The basics of epithelial-mesenchymal transition. J Clin Invest *119*, 1420–1428.

Kang, Q, Cao, Y, Zolkiewska, A. (2001). Direct interaction between the cytoplasmic tail of ADAM 12 and the Src homology 3 domain of p85alpha activates phosphatidylinositol 3-kinase in C2C12 cells. J Biol Chem *276*, 24466–24472.

Kawaguchi, N., Sundberg, C., Kveiborg, M., Moghadaszadeh, B., Asmar, M., Dietrich, N., Thodeti, C. K., Nielsen, F. C., Möller, P., and Mercurio, A. M. (2003). ADAM12 induces actin cytoskeleton and extracellular matrix reorganization during early adipocyte differentiation by regulating beta1 integrin function. J Cell Sci *116*, 3893–3904.

Kurisaki, T., Masuda, A., Sudo, K., Sakagami, J., Higashiyama, S., Matsuda, Y., Nagabukuro, A., Tsuji, A., Nabeshima, Y., and Asano, M. (2003). Phenotypic analysis of meltrin (ADAM12)-deficient mice: involvement of meltrin in adipogenesis and myogenesis. Mol Cell Biol 23, 55–61.

Kveiborg, M., Albrechtsen, R., Couchman, J. R., and Wewer, U. M. (2008). Cellular roles of ADAM12 in health and disease. Int J Biochem Cell Biol *40*, 1685–1702.

Kveiborg, M., Fröhlich, C., Albrechtsen, R., Tischler, V., Dietrich, N., Holck, P., Kronqvist, P., Rank, F., Mercurio, A. M., and Wewer, U. M. (2005). A role for ADAM12 in breast tumor progression and stromal cell apoptosis. Cancer Res *65*, 4754–4761.

Kveiborg, M., Jacobsen, J., Lee, M. H., Nagase, H., Wewer, U. M., and Murphy, G. (2010). Selective inhibition of ADAM12 catalytic activity through engineering of tissue inhibitor of metalloproteinase 2 (TIMP-2). Biochem J *430*, 79–86.

Linder, S. (2009). Invadosomes at a glance. J Cell Sci *122*, 3009–3013.

Loechel, F., Fox, J. W., Murphy, G., Albrechtsen, R., and Wewer, U. M. (2000). ADAM 12-S cleaves IGFBP-3 and IGFBP-5 and is inhibited by TIMP-3. Biochem Biophys Res Commun *278*, 511–515.

Loechel, F., Overgaard, M. T., Oxvig, C., Albrechtsen, R., and Wewer, U. M. (1999). Regulation of human ADAM 12 protease by the prodomain. Evidence for a functional cysteine switch. J Biol Chem *274*, 13427–13433.

Mendelson, K., Swendeman, S., Saftig, P., and Blobel, C. P. (2010). Stimulation of platelet-derived growth factor receptor beta (PDGFRbeta) activates ADAM17 and promotes metalloproteinase-dependent cross-talk between the PDGFRbeta and epidermal growth factor receptor (EGFR) signaling pathways. J Biol Chem *285*, 25024–25032.

Mitra, S. K., and Schlaepfer, D. D. (2006). Integrin-regulated FAK-Src signaling in normal and cancer cells. Curr Opin Cell Biol *18*, 516–523.

Murphy, D. A., and Courtneidge, S. A. (2011). The “ins” and “outs” of podosomes and invadopodia: characteristics, formation and function. Nat Rev Mol Cell Biol *12*, 413–426.

Narita, D., Seclaman, E., Ursoniu, S., and Anghel, A. (2012). Increased expression of ADAM12 and ADAM17 genes in laser-capture microdissected breast cancers and correlations with clinical and pathological characteristics. Acta Histochem *114*, 131–139.

Oh, M., Im, I., Lee, Y. J., Kim, Y. H., Yoon, J. H., Park, H. G., Higashiyama, S., Kim, Y.-C., and Park, W. J. (2004). Structure-based virtual screening and biological evaluation of potent and selective ADAM12 inhibitors. Bioorg Med Chem *14*, 6071–6074.

Owen, K. A., Pixley, F. J., Thomas, K. S., Vicente-Manzanares, M., Ray, B. J., Horwitz, A. F., Parsons, J. T., Beggs, H. E., Stanley, E. R., and Bouton, A. H. (2007). Regulation of lamellipodial persistence, adhesion turnover, and motility in macrophages by focal adhesion kinase. J Cell Biol *179*, 1275–1287.

Park, C. C., Zhang, H., Pallavicini, M., Gray, J. W., Baehner, F., Park, C. J., and Bissell, M. J. (2006). Beta1 integrin inhibitory antibody induces apoptosis of breast cancer cells, inhibits growth, and distinguishes malignant from normal phenotype in three dimensional cultures and *in vivo*. Cancer Res *66*, 1526–1535.

Peduto, L., Reuter, V. E., Sehara-Fujisawa, A., Shaffer, D. R., Scher, H. I., and Blobel, C. P. (2006). ADAM12 is highly expressed in carcinoma-associated stroma and is required for mouse prostate tumor progression. Oncogene *25*, 5462–5466.

Rao, V. H., Kandel, A., Lynch, D., Pena, Z., Marwaha, N., Deng, C., Watson, P., and Hansen, L. A. (2011). A positive feedback loop between HER2 and ADAM12 in human head and neck cancer cells increases migration and invasion. Oncogene [Epub ahead of print].

Ray, A., Dhar, S., and Ray, B. K. (2010). Transforming growth factor-1-mediated activation of NF-kappaB contributes to enhanced ADAM-12 expression in mammary carcinoma cells. Mol Cancer Res *8*, 1261–1270.

Riedl, J., Flynn, K. C., Raducanu, A., Gärtner, F., Beck, G., Bösl, M., Bradke, F., Massberg, S., Aszodi, A., Sixt, M., et al. (2010). Lifeact mice for studying F-actin dynamics. Nat Methods *7*, 168–169.

Roy, R., Rodig, S., Bielenberg, D., Zurakowski, D., and Moses, M. A. (2011). ADAM12 transmembrane and secreted isoforms promote breast tumor growth: a distinct role for ADAM12-S protein in tumor metastasis. J Biol Chem *286*, 20758–20768.

Roy, R., Wewer, U. M., Zurakowski, D., Pories, S. E., and Moses, M. A. (2004). ADAM 12 cleaves extracellular matrix proteins and correlates with cancer status and stage. J Biol Chem *279*, 51323–51330.

Sahin, U., Weskamp, G., Kelly, K., Zhou, H.-M., Higashiyama, S., Peschon, J., Hartmann, D., Saftig, P., and Blobel, C. P. (2004). Distinct roles for ADAM10 and ADAM17 in ectodomain shedding of six EGFR ligands. J Cell Biol *164*, 769–779.

Schlaepfer, D. D., Hauck, C. R., and Sieg, D. J. (1999). Signaling through focal adhesion kinase. Prog Biophys Mol Biol *71*, 435–478.

Schlaepfer, D. D., and Hunter, T. (1997). Focal adhesion kinase overexpression enhances ras-dependent integrin signaling to ERK2/mitogen-activated protein kinase through interactions with and activation of c-Src. J Biol Chem *272*, 13189–13195.

Seals, D. F., and Courtneidge, S. A. (2003). The ADAMs family of metalloproteases: multidomain proteins with multiple functions. Genes Dev *17*, 7–30.

Sjöblom, B., Salmazo, A., and Djinović-Carugo, K. (2008). Alpha-actinin structure and regulation. Cell Mol Life Sci *65*, 2688–2701.

Slack-Davis, J. K., Martin, K. H., Tilghman, R. W., Iwanicki, M., Ung, E. J., Autry, C., Luzzio, M. J., Cooper, B., Kath, J. C., Roberts, W. G., et al. (2007). Cellular

characterization of a novel focal adhesion kinase inhibitor. J Biol Chem *282*, 14845–14852.

Stautz, D., Sanjay, A., Hansen, M. T., Albrechtsen, R., Wewer, U. M., and Kveiborg, M. (2010). ADAM12 localizes with c-Src to actin-rich structures at the cell periphery and regulates Src kinase activity. Exp Cell Res *316*, 55–67.

Sundberg, C., Thodeti, C. K., Kveiborg, M., Larsson, C., Parker, P., Albrechtsen, R., and Wewer, U. M. (2004). Regulation of ADAM12 cell-surface expression by protein kinase C epsilon. J Biol Chem *279*, 51601–51611.

Suzuki, A., Kadota, N., Hara, T., Nakagami, Y., Izumi, T., Takenawa, T., Sabe, H., and Endo, T. (2000). Meltrin α cytoplasmic domain interacts with SH3 domains of Src and Grb2 and is phosphorylated by v-Src. Oncogene *19,* 5842–5850.

T. Oikawa, T. T. (2009). PtdIns(3,4)P2 instigates focal adhesions to generate podosomes. Cell Adh Migr *3*, 195–197.

Thodeti, C., Frohlich, C., Nielsen, C., Holck, P., Sundberg, C., Kveiborg, M., Mahalingam, Y., Albrechtsen, R., Couchman, J., and Wewer, U. (2005). Hierarchy of ADAM12 binding to integrins in tumor cells. Exp Cell Res *309*, 438–450.

Tamura, M., Gu, J., Matsumoto, K., Aota, S., Parsons, R., Yamada, K.M. (1998). Inhibition of cell migration, spreading, and focal adhesions by tumor suppressor PTEN. Science *280*, 1614–1617.

Thodeti, C. K., Albrechtsen, R., Grauslund, M., Asmar, M., Larsson, C., Takada, Y., Mercurio, A. M., Couchman, J. R., and Wewer, U. M. (2003). ADAM12/syndecan-4 signaling promotes beta 1 integrin-dependent cell spreading through protein kinase Calpha and RhoA. J Biol Chem *278*, 9576–9584.

Thodeti, C. K., Fröhlich, C., Nielsen, C. K., Takada, Y., Fässler, R., Albrechtsen, R., and Wewer, U. M. (2005). ADAM12-mediated focal adhesion formation is differently regulated by beta1 and beta3 integrins. FEBS Lett *579*, 5589–5595.

Urra, H., Torres, V. A., Ortiz, R. J., Lobos, L., Díaz, M. I., Díaz, N., Härtel, S., Leyton, L., and Quest, A. F. G. (2012). Caveolin-1-enhanced motility and focal adhesion turnover require tyrosine-14 but not accumulation to the rear in metastatic cancer cells. PLoS ONE *7*, e33085.

Vitale, S., Avizienyte, E., Brunton, V., and Frame, M. (2008). Focal adhesion kinase is not required for Src-induced formation of invadopodia in KM12C colon cancer cells and can interfere with their assembly. Eur J Cell Biol *87*, 569–579.

Wang, Y., and McNiven, M. A. (2012). Invasive matrix degradation at focal adhesions occurs via protease recruitment by a FAK-p130Cas complex. J Cell Biol *196*, 375–385.

Wewer, U. M., Mörgelin, M., Holck, P., Jacobsen, J., Lydolph, M. C., Johnsen, A. H., Kveiborg, M., and Albrechtsen, R. (2006). ADAM12 is a four-leafed clover: the excised prodomain remains bound to the mature enzyme. J Biol Chem *281*, 9418–9422.

Whelan, J., and Miller, N. (1996). Generation of estrogen receptor mutants with altered ligand specificity for use in establishing a regulatable gene expression system. The J Steroid Biochem Mol Biol *58*, 3–12.

Xiong, Y., Rangamani, P., Fardin, M. A., Lipshtat, A., Dubin-Thaler, B., Rossier, O., Sheetz, M. P., and Iyengar, R. (2010). Mechanisms controlling cell size and shape during isotropic cell spreading. Biophys J *98*, 2136–2146.

Yagami-Hiromasa, T., Sato, T., Kurisaki, T., Kamijo, K., Nabeshima, Y., and Fujisawa-Sehara, A. (1995). A metalloprotease-disintegrin participating in myoblast fusion. Nature *377*, 652–656.

Yang, J., Mani, S. A., Donaher, J. L., Ramaswamy, S., Itzykson, R. A., Come, C., Savagner, P., Gitelman, I., Richardson, A., and Weinberg, R. A. (2004). Twist, a master regulator of morphogenesis, plays an essential role in tumor metastasis. Cell *117*, 927–939.

Zhao, Z., Gruszczynska-Biegala, J., Cheuvront, T., Yi, H., von der Mark, H., von der Mark, K., Kaufman, S. J., and Zolkiewska, A. (2004). Interaction of the disintegrin and cysteine-rich domains of ADAM12 with integrin α7β1. Exp Cell Res *298*, 28–37.

Zolkiewska, A. (1999). Disintegrin-like/cysteine-rich region of ADAM 12 is an active cell adhesion domain. Exp Cell Res *252*, 423–431.

Chapter IV

Conclusions and Perspectives

The discovery of an important role for EMT in cancer progression has provided a new framework in which to address questions regarding how cells gain the ability to invade and metastasize. In particular, it has highlighted the importance of transcription factors, including Twist1, in inducing multifactorial changes in cells that promote metastasis. Understanding the downstream targets of these transcription factors is essential to build models that recapitulate the cellular changes that occur during EMT in cancer progression. To those ends, we characterized the roles of the tyrosine kinase receptor PDGFRα and the metalloprotease ADAM12 in promoting metastasis downstream of Twist1.

A major unanswered question regarding Twist1 is the mechanism by which it induces local invasion. Forced expression of E-cadherin in cells that have undergone a Twist1-induced EMT is insufficient to prevent invasion (Yang et al., 2004). We therefore attempted to determine how Twist1 actively regulates invasion. Using a series of mammary cancer cell lines derived from a single mouse tumor, we found that the ability to degrade gelatin correlated with Twist1 expression. Indeed, this degradation was dependent on Twist1, as knockdown of Twist1 at the protein level led to a decrease in gelatin degradation in these same cell lines. Interestingly, we observed a pattern of degradation associated with degradation mediated by invadopodia. We therefore investigated if Twist1 regulated invadopodia formation. We found that Twist1 was both necessary and sufficient for invadopodia formation in mouse mammary carcinoma cell lines and human mammary epithelial cell lines, respectively. Importantly, the structures formed were bona fide invadopodia that were localized to the basal surface of the cell, dependent on metalloprotease activity, and required Tks5 expression.

Based on the observation that Twist1 was necessary and sufficient for invadopodia formation, we went on to characterize the mechanism by which Twist1 regulates invadopodia formation. Twist1 expression in human mammary epithelial cells led to an increase in Src activity that was dependent on expression and activity of PDGFRα. Knockdown or antibody-mediated inhibition of PDGFRα was sufficient to inhibit tyrosine phosphorylation of the invadopodia component cortactin and to prevent invadopodia formation and gelatin degradation. When human mammary epithelial cells expressing knockdown constructs against either Tks5 or PDGFRα were used in a xenotransplantation model of breast cancer metastasis, we found a significant reduction of metastasis with both knockdowns. These experiments were interesting as they indicated that both invadopodia and signaling pathways regulating invadopodia formation are essential for metastasis in a mouse model.

We then went on to investigate if PDGFRα and Twist1 were correlated with survival in human breast cancer patient data. In both microarray data sets and in human patient data, Twist1 and PDGFRα correlated both with each other and poor survival. This was consistent with an additional observation based on chromatin immunoprecipitation and luciferase assays that Twist1 binds the PDGFRα promoter to directly regulate its transcription. We also described a specific role for Twist1 in mediating invadopodia formation during EMT. Both forced expression of the EMT-inducing transcription factor Snail and treatment with TGF-β induced formation of invadopodia. Importantly, Twist1 was highly upregulated downstream of both signals. Knockdown of Twist1 in both systems led to a decrease in invadopodia formation while

not leading to a reversion of the EMT process. This indicated that Twist1 has specific roles in mediating local invasion during EMT.

This study answers several important questions regarding the role of Twist1 in EMT. Significantly, it provides a mechanism to explain how Twist1 actively induces invasion during the EMT process. Formation of invadopodia is downstream of Twist1 and required for local invasion and metastasis. This was especially important as relatively few studies have directly addressed the roles of invadopodia in models of metastasis. Although cortactin was found to be necessary for dissemination in a model of breast cancer metastasis, cortactin has other roles in normal cell biology as an actin bundling protein associated with cortical actin (Li et al., 2001). Previous experiments utilizing knockdown of Tks5 in a mouse model of metastasis found that Tks5 knockdown reduced tumor growth and angiogenesis, but had no effects on metastasis (Blouw et al., 2008). This observation could be due to the effects of using Src-transformed fibroblasts instead of transformed mammary epithelial cells. Although Src-transformed fibroblasts are an excellent model of fibrosarcomas, there may be inherent differences in the details of the metastatic process in these cells versus cell lines derived from breast carcinomas (Murphy and Courtneidge, 2011).

In addition, this study was the first to propose a mechanism for transcriptional regulation of invadopodia formation. A previous publication suggested that invadopodia-mediated degradation was dependent on upregulation of MMP2 transcription by AP1, but AP1 was not required for invadopodia formation in the described system (Hasegawa et al., 2009). Interestingly, a role for post-transcriptional regulation of mRNA in podosomes has been described. In vascular smooth muscle cells,

inhibition of the microRNAs (mir)-143 and 145 downstream of PDGF signaling is essential for podosome formation (Quintavalle et al., 2010). It will be interesting to determine if other microRNAs are similarly involved in regulation of invadopodia formation in cancer cells. As transcription factors involved in EMT are increasingly being investigated as clinical biomarkers for prognosis, there is potential to integrate markers of invadopodia formation with markers of EMT. Interestingly, a recent paper reported a role for the focal adhesion protein hydrogen peroxide-inducible clone 5 (Hic-5) in regulating invadopodia formation downstream of TGF-β signaling (Pignatelli et al., 2012).

The observation that invadopodia are essential for invasion and dissemination in a mouse model of metastasis suggests that treatments targeting invadopodia formation could be clinically useful. Experiments using both small molecule inhibitors and knockdown of signaling components have demonstrated an essential and central role for Src in mediating invadopodia formation. As a tyrosine kinase, Src is relatively easily druggable with multiple small molecule inhibitors on the market (Kim et al., 2009). Unfortunately, use of Src inhibitors, including dasatinib and bosutinib, have not shown dramatic effects in treatment of solid tumors, including breast cancer (Mayer and Krop, 2010). Upstream of Src, the PDGFR inhibitor Gleevec could have obvious applications to solid cancer therapeutics (Druker et al., 1996). Although previous small clinical trials have found little benefit from Gleevec in breast cancer, these trials took place in advanced stage cancer patients in which metastasis likely had already occurred (Cristofanilli et al., 2008). The recent development of antibody-based inhibitors against MT1-MMP may provide alternative methods of inhibiting metalloproteases at

invadopodia without the toxicities associated with hydroxamate metalloprotease inhibitors (Devy et al., 2009; Gialeli et al., 2011). In order for any therapeutic targeting invadopodia to be approved, however, the patient population must be carefully selected. Observations from our lab and others suggest that agents targeting invadopodia would be most helpful in the early stages of cancer progression in which tumor cells invade the surrounding stroma and breach basement membranes.

Although this study answered many questions regarding the role of Twist1 in local invasion and invadopodia formation, it raised several other important questions. Twist1 and PDGFRα are both induced during development and required for normal craniofacial development (Chen and Behringer, 1995; Sun et al., 2000). In addition, defects in the ECM associated with the neural crest were observed in PDGFRα mice (Hoch and Soriano, 2003). This raises the obvious possibility that Twist1-induced invadopodia may function in development, particularly in neural crest cell invasion and migration. A recent report by Murphy et al. suggests a vital role for Tks5-mediated invadopodia during invasive processes in zebrafish development (Murphy et al., 2011). Similar techniques could be applied to investigate the roles of Twist1 and PDGFRα orthologous genes in zebrafish development. Alternatively, similar process could be investigated in mammalian species using fluorescently labeled genes or immunofluorescence in developing embryos. To these ends, a transgenic mouse expressing LifeAct-GFP has been developed in which all F-actin is labeled by interaction with a fluorescent LifeAct peptide (Riedl et al., 2010).

The association between EMT and invadopodia formation also suggests a possible role for invadopodia in mammalian gastrulation. During gastrulation, the

primitive ectoderm invaginates to form the mesoderm in a process that requires breakdown of a basement membrane underlying the ectoderm (Sanders, 1984). This process resembles an EMT as cells in the ectoderm lose cadherin-mediated junctions and invade individually to form the mesoderm (Thiery et al., 2009). Importantly, EMT-inducing transcription factors, most prominently Snail, are associated with mesoderm formation (Carver et al., 2001). There are multiple *in vitro* models of mammalian gastrulation that entail use of embryoid body culture. Differentiation and gastrulation may be triggered by withdrawal of leukemia inhibitory factor (LIF) to promote gastrulation, providing a convenient model of early development that is amenable to genetic and small molecule manipulation (Kurosawa, 2007). Investigation of potential roles for invadopodia in gastrulation could be performed by knocking down essential invadopodia component proteins with shRNA and investigating the integrity of the basement membrane during gastrulation with immunofluorescence. As developmental pathways are often co-opted and inappropriately expressed during cancer progression, better characterizing the functions of invadopodia in developmental systems will be key to understanding the metastastic process.

In addition, the identification of PDGFRα as a downstream target of Twist1 during EMT has other applications in addition to inhibition of local invasion and metastasis. In a recent model for cancer development, a subpopulation of cancer cells, cancer stem cells, promote sustained growth of the tumor and are resistant to many chemotherapeutics (Visvader and Lindeman, 2008). Importantly, EMT and Twist1 expression is associated with development of a cancer stem cell-like phenotype (Mani et

al., 2008). As PDGFRα is a direct target of Twist1, PDGFRα would be an appealing target for treatments aimed at depleting cancer stem cells.

Additionally, we describe a role for the metalloprotease ADAM12 in regulating both invadopodia formation and migration downstream of Twist1. ADAM12 is an interesting protein with the ability to both act as a metalloprotease and modulate integrin-dependent adhesion and signaling via a disintegrin domain. We identify roles for both of these domains in regulating Twist1-induced motility and invasion.

Upon observing a robust induction of ADAM12 in response to Twist1 expression, we went on to find that Twist1 is both necessary and sufficient for ADAM12 expression in Hs578t breast cancer cells and breast epithelial cells, respectively. Knockdown of ADAM12 in both Hs578t cells and breast epithelial cells led to a decrease in motility in both Transwell and scratch assays. In addition, knockdown of ADAM12 was associated with an increase in cell spreading independent of cell size and was associated with an increase in focal adhesion number. Consistent with an increase in focal adhesion formation, we observed a decrease in β1 integrin solubility and an increase in adhesion in ADAM12 knockdown cells. This implied a strong role for ADAM12 in regulating adhesion downstream of Twist1.

In addition to effects on focal adhesions, knockdown of ADAM12 also reduced cell invasion in a Matrigel-Transwell invasion assay. Due to the previously observed localization of ADAM12 to invadopodia, we therefore investigated the possibility that knockdown of ADAM12 affected invadopodia formation (Abram et al., 2003). Knockdown of ADAM12 was sufficient to inhibit invadopodia formation and gelatin degradation in both Hs578t and human mammary epithelial cells. ADAM12 was

necessary for local invasion in both *in vitro* and *in vivo* models. In a mouse model of metastasis, we observed a significant decrease in lung metastasis upon knockdown of ADAM12 that was associated with a similar decrease in local invasion detected with immunohistochemistry.

As ADAM12 is a multidomain protein with potential roles in invadopodia formation by both locally shedding growth factors and modulating integrin-mediated adhesions, we performed a series of rescue experiments (Kveiborg et al., 2008). We expressed constructs of ADAM12 in which the metalloprotease, disintegrin, or cytoplasmic tail were mutated in Hs578t ADAM12 knockdown cells and assayed for focal adhesion and invadopodia formation. Surprisingly, the cytoplasmic tail was dispensible for rescuing either phenotype, while the disintegrin domain was required for rescue of both the focal adhesion and invadopodia defects. The metalloprotease domain was additionally required for rescue of the invadopodia defect. Previously, the metalloprotease domain of ADAM12 has been described as essential for formation of invadopodia via directing localized shedding of EGF (Albrechtsen et al., 2011). The disintegrin domain could possess obvious roles in disrupting integrin-mediated focal adhesions. To explain the effect of the disintegrin domain on invadopodia formation, we propose two possible hypotheses. ADAM12 may be necessary for dynamic regulation of integrin-mediated adhesions at both focal adhesions and invadopodia. Alternatively, the disintegrin domain of ADAM12 may be required for localized ADAM12 proteolysis at invadopodia. A similar model has been proposed in which MT1-MMP activation of MMP2 requires an association with αvβ3 integrin to efficiently cleave the prodomain of MMP2 (Deryugina et al., 2001).

Our investigation of the role of ADAM12 in mediating Twist1-induced local invasion and migration answers several unresolved questions. Importantly, it provides information about the regulation of ADAM12 during EMT and previously undocumented roles for ADAM12 domains in both focal adhesion and invadopodia regulation.

Although ADAM12 expression has been associated with multiple cancers, relatively little was known about its transcriptional regulation. High levels of ADAM12 have been observed in breast and bladder cancer (Narita et al., 2012; Fröhlich et al., 2006). In addition, levels of soluble ADAM12 in the urine of breast cancer patients correlates with prognosis (Roy et al., 2004). The only previously described transcriptional regulator of ADAM12 is NFK-B, which induces ADAM12 in response to TGF-β signaling (Ray et al., 2010). Our data suggests that ADAM12 may be correlated with Twist1 expression or EMT in human patient samples. It should be noted, however, that ADAM12 is unlikely to be a direct target of Twist1 as the ADAM12 promoter lacks E-box elements. More work is therefore necessary to completely describe the transcriptional regulation of ADAM12 during EMT. It will be interesting to determine if ADAM12 is associated with other transcriptional regulators of EMT such as Snail or Zeb1 and Zeb2.

In addition, our data suggests a positive role for ADAM12 in promoting migration during EMT. Increased motility and migration are required for efficient metastasis and a prerequisite for invasiveness. Although an increase in migration is observed upon expression of Twist1, regulators of migration have not been as thoroughly studied. Previously activation of Rac1 has been associated with increased

motility downstream of Twist1 (Yang et al., 2012). Our data suggests ADAM12 may play roles in promoting migration downstream of Twist1 via interactions with integrin-mediated adhesions.

Previous studies have suggested a role for ADAM12 in regulating adhesion, but ours is one of the first to specifically address the role of ADAM12 in regulating focal adhesions. In adipose cells, translocation of ADAM12 to the membrane is associated with a reduction in focal adhesion-like structures and stress fibers (Kawaguchi et al., 2003). In addition, Twist1 expression has been associated with a reduction in focal adhesion formation in liver cancer (Matsuo et al., 2009). Although we observe an increase in focal adhesions upon knockdown of ADAM12, this effect may be due to changes in the dynamics of focal adhesions. The disintegrin domain of ADAM12 is capable of directly interacting with integrins and may regulate focal adhesion lifetime. It is difficult to investigate dynamic processes using immunofluorescence of fixed cells. Therefore in order to more fully understand this process, live cell imaging using total-internal reflectance fluorescence (TIRF) microscopy to study focal adhesion dynamics with fluorescently tagged paxillin would be interesting. This technique would allow one to measure the absolute lifetimes of focal adhesions in control and ADAM12 knockdown cells to characterize the potential effects of ADAM12 on focal adhesion stability. Similar techniques using fluorescently labeled actin or cortactin would more fully reveal the effects of ADAM12 on invadopodia stability.

The relative contributions of focal adhesions and invadopodia to invasion and potential interactions between these structures are still unresolved. Previous reports have identified focal adhesions as opposed to invadopodia formation with increased

focal adhesion formation correlating with decreased invadopodia (Chan et al., 2009). The authors suggest that this is due to sequestering of active Src at focal adhesions. Other investigators have reported that invadopodia can be distinguished from focal adhesions by a lack of staining for FAK with immunofluorescence (Bowden et al., 2006). In contrast, other groups have reported an essential role for FAK in invadopodia biogenesis (Hauck et al., 2002; Pan et al., 2011). FAK localizes to invadopodia in other cell lines as well (Alexander et al., 2008). This contradictory information regarding focal adhesions and their roles in invadopodia suggests that major unresolved questions remain in the field. It is possible that invadopodia can be formed through multiple mechanisms, with some invadopodia arising from nascent focal adhesions and others from *de novo* actin polymerization (Mader et al., 2011; Oikawa and Takenawa, 2009). The recent observation that focal adhesions are also capable of degrading the ECM raises additional questions regarding the relative contributions of invadopodia and focal adhesions to local invasion (Wang and McNiven, 2012). It will be necessary to perform robust *in vitro* and *in vivo* characterizations of focal adhesion and invadopodia-mediated invasion to fully understand these processes. As invadopodia and focal adhesions both behave differently in 3D culture systems, it will be necessary to investigate these relative contributions in 3D matrices to more fully resolve these questions.

Although significant process has been made to understand the regulation of invasion and metastasis during the EMT process, many open questions remain in the field. Addressing these questions will require use of sophisticated imaging and culture systems to recapitulate the environments cells experience *in vivo*. In addition, more robust *in vivo* characterization of the role of invadopodia and focal adhesions is

essential to understanding these unique cellular processes. Although these experiments will be challenging, they have the potential to reveal new targets and biomarkers for cancer treatment and diagnosis.

REFERENCES

Abram, C. L., Seals, D. F., Pass, I., Salinsky, D., Maurer, L., Roth, T. M., and Courtneidge, S. A. (2003). The adaptor protein fish associates with members of the ADAMs family and localizes to podosomes of Src-transformed cells. J Biol Chem *278*, 16844–16851.

Albrechtsen, R., Stautz, D., Sanjay, A., Kveiborg, M., and Wewer, U. M. (2011). Extracellular engagement of ADAM12 induces clusters of invadopodia with localized ectodomain shedding activity. Exp Cell Res *317*, 195–209.

Alexander, N. R., Branch, K. M., Parekh, A., Clark, E. S., Iwueke, I. C., Guelcher, S. A., and Weaver, A. M. (2008). Extracellular matrix rigidity promotes invadopodia activity. Curr Biol *18*, 1295–1299.

Blouw, B., Seals, D., Pass, I., Diaz, B., and Courtneidge, S. (2008). A role for the podosome/invadopodia scaffold protein Tks5 in tumor growth *in vivo*. Eur J Cell Biol *87*, 555–567.

Bowden, E. T., Onikoyi, E., Slack, R., Myoui, A., Yoneda, T., Yamada, K. M., and Mueller, S. C. (2006). Co-localization of cortactin and phosphotyrosine identifies active invadopodia in human breast cancer cells. Exp Cell Res *312*, 1240–1253.

Carver, E. A., Jiang, R., Lan, Y., Oram, K. F., and Gridley, T. (2001). The mouse snail gene encodes a key regulator of the epithelial-mesenchymal transition. Mol Cell Biol *21*, 8184–8188.

Chan, K. T., Cortesio, C. L., and Huttenlocher, A. (2009). FAK alters invadopodia and focal adhesion composition and dynamics to regulate breast cancer invasion. J Cell Biol *185*, 357–370.

Chen, Z. F., and Behringer, R. R. (1995). twist is required in head mesenchyme for cranial neural tube morphogenesis. Genes Dev *9*, 686–699.

Cristofanilli, M., Morandi, P., Krishnamurthy, S., Reuben, J. M., Lee, B.-N., Francis, D., Booser, D. J., Green, M. C., Arun, B. K., Pusztai, L., et al. (2008). Imatinib mesylate (Gleevec) in advanced breast cancer-expressing C-Kit or PDGFR-beta: clinical activity and biological correlations. Ann Oncol *19*, 1713–1719.

Deryugina, E. I., Ratnikov, B., Monosov, E., Postnova, T. I., DiScipio, R., Smith, J. W., and Strongin, A. Y. (2001). MT1-MMP initiates activation of pro-MMP-2 and integrin alphavbeta3 promotes maturation of MMP-2 in breast carcinoma cells. Exp Cell Res *263*, 209–223.

Devy, L., Huang, L., Naa, L., Yanamandra, N., Pieters, H., Frans, N., Chang, E., Tao, Q., Vanhove, M., and Lejeune, A. (2009). Selective inhibition of matrix metalloproteinase-14 blocks tumor growth, invasion, and angiogenesis. Cancer Res *69*, 1517–1526.

Druker, B. J., Tamura, S., Buchdunger, E., Ohno, S., Segal, G. M., Fanning, S., Zimmermann, J., and Lydon, N. B. (1996). Effects of a selective inhibitor of the Abl tyrosine kinase on the growth of Bcr–Abl positive cells. Nat Med *2*, 561–566.

Fröhlich, C., Albrechtsen, R., Dyrskjøt, L., Rudkjaer, L., Ørntoft, T. F., and Wewer, U. M. (2006). Molecular profiling of ADAM12 in human bladder cancer. Clin Cancer Res *12*, 7359–7368.

Gialeli, C., Theocharis, A. D., and Karamanos, N. K. (2011). Roles of matrix metalloproteinases in cancer progression and their pharmacological targeting. FEBS J *278*, 16–27.

Hasegawa, H., Senga, T., Ito, S., Iwamoto, T., and Hamaguchi, M. (2009). A role for AP-1 in matrix metalloproteinase production and invadopodia formation of v-Crk-transformed cells. Exp Cell Res *315*, 1384–1392.

Hauck, C. R., Hsia, D.A., Ilic, D., Schlaepfer, D. D. (2002). v-Src SH3-enhanced interaction with focal adhesion kinase at beta 1 integrin-containing invadopodia promotes cell invasion. J Biol Chem *277*, 12487–12490.

Hoch, R. V., and Soriano, P. (2003). Roles of PDGF in animal development. Development *130*, 4769–4784.

Kawaguchi, N., Sundberg, C., Kveiborg, M., Moghadaszadeh, B., Asmar, M., Dietrich, N., Thodeti, C. K., Nielsen, F. C., Möller, P., and Mercurio, A. M. (2003). ADAM12 induces actin cytoskeleton and extracellular matrix reorganization during early adipocyte differentiation by regulating beta1 integrin function. J Cell Sci *116*, 3893–3904.

Kim, L. C., Song, L., and Haura, E. B. (2009). Src kinases as therapeutic targets for cancer. Nature Rev Clin Oncol *6*, 587–595.

Kurosawa, H. (2007). Methods for inducing embryoid body formation: *in vitro* differentiation system of embryonic stem cells. J Biosci Bioeng *103,* 389–398.

Kveiborg, M., Albrechtsen, R., Couchman, J. R., and Wewer, U. M. (2008). Cellular roles of ADAM12 in health and disease. Int J Biochem Cell Biol *40*, 1685–1702.

Li, Y., Tondravi, M., Liu, J., Smith, E., Haudenschild, C. C., Kaczmarek, M., and Zhan, X. (2001). Cortactin potentiates bone metastasis of breast cancer cells. Cancer Res *61*, 6906–6911.

Mader, C. C., Oser, M., Magalhaes, M. A. O., Bravo-Cordero, J., Condeelis, J. S., Koleske, A. J., and Gil-Henn, H. (2011). An EGFR-Src-Arg-cortactin pathway mediates functional maturation of invadopodia and breast cancer cell invasion. Cancer Res *71*, 1730–1741.

Mani, S. A., Guo, W., Liao, M.-J., Eaton, E. N., Ayyanan, A., Zhou, A. Y., Brooks, M., Reinhard, F., Zhang, C. C., Shipitsin, M., et al. (2008). The epithelial-mesenchymal transition generates cells with properties of stem cells. Cell *133*, 704–715.

Matsuo, N., Shiraha, H., Fujikawa, T., Takaoka, N., Ueda, N., Tanaka, S., Nishina, S., Nakanishi, Y., Uemura, M., and Takaki, A. (2009). Twist expression promotes migration and invasion in hepatocellular carcinoma. BMC Cancer *9*, 240.

Mayer, E. L., and Krop, I. E. (2010). Advances in targeting Src in the treatment of breast cancer and other solid malignancies. Clin Cancer Res *16*, 3526–3532.

Murphy, D. A., and Courtneidge, S. A. (2011). The “ins” and “outs” of podosomes and invadopodia: characteristics, formation and function. Nat Rev Mol Cell Biol *12*, 413–426.

Murphy, D. A., Diaz, B., Bromann, P. A., Tsai, J. H., Kawakami, Y., Maurer, J., Stewart, R. A., Izpisúa-Belmonte, J. C., and Courtneidge, S. A. (2011). A Src-Tks5 pathway is required for neural crest cell migration during embryonic development. PLoS ONE 6, e22499.

Narita, D., Seclaman, E., Ursoniu, S., and Anghel, A. (2012). Increased expression of ADAM12 and ADAM17 genes in laser-capture microdissected breast cancers and correlations with clinical and pathological characteristics. Acta Histochem *114*, 131–139.

Oikawa, T., and Takenawa, T. (2009). PtdIns(3,4)P2 instigates focal adhesions to generate podosomes. Cell Adh Migr *3*, 195–197.

Pan, Y. R., Chen, C. L., and Chen, H. C. (2011). FAK is required for the assembly of podosome rosettes. J Cell Biol *195*, 113–129.

Pignatelli, J., Tumbarello, D. A., Schmidt, R. P., and Turner, C. E. (2012). Hic-5 promotes invadopodia formation and invasion during TGF-beta-induced epithelial-mesenchymal transition. J Cell Biol. In Press.

Quintavalle, M., Elia, L., Condorelli, G., and Courtneidge, S. A. (2010). MicroRNA control of podosome formation in vascular smooth muscle cells *in vivo* and *in vitro*. J Cell Biol *189*, 13–22.

Ray, A., Dhar, S., and Ray, B. K. (2010). Transforming growth factor-1-mediated activation of NF- B contributes to enhanced ADAM-12 expression in mammary carcinoma cells. Mol Cancer Res *8*, 1261–1270.

Riedl, J., Flynn, K. C., Raducanu, A., Gärtner, F., Beck, G., Bösl, M., Bradke, F., Massberg, S., Aszodi, A., Sixt, M., et al. (2010). Lifeact mice for studying F-actin dynamics. Nat Methods *7*, 168–169.

Roy, R., Wewer, U. M., Zurakowski, D., Pories, S. E., and Moses, M. A. (2004). ADAM 12 cleaves extracellular matrix proteins and correlates with cancer status and stage. J Biol Chem *279*, 51323–51330.

Sanders, E. J. (1984). Labelling of basement membrane constituents in the living chick embryo during gastrulation. J Embryol Exp Morphol *79*, 113–123.

Sun, T., Jayatilake, D., Afink, G., Ataliotis, P., Nister, M., Richardson, W., and Smith, H. (2000). A human YAC transgene rescues craniofacial and neural tube development in PDGFRalpha knockout mice and uncovers a role for PDGFRalpha in prenatal lung growth. Development *127*, 4519–4529.

Thiery, J. P., Acloque, H., Huang, R. Y. J., and Nieto, M. A. (2009). Epithelial-mesenchymal transitions in development and disease. Cell *139*, 871–890.

Visvader, J. E., and Lindeman, G. J. (2008). Cancer stem cells in solid tumours: accumulating evidence and unresolved questions. Nat Rev Cancer *8*, 755–768.

Wang, Y., and McNiven, M. A. (2012). Invasive matrix degradation at focal adhesions occurs via protease recruitment by a FAK-p130Cas complex. J Cell Biol *196*, 375–385.

Yang, J., Mani, S. A., Donaher, J. L., Ramaswamy, S., Itzykson, R. A., Come, C., Savagner, P., Gitelman, I., Richardson, A., and Weinberg, R. A. (2004). Twist, a master regulator of morphogenesis, plays an essential role in tumor metastasis. Cell *117*, 927–939.

Yang, W. H., Lan, H. Y., Huang, C. H., Tai, S. K., Tzeng, C. H., Kao, S. Y., Wu, K. J., Hung, M. C., and Yang, M. H. (2012). RAC1 activation mediates Twist1-induced cancer cell migration. Nat Cell Biol *14*, 366–374.